Modelling the critical role of cold acclimation for vegetation survival during extreme winter weather

Marius S. A. Lambert

Dissertation for the degree of Philosophiae Doctor (PhD)

Section for Meteorology and Oceanography
Department of Geosciences
University of Oslo

December 2022

Series of dissertations submitted to the
Faculty of Mathematics and Natural Sciences, University of Oslo
No. 2583

ISSN 1501-7710

Cover: UiO.
Print production: Graphics Center, University of Oslo.

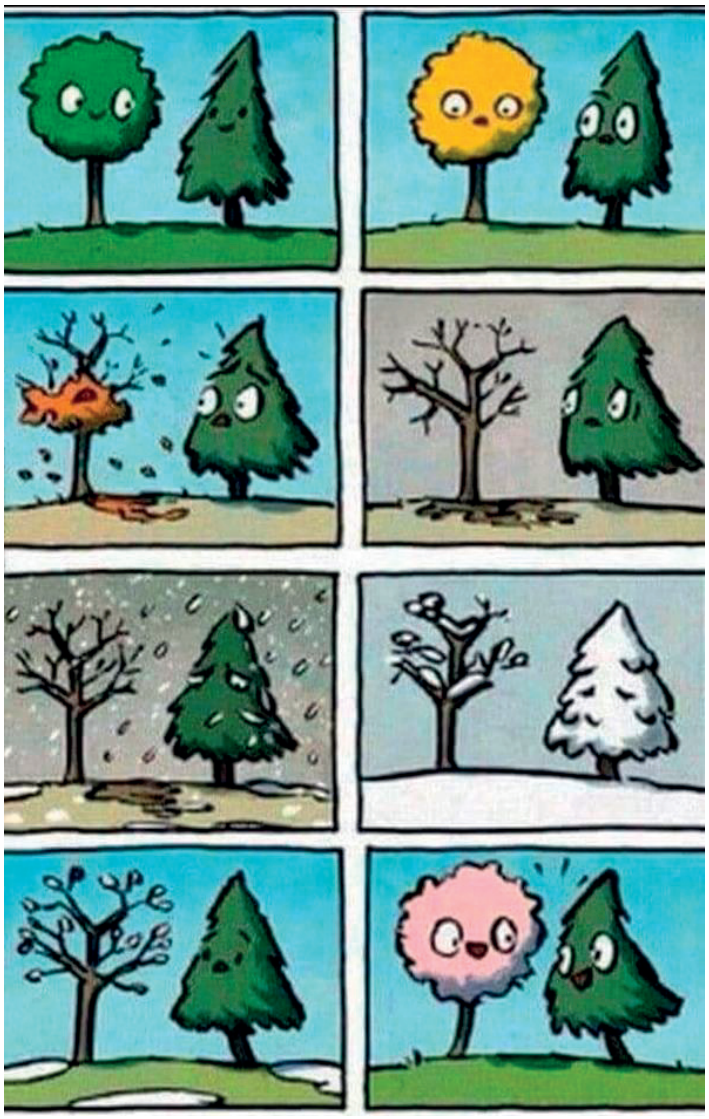

Acknowledgements

In 2018, during the few months preceding the accomplishment of my Master thesis, driven by the curiosity to discover upcoming opportunities, I read countless PhD proposals from all around the world. Most were interesting, but one stood out and straight away I was convinced it was for me. It distinguished itself by its gripping text, the requirements that perfectly fitted my background, and above all, the urgency and significance of the tasks. A couple of months after applying, I flew to Norway and started working at the section of Meteorology and Oceanography (MetOs), University of Oslo. Today, more than three years later, I realize how much I have learned during my time as a PhD candidate. This journey and its fulfilment would not have been possible without some key people I would like to thank.

At MetOs, I want to thank my main supervisor Frans-Jan W. Parmentier who made this PhD thesis possible for me to accomplish, gave me the opportunity to do research in several enriching environments, guided me along the way and defended my interests. I respect him for his broad knowledge, his relaxed and positive attitude in all circumstances and his impressive writing skills. My co-supervisor Hui Tang, for its tenacious contributions during the darkest periods of my PhD. Your help understanding and solving land surface modelling errors, have saved me considerable amounts of time. It is without hesitation during the time I spent with you, that I have gained most knowledge about the structure of our model and the technicalities of how to improve it. Kjetil Aas, for your active participation in the planning and structuring of the thesis. From sharing my first office with you, I benefited from your guidance and support when I most needed it. Frode Stordal, for the interesting discussions we have had and the constructive comments which nicely complemented help from my other co-supervisors.

Furthermore, I want to thank my colleagues, Stephanie for assisting me on some particular modelling issues, Britta for the numerous scientific and non-scientific discussions at work. Thanks also to all the other colleagues and friends with whom I shared ping-pong breaks, lunch breaks and most needed, other more entertaining after-work activities.

Part of my scientific work was enhanced by the valuable input of Rosie Fisher and Jarle Bjerke. I want to warmly thank both of them for their external guidance. I would like to thank Jacqueline Shuman and David Lawrence at National Center for Atmospheric Research (NCAR) in Boulder as well as Ryan Knox and Charles Koven at Berkeley Lab for welcoming me and supporting my work. I am grateful to Sarah and John Pitcher for their hospitality during my research stay at NCAR.

I would also like to thank my parents, who supported me and my choices and enabled me to get access to such an opportunity. My master thesis supervisor Xavier Fettweis, who introduced me to climate modelling and opened the door to research. My brother Baptiste, whose skills in mathematics have been briefly recruited. And huge thanks to Taletta for being an outstanding support. You managed to endure my complicated and disturbed character with ease during the last phase of my PhD.

Last but not least, I want to thank the Research council of Norway for funding this research, the strategic research initiative LATICE and the Centre for Biogeochemistry in the Anthropocene for their collaboration and the interesting meetings they provided.

Marius Lambert, Oslo 2022

Contents

Part I: Thesis

1. Introduction

1.1. Motivation

Climate models are idealised representations of a complex reality, and while they involve some degree of ignorance, distortion and approximations, they have the powerful capacity to enhance our understanding of the system we live in. These models allow us to quantitatively formulate and test hypotheses about the causes and mechanisms of past and future climate change. The climate is not stable in time but varies naturally on a range of timescales, as proven by observations and proxy records (Houghton, 1990; Pelletier, 1997). In addition, there is vast evidence that climate is now also changing due to greenhouse gas emissions resulting from human activity. These recent changes have already contributed to a global increase in temperature, and in the Arctic, the warming is four times faster than in the rest of the world (Rantanen et al., 2021). Even more worrying is that temperatures will continue to rise along with human emissions. As concerns are rising, the necessity of climate models and climate research is clear.

In global climate models, the Earth system is described by a myriad of mathematical equations based on well-established physical, biological and chemical processes predicting matter and energy transfers. The processes that are represented in global climate models are generally divided into components such as the atmosphere, ocean and land surface. In short, the atmospheric component simulates cloud formation and transport of heat and water through wind. The oceanic component represents current movements and mixing as well as ocean biogeochemistry, while the land surface component predicts surface characteristics such as vegetation, snow cover, soil water, rivers and carbon storage.

Among these components, the land surface generates most uncertainty in climate projections of future atmospheric CO_2 concentrations (Fatichi et al., 2019). The terrestrial part of the global carbon cycle, including carbon storage by vegetation through growth (carbon sink), is the least constrained (Le Quéré et al., 2018), resulting in uncertain projections of future atmospheric CO_2 concentrations (Friedlingstein, 2015). The complexity of land surface processes and the inaccuracy or sometimes even absence of crucial biogeochemical and physical processes are part of the uncertainty resulting from the land component. At high northern latitudes for example, a major consequence is that most land surface models project an increase in ecosystem productivity (Xia et al., 2017; Zhang et al., 2014), despite a sizeable proportion of the land area showing declining productivity, commonly known as browning trends (Berner et al., 2020; Frost et al., 2021; Phoenix & Bjerke, 2016). Arctic browning has been linked to extreme winter events that cause vegetation damage (Bokhorst et al., 2009; Phoenix and Bjerke, 2016), which are expected to become more frequent in the future (Bokhorst et al., 2010; Vikhamar-Schuler et al., 2016).

Ecosystem responses to arctic warming may positively or negatively feedback into the Earth's climate system depending on the geographical location, vegetation distribution and the changes resulting from the disturbance (McGuire et al., 2009). Forests have a lower albedo than tundra and this provides a positive feedback to rising temperatures (Bala et al., 2007). An increase in vegetation productivity due to a warming Arctic would increase CO_2 uptake by photosynthesis and hence result in a negative feedback on temperature (Speed et al., 2010), but increased root activity from this increase in vegetation productivity will also re-activate old carbon stored in tundra soils, resulting in a net release of carbon and contribute to the positive feedback (Hartley et al., 2012). Moreover, modifications of the surface energy balance from ecosystem changes may enhance permafrost thaw (Schuur & Mack, 2018). Permafrost soils store almost twice as much carbon as the atmosphere currently contains (MacDougall et al., 2012). Although the rate of carbon release from microbial activity in previously

frozen soils is uncertain, it is predicted to be a major contributor to a positive temperature feedback (Jansson & Taş, 2014). This emphasizes the need to realistically simulate current ecosystem productivity, vegetation distribution and total biomass in the arctic and boreal regions, to accurately predict future climate.

When winter approaches, plants start to develop their ability to withstand frost events. This process, which prevents cellular freezing, is called hardening and takes place every year during autumn, when days become shorter and temperatures start to drop. Its reversal occurs when temperatures start to rise again, and this is crucial for the reactivation of plant metabolism. Cold-acclimated plants go through a set of structural and physiological changes which protect them from frost and drought, but also slows down their metabolism and stops the synthesis of carbon compounds. The mechanisms that enable trees to survive include modifications of the cell membranes (Vaultier et al., 2006; Moellering et al., 2010), accumulation of cold-induced proteins and of cryoprotective compounds (Schrader & Sauter, 2002; Knaupp et al., 2011, Close, 1997; Kjellsen et al., 2013) and modifications of the photosynthetic machinery (Savitch et al., 2002; Ensminger et al., 2006; Demmig-Adams et al., 2012).

It has become clear that the influence of the cold season on the arctic carbon cycle (through processes such as frost, drought, and rain on snow) is much stronger than previously thought (Parmentier et al., 2017). Hardiness can be dramatically disturbed when extreme winter warming events lead to spring-like conditions. Such events prematurely initiate dehardening and expose vegetation by melting the protective snow cover (Bokhorst et al., 2011). When temperatures abruptly return to freezing following a warm spell, strong damage to trees, shrubs and sedges is likely to occur. Winter warm spells have already been observed at multiple northern locations, and their frequency is expected to increase (Bjerke et al., 2014; Bokhorst et al., 2009; Vikhamar-Schuler et al., 2016). The occurrence of vegetation-damaging events during several successive winters may result in ecosystem composition shifts (Zhao et al., 2017). Such events reduce vegetation productivity and carbon uptake by temperate, boreal and arctic ecosystems (Parmentier et al., 2018; Treharne et al., 2020). However, neither plant hydraulic adaptations during frost nor vegetation damage caused by extreme winter events, are well represented in land surface models. As a result, models lack the ability to simulate the cold season accurately. Land surface models urgently need to be updated with novel pathways and processes (e.g. delayed methane fluxes, microbial activity, cold acclimation and freezing plant water), to more accurately quantify future surface-atmosphere carbon fluxes in norther regions.

The focus of this thesis is to further expand the understanding of the impacts of cold-season processes in temperate, boreal and arctic ecosystems by improving CTSM5.0-FATES. The functionally assembled ecosystem simulator (FATES) is a size and age-structured representation of vegetation dynamics which may be coupled to a land surface model or an Earth system model. The Community Terrestrial Systems Model (CTSM) and the Energy Exascale Earth System Model (E3SM), have both been coupled to FATES and used by numerous scientists across the globe to simulate land surface processes (Christoffersen et al., 2016; Lawrence et al., 2019).

1.2. Scope and objectives

The overall goal of this work is to improve the representation and understanding of winter processes undergone by temperate and boreal vegetation during the cold seasons in a terrestrial biosphere model (CTSM5-FATES).

This goal is met by addressing a series of sub objectives:

1) *Hardening scheme:*
   a) Implement a globalized version of the hardening scheme based on the work of Rammig et al. (2010) into the ecosystem simulator (FATES) hosted by CTSM5.0.
   b) Adapt the hardening scheme to make it performant in all climates/locations since the hardening scheme of Rammig et al (2010) was parametrized to be effective only in Farstanäs (Sweden).
   c) Adapt the hardening scheme to all plant functional types (PFTs) since the version of Rammig et al. (2010) was parametrized to fit Norway spruce (*Picea abies*).
2) *Hydro-hardening:*
   a) Implementing a novel scheme to use the hardiness level of plants to constrain plant hydraulic variables during winter in order to mimic the impacts of cold acclimation on plant hydraulics in the field.
   b) Assess the effects of hardiness on transpiration, root water fluxes, mortality, and vegetation productivity, and examine the sensitivity of parameters and variables involved in the hardening scheme
3) *Frost hardening*:
   a) Implement a frost mortality scheme based upon the previously implemented hardening scheme. The frost mortality scheme uses the varying hardiness levels instead of a fixed tolerance threshold to calculate frost mortality.
   b) Examine the trends, annual distribution and spatial patterns of the hardiness-dependent frost mortality scheme and compare it to the previous frost mortality scheme.
4) *Frost droughts:*
   a) Using the newly implemented schemes in (1)-(3) to evaluate the capacity of FATES-Hydro to accurately represent frost droughts in cases where the soil is still frozen, but mild atmospheric conditions trigger excess transpiration.
   b) Assess the vulnerability of deciduous versus evergreen shrubs (differentiated by their capacity to remain cold acclimated) during winter warming events.

These four main objectives are treated in the following three papers, and as detailed below, some of the papers cover sub-objectives from different main objectives.

Paper I: FATES has recently been improved with an advanced hydraulic model based on the continuous porous media approach (Sperry et al., 1998; Christoffersen et al., 2016). However, this improvement was initially developed to fit specific sites in the tropics. This implies that the model performs poorly at representing hydraulic processes in the cold regions of the world, where extreme winters can cause soils to freeze to temperatures well below −20°C causing dehydration by the activation of reverse water flow through roots in the model. The main purpose of Paper I is to make FATES-Hydro more realistic in cases where plants acclimate to cold temperature. The objectives met in Paper I are 1a, 1b, 2a and 2b and aim to show that the hydraulic changes prescribed by the hardening scheme are necessary to model realistic vegetation growth in northern regions and make it possible to use CTSM5-FATES to model realistic impacts from droughts on vegetation growth and photosynthesis.

Paper II: In FATES, each PFT is assigned a minimum temperature threshold (between 2.5 °C and −80°C) to which it is tolerant. These thresholds are fixed parameters of the model and are used to predict frost mortality and hence influence the spatial distribution of PFTs. However, depending on the climate (e.g. average winter temperatures of −20°C) of a grid-cell (location), the outcome is that plants with a low freezing tolerance (e.g. 2.5°C) are likely to die out in the course of a few winters, while plants with a high freezing tolerance (e.g. −80°C) will never incur frost injury. In Paper II, we replace the fixed temperature threshold by the hardiness level of plants in the calculation of frost mortality. The objectives of Paper II are described by 1c, 3a and 3b. Our goal with paper II is to show that the hardening-frost scheme is necessary to model (realistic) frost mortality in northern regions of the globe and to examine how it may lead to significant changes of PFT distribution ranges by enhancing the competitiveness of frost-tolerant PFTs.

Paper III: Winter warming events in the Arctic are predicted to increase in the future. However, to date, no ecosystem models have studied the effects of frost droughts on cold-acclimated plants. Frost droughts occur when sudden winter atmospheric warming causes leaf transpiration while frozen soils prevent water uptake. In paper III, we take advantage of the complex tissue level-trait plant hydraulics of FATES-Hydro and its newly implemented hydro-hardening scheme to assess how the model performs to represent the 2013/14 winter warm spells that were experienced by deciduous and evergreen shrubs along the Norwegian coast. The objectives met in Paper III are 4a and 4b and aim to show that the extreme winter of 2013/14 led to excess transpiration, vegetation mortality and ultimately affected the carbon cycle, and that evergreen species are more vulnerable to acute frost desiccation than deciduous genotypes.

1.3. Outline of this thesis

This thesis is composed of two parts. The first part provides an overview of the presented research and is divided in several chapters. Chapter 2 presents a general overview over the relevant scientific background needed to understand the scientific work in this thesis. Chapter 3 describes the model used in the thesis (i.e. CLM5-FATES-Hydro) and the data that serves as atmospheric forcing (i.e. GSWP3v1, COSMOREA6 and ERA5-Land). Chapter 4 contains a summary of the scientific findings from each of the four papers and relates these to the objectives listed above. Chapter 5 discusses the results and presents recommendations for further research.

The second part of the thesis contains the three scientific papers. All papers have been submitted to internationally recognized scientific journals.

2. Scientific background

This chapter presents an overview of the scientific background related to the topics investigated in this thesis. I start by briefly defining and documenting the Arctic browning phenomenon in Section 2.1. This first section complements the motivation section and broadly introduces the concepts and processes related to extreme winter warming events, vegetation biomass and mortality, and how their feedback to climate is. In Section 2.2, the capacity of temperate and boreal plants to acclimate to cold and tolerate freezing during winter is described in detail. In a set of successive subsections, I discuss the emergence of cold tolerance, cold acclimation, and explain the pathways and reasons for plants to acclimate to cold and elaborate on some relevant aspects and impacts of freezing tolerance and dormancy. In Section 2.3, I describe the existing types of droughts with a particular emphasis on winter droughts and I discuss how they impact plant hydraulics and can lead to mortality. Finally, in Section 2.4, I first present the capacity and utility of land surface models as part of Earth system models, and then I describe how land surface and dynamic vegetation models represent phenology and frost mortality, and plant hydraulics and transpiration.

2.1. Winter warming-induced greening and browning

Arctic, boreal and temperate ecosystems have experienced substantial changes throughout the past forty years and are expected to be dramatically transformed over the coming decades (Francis & Vavrus, 2012; Serreze & Francis, 2006). For example, surface temperatures have risen much faster in the arctic region than the global average (Serreze & Barry, 2011), and northern parts of the world have experienced major extreme winter events (Bjerke et al., 2017; Hansen et al., 2014). Extreme winter events in northern regions can be in many forms and include for example excessive winter rainfall, abrupt and abnormally low temperatures, and winter warm spells. Warm spells are a number of consecutive winter days with maximum temperatures peaking above 0°C. As an example, in February 2012, Svalbard was hit by heavy rainfall (272 mm in two weeks) and maximum temperatures exceeded 4° C during 6-12 days before they dropped to −10° C again (Hansen et al., 2014). With global warming, extreme winter events are expected to become more frequent in the future (Screen et al., 2015).

Mid-winter warm spells (or warm pulses) can be extremely damaging to vegetation as they interrupt and disturb vegetation in their dormancy (Fig. 1). Because of their damaging effect on vegetation, extreme winter events may explain a large part of Arctic browning (Phoenix & Bjerke, 2016). For example, areas with vegetation damage, or browning, as large as 1424 km^2 have been observed in the arctic region in the past decade (Bi et al., 2013; Bokhorst et al., 2008). Such browning events are defined as an area where living biomass or vegetation productivity decreases during at least 3 consecutive years (Fig. 2). The normalized difference vegetation index (NDVI, a proxy for live green vegetation) is generally used to illustrate such browning or greening. However, huge uncertainties remain concerning the relative contributions of factors causing Arctic browning, which include extreme events, wildfires, insect attacks, diseases, and consequences thereof in particular. While the drivers of Arctic browning have been widely studied, its consequences on the Earth's climate have not been clearly defined yet.

One major cause of arctic browning, frost damage, can occur in several ways. Periods of abnormally warm weather, particularly in the middle of arctic winter, simulate autumn-like conditions leading to mid-winter loss of freezing tolerance or premature bud burst in extreme cases (Phoenix & Bjerke, 2016). During sudden and strong warm spells, plants typically start transpiring as a response to the higher temperatures, while the still frozen soil prevents root water uptake (Larcher & Siegwolf, 1985; Sakai & Larcher, 1987; Tranquillini, 1982). This process is called frost drought (in contrast to summer drought where the soil is not frozen) and results in dehydration of plant tissues through

excessive transpiration. Alternatively, when temperatures rapidly drop below freezing after a warm spell, frost may further damage plants by causing inter- and intra-cellular freezing of tissues (S. Bokhorst et al., 2011).

Under normal circumstances, the exposure of plants to low temperatures increases their frost tolerance, a process known as cold acclimation, and this involves the expression of cold-induced genes (Chang et al., 2021; Leinonen et al., 1997; Thomashow, 1999). However, when temperatures drop too rapidly after a warm spell, plants do not have the time to re-acclimate (Arora & Rowland, 2011; Kalberer et al., 2006; Welling & Palva, 2006). During warm pulses, the loss of freezing tolerance is often accompanied by substantial snow melt that increases vegetation's vulnerability to freezing temperatures. Snow cover is crucial for insulating and protecting vegetation from cold atmospheric winter air. During a warm pulse, even a partial loss of this protective snow cover can lead to observed damage to the plant (or parts of the plant sticking out from the snow) (Bokhorst et al., 2009). In addition, the simulation of spring-like conditions triggers bud burst, which is crucial for reproduction but also makes plants highly vulnerable to a return to freezing temperatures (Bokhorst et al., 2008).

Figure 1: Damage to Empetrum nigrum in north-west Scandinavia caused by an extreme winter warming event. (From Phoenix & Bjerke, 2016)

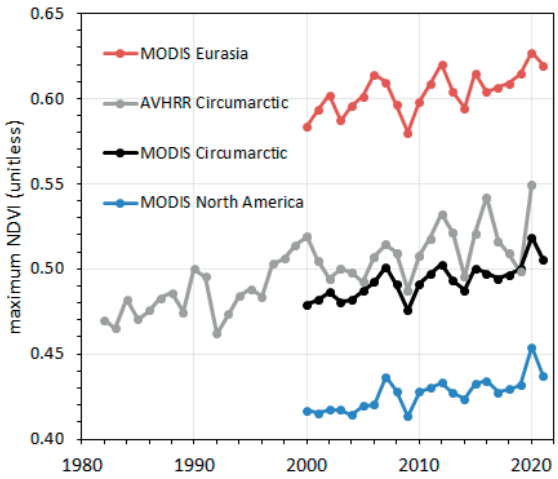

Figure 2: Time series of MaxNDVI (Maximum Normalized Difference Vegetation Index) from the MODIS MCD43A4 (2000-21) dataset for the Eurasian Arctic (in red), North American Arctic (in blue), and the circumpolar Arctic (in black), and from the long-term AVHRR GIMMS-3g+ (1982-2020) dataset for the circumpolar Arctic (in grey). (Frost et al., 2019)

Changes in vegetation productivity will have considerable impacts on the climate system through, among others, modifications of the surface albedo (Loranty et al., 2011), carbon uptake, evapotranspiration (Law et al., 2002), biogenic volatile organic compound (BVOC) emissions (Peñuelas & Staudt, 2010), and permafrost stability (Nauta et al., 2015; Yi et al., 2007). Since vegetation damage in winter has consequences for plant health in summer, it has been suggested that extreme events may contribute to climate warming when considering the albedo effect (Diffenbaugh et al., 2005). Moreover, damaged vegetation means a reduced CO_2 uptake, a potential feedback on climate that follows from extreme winter events (Parmentier et al., 2018). Also, if northern regions are browning, transpiration is expected to decrease, leading to less water vapour – an important greenhouse gas – which influences cloud formation (Law et al., 2002). To conclude, the effects of browning on the surface energy balance, carbon exchange, permafrost stability and feedbacks on climate change are mixed and have not been clearly defined yet (Pearson et al., 2013; Swann et al., 2010; Yi et al., 2007). The potential for large impacts emphasizes the need to implement relevant processes in models and to explore their future development.

2.2. Cold tolerance

Since the late Eocene, the Earth has experienced countless cooling events resulting in a contraction of the tropics and the appearance of temperate zones in both hemispheres (Stickley et al., 2009; Zachos et al., 2001). As a response to this cooling, several tropical species have successively diversified in order to survive outside of their initial ecologic niche by becoming resistant to colder and often more seasonal environments (Axelrod, 1952; Sandve & Fjellheim, 2010; Schluter, 2016).

Both in cold temperate zones and tropical highlands, plants experience freezing temperatures which may be detrimental to their fitness. However, the timing and duration of cold events is quite dissimilar in these regions, either occurring on an annual cycle in temperate regions or on a diurnal cycle in tropical highlands (Greenup et al., 2011; Preston & Sandve, 2013). Despite these two different cases of timing for frost, and their implication on the strategies adopted by plants of a given environment, there is evidence for similar genetic responses to cold (Teutonico & Osborn, 1995). In this thesis, we focus on the physiological and morphological adaptations adopted by temperate and boreal plants exposed to seasonal freezing temperatures.

Unlike animals, who can migrate, plants are static. Hence, in order to survive cold winters, they must coordinate their most vulnerable phenological states (e.g. budburst, flowering and germination) with favourable environmental conditions, usually met during spring and summer (King & Heide, 2009). As a result, activities such as germination, growth and reproduction take place during the warm season, while plants become dormant and reduce or completely stop growth during winter.

Among vegetation species found in nature, some are called spring annuals, meaning that they perform their entire life cycle in the course of a single growing season, from the moment they germinate in response to inductive conditions in spring, to flower and back to seed. These plants die annually and only cold-resistant seeds bridge the gap between two generations. In contrast, plants that persist several years without completely dying off are called perennials. Since the vegetative structures (roots, stem and leaves) of perennials are subject to cold/frost during winter, these plants are often induced into a cold and/or frost-tolerant state. Woody perennials (i.e. trees and shrubs) can be either

qualified as evergreen, if they keep their leaves/needles, or as deciduous if leaves/needles fall off in autumn. Plants with needles are called needleleaf while plants with leaves are called broadleaf. These definitions will be used throughout this thesis.

2.2.1. *Introduction to cold acclimation*

The development of tolerance to frost in seasonal temperate and boreal woody perennials involves a sequence of interdependent stages (Glerum, 1973; Sakai & Larcher, 1987; Weiser, 1970). The first stage appears to be induced by a shortening of days at still fairly warm temperatures (10° to 20°C in fall) and takes place only after growth has ceased. During this stage, plants accumulate materials such as reserve starch and neutral lipids. These stored substrates are essential energy sources for the fulfilment of the second stage. During the second stage, low non-freezing temperatures become the main driver, but sub-zero temperatures are even more effective and will further enhance the frost tolerance level of plants. Stage two is accompanied by the neo-synthesis of proteins and membrane lipids as well as structural changes that will ultimately lead to the maximum hardiness level (Welling et al., 2002).

The maximum level to which plants can acclimate, as well as the timing and the rate at which they harden, is under genetic control and varies between and within species, depending on their developmental stage (Chang et al., 2021; Johansson et al., 2015; Sakai & Larcher, 1987). If transported to grow in the same outdoor location, like a common garden, northerly and highland ecotypes are likely to start hardening earlier than those originating from southerly or low latitude locations (Stevenson, 1994). After exposure to moderately warm conditions, a decrease in frost hardiness takes place (Pagter & Arora, 2013; Vyse et al., 2019). The rate and temperature range at which plants deharden or deacclimate depends on the development status and genotype of species (Arora & Rowland, 2011).

The process of deacclimation is typically faster than acclimation (Arora et al., 1992). An extreme example shows that leaves of *Solanum commersonii* (wild potato species) only required one day to completely lose their freezing tolerance when exposed to 20°C (Chen & Li, 1980). In comparison, if exposed to 2°C, 15 days were needed. Observations of *Pinus sylvestris* indicate that hardening rates are around −1°C per day, while dehardening rates are ca. 2°C per day (Beck et al., 2004; Repo, 1991).

2.2.2. *Synchronization with dormancy*

A growing amount of research has focused on identifying the molecular mechanisms controlling dormancy and freezing tolerance separately, due to their complexity and distinct regulation (Welling & Palva, 2006; Wisniewski et al., 2003). However, as they are synchronized processes (Fig. 3), regulated by common environmental cues and mutually impacting each other, it is essential to take both dormancy and freezing tolerance into account when trying to understand overwintering strategies of trees.

Similar to frost tolerance, the onset of dormancy is initiated in response to shorter days, when the region of cells capable of division and growth in the root and shoot tips of plants (apical bud meristem) cease their activity (Rinne et al., 2001). From the moment plants stop growing, the development of dormancy is initiated, and in a few weeks' time, the apical bud meristem but also the buds occurring at leaf nodes (auxillary buds) enter endodormancy (Lang, 1987). Endodormancy refers to a state of buds, where an internal inhibitor system prevents growth until exposed to sufficient

amounts of chilling temperatures (low but above zero). For the second stage of the development of freezing tolerance, the progression of dormancy requires chilling and freezing temperatures (Cox & Stushnoff, 2001; Welling et al., 1997). During this stage, buds are released from endodormancy and maintain a hardened resting state (ecodormancy) until growth conditions turn favorable again in spring (Lang, 1987). The increasing mean temperatures in spring also result in a gradual loss of freezing tolerance and in most cases endodormancy is a prerequisite for woody perennials to deacclimate and lose freezing tolerance. However, fluctuating temperatures can stop deacclimation and result in a transient increase of tolerance (reacclimation) (Welling et al., 2004). The capacity of plants to reacclimate and resist deacclimation play a significant role during a period when plants are particularly vulnerable to injury due to their emergence from dormancy (Kalberer et al., 2006; Pagter et al., 2011).

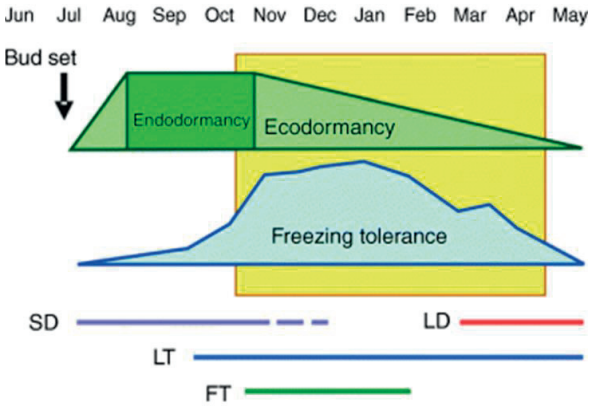

Figure 3: "*Annual development of dormancy and freezing tolerance in adult, field-grown birch during overwintering in northern Finland. After growth cessation and bud set in July, buds gradually enter into endodormancy, in which they are incapable of bud break until they have received sufficient chilling treatment. Endodormancy is released by November, and ecodormant buds are able to burst under favorable conditions. Freezing tolerance starts to increase during autumn in response to shorter day lengths. Subsequent low and freezing temperatures increase freezing tolerance to its maximum values. From February onwards, trees start to de-acclimate and their freezing tolerance decreases with increasing mean temperature. If temperature decreases transiently, trees are able to reacclimate. The yellow box refers to time of the year when mean temperature remains below zero. Horizontal bars denote the time of the year when different environmental factors are most likely to have the greatest impact on the growth of trees. LD, long day length; LT, low, non-freezing temperature; FT, freezing temperature; SD, short day length". (*From Welling & Palva, 2006)

2.2.3. Deacclimation and reacclimation

While maximum freezing tolerance is generally reached mid-winter, and is associated with the absence of growth, plants deacclimate upon exposure to favorable temperatures and increasing daylength so they can start growing again (Arora & Rowland, 2011). If deacclimation occurs too late, valuable growing season time will be lost. In contrast, plants that deacclimate too early, risk being exposed to damaging temperatures during cold spells. Unless of course, they have the ability to rapidly reacclimate in spring (Kalberer et al., 2006). Compared to the large body of research on cold acclimation, little is known on how plants maintain or reacquire frost tolerance in late winter and spring. It has been established that, depending on the degree of deacclimaton and the time plants spent in an unhardy state, some overwintering plants have the capacity to reharden to some extent. The

degree to which plants reacclimate has been suggested to progressively decrease after successive cycles of reacclimation (Shin et al., 2015). The loss of reacclimation capacity is believed to be either linked to the lack of available energy sources from stored substrates, or due to irreversible developmental changes resulting from deacclimation, or a combination of both (Pagter & Arora, 2013; Saxe et al., 2001).

2.2.4. *Molecular level of cold acclimation*

Although the physiological consequences of hardening are well established, less is known about the pathways triggering cold acclimation and the ways cold temperatures are sensed by a plant (Guo et al., 2018; Ruelland et al., 2009; Shi et al., 2018). Research suggests that the low-temperature signal is translated into cellular responses through an array of mechanisms involving cell and organelle membranes (Örvar et al., 2000; Sangwan et al., 2001). A change of the membrane rigidity and rearrangement of the cytoskeleton (which is the network of protein filaments giving coherence and shape to cells), may trigger an influx of calcium (Ca++) and the expression of cold-responsive (COR) genes (Welling & Palva, 2006). Alternatively, the expression of COR genes can also be regulated by C-repeat-binding factor (CBF) dependent pathways (Thomashow, 1999). CBFs, or homologs, are rapidly expressed when temperatures drop, but can also be regulated by the circadian clock, light quality and photoperiod under normal (e.g. 22°C) temperatures (Dong et al., 2011). The products of COR genes associated to the acquisition of cold acclimation are numerous and include among others: late embryogenesis abundant (LEA) proteins such as dehydrins (Close, 1997), protein kinases (PK) (Weckwerth et al., 2015), proteins associated with lipid metabolism (Holliday et al., 2008), proteins for hormone responses such as ABA (Umezawa et al., 2010), cell wall modifiers, and chloroplast proteins (Tai et al., 2007; Ueno et al., 2013).

The protective compounds synthesized during cold acclimation have been identified to prevent intercellular freezing and associated dehydration effects, enhance the capacity of plants to tolerate freezing, or promote both tolerance and avoidance of freezing (Janská et al., 2010; Levitt, 1980). The avoidance of interstitial ice crystallization can be achieved by keeping tissues isolated from the cold or decrease the temperature of ice nucleation. When anti-freeze proteins such as dehydrins are synthesized, the nucleation point of ice in tissues can be suppressed down to −38°C (Hanin et al., 2011). Then, at temperatures between −20°C and −30°C, the formation of intracellular glass, also named vitrification, further enables cold-acclimated woody plants to develop a resistance to much lower temperatures. Experiments have demonstrated that in extreme conditions, it is possible for trees to resist temperatures as low as the temperature of liquid nitrogen (−196°C) (Rinne et al., 1998).

In frost-tolerant plants, cryoprotective mechanisms improve membrane fluidity through changes in lipid composition (Steponkus, 1993; Uemura & Steponkus, 1997). The accumulation of sucrose and other sugars or LEA proteins contributes to the stabilization of membranes protecting them against frost-induced damage (Anchordoguy et al., 1987; Strauss & Hauser, 1986).

2.2.5. *Cold damage*

When temperatures get below the cold tolerance threshold of plants, damage can occur (Sakai & Larcher, 1987). In some cases, plants already experience injury at low temperatures (chilling temperatures) well above their freezing point (~1 to ~10 °C), a process called chilling injury (Lyons, 1973). In contrast, freezing injury requires freezing temperatures and results in ice formation in and around plant tissues (Burke et al., 1976).

Chilling temperatures generally result in symptoms such as reduced growth, increased permeability of the membrane and metabolism dysfunction, which lead to chlorosis (lack of iron in leaves) or necrosis (degeneration of tissues) (Cohen et al., 1994; Wang & Wallace, 2004). In general, the duration of exposure to chilling is directly proportional to the degree of damage, and in extreme cases, chilling temperatures can cause wilting and death. Chilling injuries develop slowly and usually become visible only after several days or weeks (Lyons, 1973).

In cases of freezing injury, the primary form of damage is mechanical stress to the membrane systems due to intercellular (occurring in the space between cells) ice crystallization and fragility of the tissues (Levitt, 1972). If intracellular (within cells) freezing takes places, cells always die (Asahina, 1956; Modlibowska & Rogers, 1955). Fortunately, due to the lower concentration of solutes and the consequently higher freezing point of water, ice generally starts to form in intercellular spaces before it forms in cells. Since ice has a lower chemical potential than liquid water, the formation of ice crystals in intercellular spaces makes the water potential decrease locally and provokes cellular dehydration.

Water potential is a measure of energy and quantifies the tendency of water to move from an area to another due to osmosis (presence of solutes), gravity, mechanical pressure and capillary action (Papendick & Campbell, 1981). When the formation of ice crystals takes place in extracellular spaces, water flows out of cells along the water potential gradient resulting in cellular dehydration (Steponkus, 1984). The removal of water from cells causes membrane defects and alteration of lipid-protein complexes. The loss of membrane integrity of cells that are insufficiently cryo-protected, in turn, results in solute leakage and water loss (Sakai & Larcher, 1987; Steponkus, 1984). If dehydration exceeds a certain threshold, cell membranes can be damaged leading to multiple physiological impacts: death of tissues, yellowing of leaves, smaller leaves, reduced reproduction, or even plant death.

2.2.6. Photosynthesis inhibition and photosystem damage

Beyond chilling and freezing injury, low temperatures inhibit the synthesis and pathways for repair of the core protein D1 of the photosystem 2. This can cause the near to complete loss of photosynthetic core proteins, which disrupts metabolic processes such as the fixation of CO_2 (Ebbert et al., 2005; Ensminger et al., 2004). Freezing can also impair the Calvin cycle by decreasing the efficiency of rubisco carboxylation and slowing down the regeneration of ribulose biphosphate (Crosatti et al., 2013; Ensminger et al., 2012). Despite the dysfunction of the photosystem and the absence of photosynthesis in overwintering evergreen needles or leaves, light is still perceived by the chloroplasts although it cannot be used for photosynthesis. This excess light can induce a process called photo-inhibition, which leads to the formation of reactive oxygen species (ROS), both of which can cause large photo-oxidative damage (Adams et al., 2004). For example, there is evidence that the production of ROS leads to membrane damage (Das & Roychoudhury, 2014). While deciduous trees avoid the stress resulting from high light intensities and freezing by shedding their leaves, evergreens have evolved mechanisms to prevent damage from excess light during winter. Conifers decrease light absorption through the degradation of leaf chloroplasts and some membrane proteins of photosystem 2, and through the increased synthesis of photoprotective carotenoids (Ottander et al., 1995). The photoprotective mechanisms plants use to avoid the formation of ROS are called non-photochemical quenching (NPQ) and relies on the dissipation and conversion of excess light into heat.

2.3. Winter plant hydraulics

2.3.1. Basics of plant hydraulics

Photosynthesis is the chemical process by which plants transform water and atmospheric CO_2 into sugar molecules and oxygen in their leaves. Photosynthesis requires energy from light to carry out this reaction. Leaves are covered by pores (stomata) which capture the atmospheric CO_2 in exchange for water. Stomata can open (usually during the day), when CO_2 molecules move in and energy sources (sugars) are synthesised. At night, or when plants face dry conditions, stomata may close to avoid large water losses, but this means that less CO_2 enters, and if stomata remain closed for too long, plants may starve. To compensate for leaf water loss, plants depend on the performance of water transport systems (Cochard, 2013). Xylem and phloem make up the vascular tissue of a plant (Carlsbecker & Helariutta, 2005). Phloem cells transport the products of photosynthesis from leaves to other plant tissues (De Schepper et al., 2013), while the xylem tissue (elongated, hollow and dead cells, i.e. tracheids and vessel elements) transports water, salt and minerals from roots to stems and leaves (Kim et al., 2014). Through xylem vessels, continuous columns of liquid water connect the soil to the leaves. Because the atmosphere is drier than the leaves, water evaporates through stomata (transpiration) at the very top of the water column (Meinzer, 1993). This creates a strong negative pressure or tension which pulls up the whole water column, and enhances capillary forces (Steudle, 2001). Moreover, water molecules stick together putting the column under high cohesion. The combination of the pulling force or tension exerted by evaporation at the leaf surface, and cohesion of water molecules sticking together, is described by the cohesion-tension (C-T) theory (Bohm, 1893; Dixon & Joly, 1894).

Over the past decades, the C-T theory of water ascent has been challenged by a large body of experimental evidence (e.g., Bentrup, 2017; Wistuba et al., 2000; Zimmermann et al., 2013). This evidence suggests that plants acquire and transport water via an interplay of several mechanisms covered by the multi-force (M-F) theory (Zimmermann et al., 2004). According to this theory, several forces interact to dictate movement of water including cohesion, tension, capillarity, xylem-phloem re-circulation, cell osmotic pressure gradients and hydrogel-bound gradients of the chemical activity of water (Bentrup, 2017). This clearly implies a segmentation of the xylem conduit. Evidence of discontinuous water columns in birch trees was documented by Westhoff et al. (2009). They showed that water was lifted by means of short-distance tension gradients and mobilization of water from parenchyma (i.e. living cells around the xylem) as well as moisture uptake through lenticels (i.e. pores in the stem). With these principles, the impact of droughts on vegetation can be better understood and modeled.

2.3.2. Types of droughts

Climatologically, drought is defined as a prolonged period of abnormally low precipitation, either as snow or rainfall (Wilhite & Glantz, 1985). The lack of precipitation is one of the most demanding weather events for plants. Droughts have attracted the attention of a large community of hydrologists, ecologists, modellers, and crop scientists since it typically results in reduced soil moisture, vegetation desiccation, increased wildfires and other environmental disasters. From an ecological point of view, a drought is defined as an episodic deficit in water availability that drives ecosystems beyond thresholds of vulnerability and may lead, among others, to reduced plant growth, enhanced plant mortality and landscape-level transitions (Crausbay et al., 2017). We distinguish two main types of

plant ecological droughts: summer droughts, which are related to the lack of precipitation (Archaux & Wolters, 2006), and winter droughts which require low or freezing temperatures and often develop due to the freezing of liquid water in soil (Tranquillini, 1982). As this review is about cold season processes, the next paragraphs will focus on describing winter droughts, which may occasionally be designated simply as droughts.

2.3.3. The origin of winter droughts

Nearly 150 years ago, in the early days of plant physiology research, Ebermayer (1873) attributed extensive winter damage of Scots pine (*Pinus sylvestris*) plantations – which led to a massive shedding of needles – to winter desiccation. Ebermayer hypothesized that the needle loss was caused by severely reduced or completely interrupted water transport at chilling or freezing temperatures, so that gradual transpiration could not be adequately replaced. With continued desiccation, plant organs reached a critically low water content, a threshold at which they lost all the water they could afford to lose without incurring injury. Ebermayer's theorem was first challenged by Neger (1915), who argued that damage to forest trees following harsh winters was purely due to intracellular freezing. Around 1930, rapid advances in ecophysiology provided evidence of large decreases in plant osmotic potential after harsh winters, indicating that plants had suffered from water deficiency, and thereby confirming the validity of Ebermayer's winter desiccation theory (Walter, 1929; Walter & Thren, 1934).

Here, we distinguish two types of winter droughts (Fig. 4), chronic winter desiccation and acute frost desiccation. Chronic winter droughts are defined as the slow dehydration of plants via cuticular or peridermal, rather than stomatal transpiration. Such droughts are especially strong on sunny days, but they occur throughout the winter (Larcher, 2003; Tranquillini, 1982). In contrast, during acute frost droughts, excessive and strong stomatal transpiration is triggered by winter warm pulses or fast transitions from winter to summer, while the frozen soil prevents plants to replace transpiration losses (Tranquillini, 1980). Although transpired water is not adequately replaced, it can take several days before plants respond and stomata fully close (Larcher and Siegwolf, 1985). Despite the different pathways of water loss between drought types, the mechanism of injury is similar.

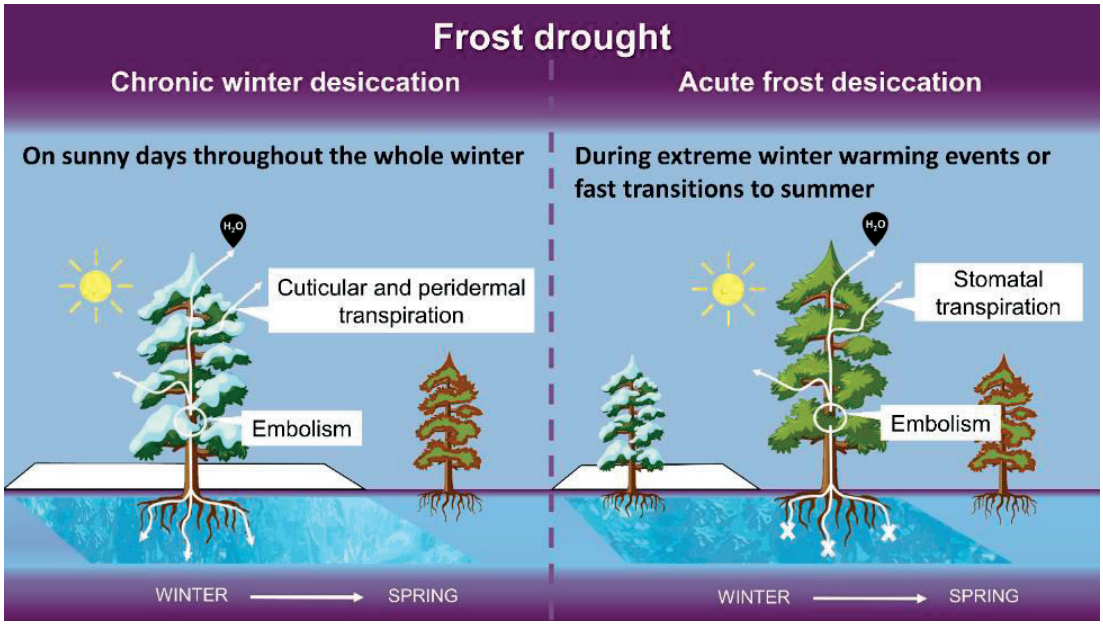

Figure 4: Types of drought: left) Chronic winter desiccation, right) Acute frost desiccation.

2.3.4. *Drought injury*

Drought conditions lower the amount of available liquid water in the soil, and hence increase the tension of soil water. Under such conditions, xylem sap must increase its tension accordingly to continue to extract water. Xylem tension additionally increases due to desiccation via excess stomatal transpiration in the absence of root water uptake. Beyond a certain pressure threshold (i.e. different among species) cavitation takes place, breaking the water column and disrupting the mechanism of sap ascent (Sperry & Tyree, 1990). Several mechanisms for the nucleation of cavitation in plants have been proposed. The most studied one is called "homogeneous nucleation" (Pickard, 1981). According to this mechanism, when the pressure of a liquid drops below its vapour pressure, vapour-filled cavities, also called "bubbles", are formed. The presence of air bubbles in xylem vessels interrupt the transmission of tension from the roots to the leaves in a process called embolism (Tyree & Sperry, 1989). Further evidence points out that cavitation can occur by air seeding through pores and hydrophobic cracks in the inter-vessels or inter-tracheid pit membranes (Tyree & Zimmermann, 2002). The structure of the pits varies between species, and determines the vulnerability to drought-induced cavitation (Cochard, 2006; Hacke et al., 2004). For example, coniferous species have a structure in their pits called "torus", which seals the opening and prevents the embolism to spread to all of the xylem conduit (Fig 5). To avoid cavitation, the first response of plants is to regulate stomata openings, so that the xylem tension remains below the vulnerability threshold, this threshold is found around 50% and 90% for conifer and angiosperms (flowering seed plants, includes broadleaf deciduous trees), respectively (Johnson et al., 2012). While stomatal closure might efficiently maintain tension below the critical value, the extended absence of CO_2 uptake and photosynthesis results in carbon starvation. If stomata remain open to avoid carbon starvation, cavitation might occur instead; hence, it is a compromise. Maintained cavitation will also result in carbon starvation, but also reduces water content and potential of vegetation organs which can damage cell membranes (Sperry and Tyree, 1990). However, if the degree of cavitation remains low, leaves can recover their functions and new xylem conduits may be formed. Alternatively, species may generate positive root pressures to refill embolized conduits which allows air to re-dissolve in the xylem solution.

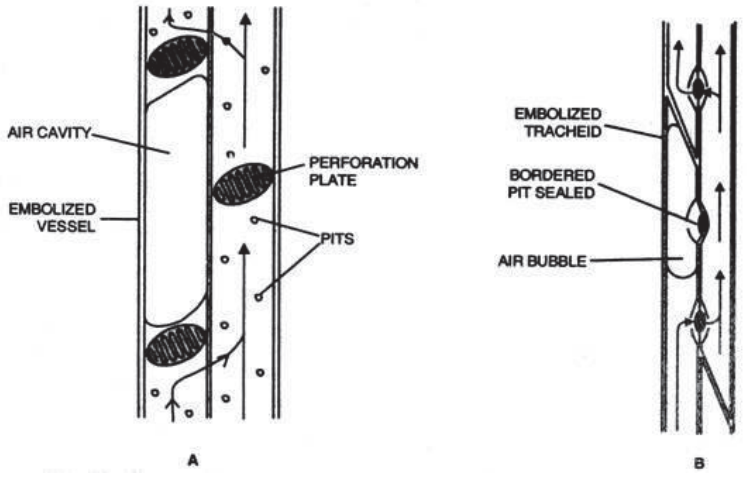

Figure 5: Schematic representation of upward movement of water (shown by arrows) in xylem vessels (A) and tracheids (B) bypassing the embolized zones. (Koratkar, 2016)

2.4. Earth system modelling

Climate is defined as the long-term pattern of weather in a particular area. In contrast to weather, which can change dramatically from day to day, climate is much slower to evolve as it is the average condition of the weather (Barry & Chorley, 2009). While meteorologists forecast weather for days or weeks ahead, climate researchers and modellers look at the evolution of the climate up to several hundreds of years in the future. Despite the remarkable differences between weather and climate, the physical laws that build forecasting and climate models are the same (Hasselmann, 1976). Both types of models assemble physical laws into a complex set of equations to represent the Earth, or at least parts of it. Moreover, weather and climate models rely on initial and boundary conditions to predict future conditions (e.g. wind, precipitation, temperature). However, the challenges faced by forecasters and climate modellers are different. Weather is chaotic. Small errors in the initial conditions used by the model magnify over time, and a weather forecast usually becomes very uncertain beyond a couple of days (Ferranti et al., 2015). In contrast, since climate predictions do not focus on getting the conditions of a particular day correct, the boundary conditions become more important (Wu et al., 2005). Long-term climate predictions strongly rely on how much energy enters and leaves the system and how it is distributed.

A climate model is a representation of the major climate system components (land, ocean, atmosphere, cryosphere…), and their interactions (Flato, 2011; Stocker, 2011). Earth system models (ESM) divide the Earth in a three-dimensional grid, where each grid cell represents a specific area (with an altitude and geographical coordinates). At each time step of a climate simulation, fluxes of heat, water and momentum are computed between grid cells. This means that a simulation of higher resolution (i.e. the earth is divided into more but smaller grid cells), at the expense of being computationally more costly, will be more accurate with better detailed physics (Roberts et al., 2018). Today, a large number of Earth system models exist, such as the Community Earth system model (CESM) and the Norwegian Earth system model (NorESM) — developed in the United States and Norway, respectively.

ESMs enable us to improve our understanding of the physical, biological and chemical laws that govern our planet and to predict its future. They allow us to focus on specific features of the Earth system and explore climate sensitivities with experiments that would not be possible on the actual planet Earth (Stocker, 2011). Although there is some degree of disagreement between different Earth system models, and despite some approximations in their equations, models generally produce current and past large-scale results that agree with observations. Even if they do not agree with particular observations, they would be useful tools to test hypotheses and make assumptions about the reasons of disagreement. Improving the accuracy of climate model predictions involves continually completing and correcting the equations of the model and enhancing the resolution of model simulations.

As mentioned in the introduction, climate modelling is crucial to better understand processes underlying climate, motivate societal actions, mitigate changes and better equip society to climate-related risks. Since knowledge generated by climate models serves as scientific basis for decision and policymakers (Hewitt et al., 2021), it is essential to further improve those models, and particularly their land surface component as it is known to contribute most to uncertainty when running future climate projections (Fatichi et al., 2019).

2.4.1. Land surface modelling

The land surface is the habitat of most humans, terrestrial animals and plants, and its processes mediate a majority of the impacts of climate on human societies and ecosystems. The accurate

representation of land surface processes is critical for our understanding of how climate change affects living systems. Each ESM contains a land surface model (LSM) that represents the coupled exchanges of water, carbon and energy between the land surface and the atmosphere, within the context of ecological dynamics and human forcings. It has been argued that LSMs are the most sophisticated tools that society currently possesses to predict how living conditions will evolve on Earth in the coming years, decades, and centuries (Fisher & Koven, 2020, Fig. 6). Land surface modeling activities encompass numerous interconnected and overlapping disciplines.

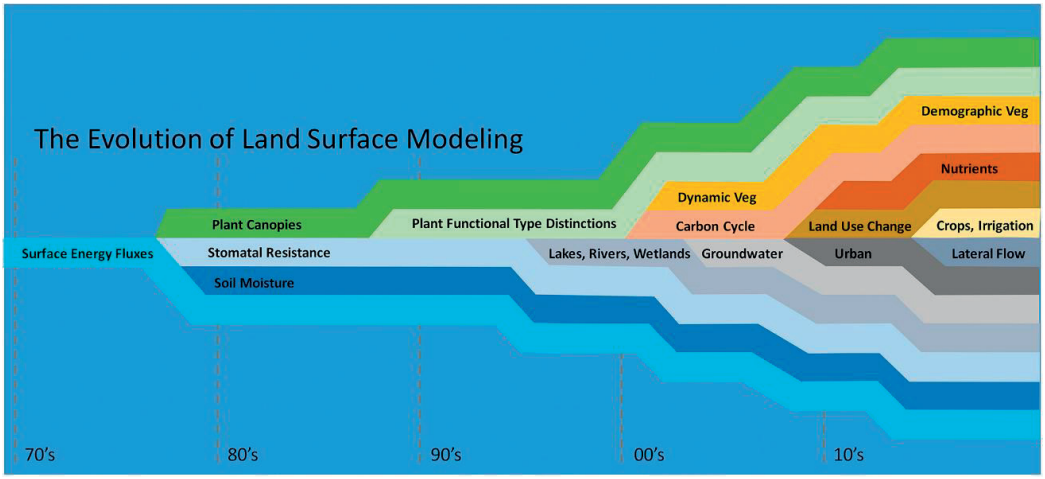

Figure 6: Schematic description of the evolution of land surface model process representation through time, representing the approximate timing of emergence of different model components as commonly employed features of Earth system models. Note that all modeling groups follow a different pathway and that this diagram is primarily intended to act as an illustration of increasing complexity through time. (From Fisher & Koven, 2020)

While LSMs typically provide a set of variables related to the feedbacks of land on global biogeochemical cycles, they also provide information on the risks to human societies and natural ecosystems related to future climate scenarios. Through time, LSMs have complexified and are increasingly called upon to represent how climate influences ecosystems, water resources, land use and land use change. They are additionally used to assess how the effects of climate on the biosphere feedback to the atmosphere through water, CO_2 and heat fluxes (Fisher et al., 2014). Representations of numerous processes known to impact dynamics of the system have been incrementally added to LSMs through time, driven by the needs of various user communities (e.g. hydrologists, ecologists and biogeochemists), and by arguments that the overall biospheric feedbacks are importantly affected by the added feature. Initially simple biophysical configurations (Sellers et al., 1986), some LSMs have now reached such a high complexity that no individual can comprehensively understand all facets of the model (Fisher & Koven, 2020).

Many processes are required to make long-term projections of the land surface, and their complexification has touched a set of different disciplines. The representation of biogeochemistry, for example, has evolved from a small set of equations required to represent photosynthesis at the leaf scale (Dickinson et al., 1991), through full carbon cycle models (Ostle et al., 2009), to models coupling several nutrient cycles (Fisher et al., 2019). Hydrology has proceeded from being represented by the simple bucket model (Manabe, 1969), through a 1-D Richards equation (Bonan, 1996), to a 3-D flow model that spans from soil to plant tissues (Bisht & Riley, 2019). The shift to represent agents of climate change has brought modelers to include microbial types and their population dynamics in soil biogeochemical models (Wieder et al., 2013). Missing in early land surface models, another major focus has been to represent the many effects humans have on

modifications of the land surface through anthropogenic disturbance (Yue et al., 2018). Further examples of process complexification include canopy radiative transfer, fire, permafrost, rivers and trace gases (Fisher & Koven, 2020).The representation of any specific process is extremely heterogeneous across models. While some models may represent a process in great detail, other models may completely neglect it. This often makes the comparison of model projections difficult or uninformative (Clark et al., 2011).

2.4.2. *Land surface modelling terminology*

While the term LSM is historically used to refer to the terrestrial component of an ESM, it is an uninformative descriptor of model capabilities. To describe the continuum of models representing ecosystem processes and their chemical, physical and biological behavior at relevant spatial and temporal scales, the term terrestrial biosphere model (TBM) is frequently used (Bonan, 2019; Fisher et al., 2014). TBMs encapsulate a large range of models including the ones focusing on biogeochemical pools and fluxes, those who focus on individual plants or size cohorts, those with emphasis on coupling leaf physiological processes with canopy physics, and the global models of the land surface (i.e. LSMs mentioned above) used to simulate climate. TBMs represent the intersection between the hydrosphere, atmosphere, geosphere and biosphere, and depending on the discipline and study interests, they depict the ecosystem in various ways (Bonan, 2019).

Biogeochemical models simulate the terrestrial carbon cycle given a geographic distribution of input biomass in the model (Berardi et al., 2020). In these models, the ecosystem is represented by aggregating litter, soil, root, stem and leaf carbon pools, and the flow between pools is described by allocation, primary production, and other physiological processes. Biogeochemical models represent the physical environment in a simplified manner and do not incorporate the variability among individual plants or plant functional groups. However, concurrent with carbon flows, nitrogen and other nutrient transfers are explicitly described.

In contrast to the compartment-based biogeochemical representation of the ecosystem, individual-based and gap models have their roots in the life cycle of species and depict the behaviour of the ecosystem as individual plants competing for resources and light. By simulating demographic processes such as competition, mortality and establishment, these models describe changes in community composition. To reduce the computational demands of individual-based models, ecosystem demography (ED) models represent similar dynamics but regroup plants of similar age and size into cohorts (Fisher et al., 2018; Hurtt et al., 1998; Moorcroft et al., 2001, Fig. 7). Another type of TBM, called dynamic global vegetation model (DGVM), also simulates changes in community composition at a cohort level, biomass and nutrient cycling (Prentice et al., 2007). DGVMs are applied globally and therefore employ plant functional types, typically distinguished by region (boreal, temperate or tropical), deciduous or evergreen leaf longevity, broadleaves or needleleaves, and woody or herbaceous biomass.

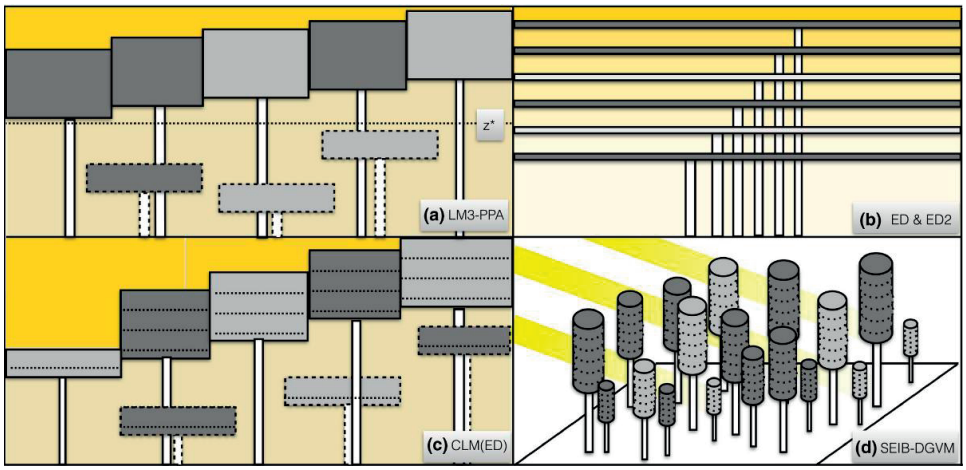

Figure 7: Organization of canopy schemes in four vegetation demographic models. Shades of yellow represent incident light levels. Shades of gray indicate alternative PFTs. Boxes represent cohorts as represented by: a) LM3-PPA, b) ED & ED2 and c) CLM(ED). Dotted cohort boundaries denote cohorts that belong to the understory. In the cohort-based schemes, horizontal positioning is for illustrative purposes only and not represented by the model, which is one-dimensional. Dotted lines in the CLM(ED) figure illustrate within-canopy leaf levels resolved by the radiation transfer scheme. In the LM3-PPA, "z" indicates the cohort height above which canopy/understory status is defined. In the CLM(ED), there is no "z*" threshold, and larger cohorts in the understory may in principle be taller than the shorter cohorts in the canopy layer (reflecting imperfect competition processes, per Fisher et al., 2010). Note that for ED-derived models (ED, ED2, CLM(ED)), cohort organization is illustrated only for a single patch, though each model represents a multitude of patches having different ages since disturbance within a single site. The SEIB-DGVM (Spatially-Explicit Individual-Based Dynamic Global Vegetation Model, http://seib-dgvm.com) is an individual based model, representing variability in light in both the vertical and horizontal dimensions. (From Fisher et al., 2018)*

With the diversification and complexification of TBMs, most LSMs have been coupled to a DGVM or a biogeochemical model to simulate detailed ecosystem dynamics and their influence on the global nutrient cycles, and feedbacks on the atmosphere and other components of the Earth system. In LSMs with a DGVM, energy, water, momentum and CO_2 are exchanged between land and atmosphere though physiological, hydrological, physical and biogeochemical processes over short timescales (minutes to hours). The timing of phenological features such as budburst, senescence, leaf abscission and germination in response to weather conditions occur over periods of days to weeks. Changes in soil carbon community composition and biomass take several years in response to primary productivity, respiration, mortality and the allocation of primary production to grow roots, stem and leaves. The growth and survival of PFTs depends on specific traits such as the tolerance to cold, the threshold for water stress, and the efficiency of photosynthesis (Bonan, 2019).

2.4.3. *Phenology and frost mortality modelling*

Phenology models simulate phenology, i.e., timing of seasonal events such as germination, budburst and flowering. LSMs are equipped with a phenology model to predict the timing of leaf onset, leaf abscission and sometimes also germination or other phenological events. Phenology is a crucial component of LSMs as it controls many feedbacks of vegetation to the climate system (Richardson et al., 2013). In particular, the timing and length of the growing season has large influences on the seasonality of albedo, canopy conductance, and fluxes of CO_2, water and energy (Keenan et al., 2014;

Richardson et al., 2010). However, current approaches to model spring and autumn phenology in LSMs are simplified parametrization which contain large uncertainties (Keenan et al., 2012; Richardson et al., 2012). Without enough emphasis on accurately modelling vegetation phenology, many of the important feedbacks vegetation has on the climate system are likely to be misrepresented.

Although variations exist among LSMs, the moment of leaf onset of each deciduous PFT is typically predicted by applying a warmth and moisture stress criteria to the weather forcing conditions of the past days, weeks or months (Krinner et al., 2005). In most LSMs, day length (photoperiod) is not considered, despite observational proofs of its potential importance in predicting the timing of leaf onset (Nizinski & Saugier, 1988). The calculation of leaf onset usually involves the calculation of the number of growing degree days over a given period, i.e. budburst when the temperature sum accumulation gets above a threshold value, modelled as a linear or logistic function. For some PFTs, the number of chilling degree days (days with mean temperature below a threshold) during the winter season may also be accounted for (Hänninen, 1995; Murray et al., 1989) and for drought-sensitive PFTs, the start of the growing season may depend on the minimum available moisture. When leaves appear, some of the carbohydrate reserves stored in plants (accumulated during the previous summer) are removed in compensation (Arora & Boer, 2005). If the storage pools are empty, due to large respiration rates during extended winters or other excessive winter metabolic activities, leaf onset cannot occur and the PFT will undergo strong mortality rates, leading to extinction (FATES Development Team, 2018). Senescence or leaf abscission also depends on the meteorological criterion of temperature and water stress (Sitch et al., 2003). For example, some PFTs might shed their leaves after temperatures have fallen below a threshold for a given period of time (Sitch et al., 2003). Similarly, if the carbohydrate pools are empty, total leaf abscission leads to death. In some LSMs, the age of leaves itself is involved in the fraction that is shed (Krinner et al., 2005). When the leaves are young, small fractions are shed, while as a critical leaf age is approached, the abscised fraction strongly increases.

A challenge faced by ecosystem-scale phenology models emerges from the aggregation into plant functional groups of unique reaction strategies of species to environmental cues. It is difficult to aggregate the responses into a single model when it comes to selecting the temperature thresholds above or below which chilling and growing degree-days take place, the temperature data to use (e.g. daily mean, minimum, maximum or other timesteps), and the critical status of chilling and growing degree-days. Despite the difficulty to develop robust and accurate phenology models at ecosystem scales, recent phenology data and advances in measuring methods pave the way for further improving phenology models as critical components of LSMs (Basler, 2016).

Beyond the capacity of phenological models to predict leaf onset and abscission, they can also be applied to estimate the risk of frost (Augspurger, 2013; Leinonen et al., 1997). Specific phenological phases differ in their sensitivity to frost, meaning that the developmental stage of a species at the time of frost affects the extent of frost damage (Hänninen, 2006; Kreyling et al., 2012). In general, plants are more vulnerable during reproductive than vegetative phases (when growth happens) (Sakai & Larcher, 1987). Despite the existence of several schemes predicting phenology-dependent frost mortality (Ferguson et al., 2011; Hänninen, 2006), phenology is generally not involved in the calculation of frost mortality of LSMs.

While the impact of freezing on photosynthesis is usually represented in LSMs, the effect of freezing on vegetation mortality is absent in most LSMs. Still, in most DGVMs, a fixed temperature threshold is typically used to predict the rate of frost mortality (Albani et al., 2006; Krinner et al., 2005). Fixed freezing tolerance temperature thresholds generally differ among PFTs, and hence predict the distribution of PFTs across the tropical, temperate and boreal regions, but they generally do not simulate frost damage to PFTs adapted to these climatic regions. In this context, a boreal or arctic PFT, which is assigned a tolerance threshold of −80°C won't incur freezing injury as long as

surface/vegetation (depending on the model) temperatures remain above −80°C. In other words, such a PFT is unlikely to be damaged by freezing anywhere on Earth. On the other hand, a tropical PFT with a tolerance threshold of −2°C, will be limited to regions where temperatures rarely (if ever) get below −2°C and is therefore unlikely to thrive in temperate regions and beyond.

2.4.4. *Modelling plant hydraulics and drought*

While several approaches exist to model plant hydraulics in LSMs, all rely on Darcy's law, whether they do so for the soil domain only or for the soil-plant continuum (Darcy, 1856). Following Darcy's law, the movement of water from one place to another is dictated by the gradient of water potential and the hydraulic conductivity between these two places. To respond to drought situations, hydraulic conductivity within the soil-plant continuum of LSMs must somehow be able to react to dryness. Current LSMs generally adopt one of three approaches to represent moisture stress and its impacts on plant hydraulic conductivities (Christoffersen et al., 2016).

Until recently, most LSMs used the soil moisture stress (SMS) parametrization to regulate vegetation transpiration and photosynthesis as a function of variations in water availability (Egea et al., 2011; Verhoef & Egea, 2014). In SMS, stomatal conductance is directly related to an empirical metric of soil moisture as xylem hydraulic conductances are not represented. While this simple approach has proven useful (Fisher et al., 2007; Williams et al., 1998), it has also been shown to perform poorly due to the misattribution of droughts within trees to the soil (Powell et al., 2013), systematically overestimating the effects of soil moisture on transpiration (Bonan et al., 2014; Ukkola et al., 2016).

In another approach, xylem water potential and variable xylem conductivities are tracked (Duursma & Medlyn, 2012; Williams et al., 2001; Xu et al., 2016). To reduce computational need, dynamic changes in the volume of plant water storage are represented by a constant ratio proportional to the change in water potential (Kennedy et al., 2019). Under strong droughts, this simplification may however overestimate the buffering capacity of plant-stored water when small declines in stored water induce large reductions in water potential. Another disadvantage of these models is the inability to represent reverse flow of water at the root-soil interface. Root water release is a well-known and impactful process which intervenes in hydraulic redistribution (Nadezhdina et al., 2010; Oliveira et al., 2005; Prieto et al., 2012), and may play a role in the mediation of desiccation under water stress (North & Nobel, 1997).

To address these issues, a third approach extends the modelled mass balance of water from the soil domain to the plant by linking changes in water content to changes in water potential everywhere in the soil-plant-atmosphere continuum (Christoffersen et al., 2016; Edwards et al., 1986; Mirfenderesgi et al., 2016; Sperry et al., 1998). Although more computationally expensive, in addition to addressing water storage and bidirectional flow, this approach offers the advantage of representing the soil-plant system by a single mass balance equation such that plant water uptake and loss simply emerge from the solution of this equation. In addition, similarly to the water retention curves used in soil physics, the model relies on a description of the relationship between the potential and content of plant water (the pressure-volume, PV curves). The use of PV curves corresponding to plant organs increases the number of complex parameters that must be specified (e.g. hydraulic traits for leaves and stems (Christoffersen et al., 2016; Sperry et al., 2017; Xu et al., 2016). While models increasingly become more capable in representing the complex reality of nature, it also becomes possible to apply these models to new scientific questions, such as what drives the greening and browning of vegetation in cold regions.

3. Methods

In this thesis, we used and further developed the CLM5-FATES model, where CLM5 (Lawrence et al., 2019) is the LSM of both the Community Earth System Model and Norwegian Earth system model (Seland et al., 2020) (Danabasoglu et al., 2020). FATES (Fisher et al., 2010; Fisher et al., 2015; Koven, 2019) is a demographic vegetation model hosted by CLM5. Paper I implements a hardening scheme in CLM5-FATES, which is based on the work of Rammig et al. (2010) and aims at better representing winter hydraulics during cold hardening. Paper II updates the formulation of frost mortality in FATES by involving a hardiness parameter into its calculation. Then, in contrast to the two other papers, Paper III does not involve model development in itself. In Paper III, the developments made in Paper I (i.e. coupling between hardening and hydraulics of plants) are used to study and assess the capacity of CLM5-FATES (with Hydro) to predict processes of winter droughts during an extreme year in Northern Norway.

Note that Paper I and Paper III focus on plant hydraulics. Therefore, the experimental hydraulic scheme (i.e. Hydro — unique water balance equation to represent water potentials and fluxes throughout the whole soil-plant continuum) of FATES was turned on in those two papers but not in paper II.

In the following sections, we describe (a) the CLM5-FATES model used in Paper I, II and III, (b) the complex hydraulic scheme of FATES used in Paper I and III, (c) the original hardening scheme of Rammig et al. (2010) before it was adapted to successfully integrate into FATES at the ecosystem and global scales, and (d) the atmospheric datasets used as forcing in our simulations (i.e. different for each paper). Note that the information about the tools (models and datasets) given in the next sections is only a brief overview as more detail is included in each of the papers and available in cited literature.

3.1. Models

3.1.1. Introduction to CLM5-FATES

The main tool of this thesis is the CLM5-FATES model, which was used in each paper and further developed in two of them. CLM5.0-FATES stands for the fifth version of the Community Land Model, coupled to the Functionally Assembled Ecosystem Simulator (FATES). In this context, CLM5.0 represents the biogeophysical aspects of the land surface, including energy balance, soil hydrology, biophysics and cryospheric processes, as well as soil biogeochemistry and other land surface types (lakes, urban, glaciers, crops) (Lawrence et al., 2019). FATES (Fisher et al., 2015; Koven, 2019) is a cohort-based vegetation demographic model integrated into CLM5.0 to represent vegetation processes and dynamics while tracking the vertical (in terms of plant height), spatial (in terms of successional age) and biological (in terms of plant functional type) heterogeneity of terrestrial ecosystems. When coupled to the CLM, FATES handles all processes related to live vegetation (inclusive of photosynthesis, stomatal conductance, respiration, growth, and plant recruitment and mortality) as well as fire and litter dynamics.

CLM has expanded and seen considerable developments over the last decades into a comprehensive platform for researchers to study weather, climate change and climate variability in response to terrestrial contributions. For example, the soil moisture stress (SMS) plant hydraulic theory of CLM has recently been replaced with a more complex approach called plant hydraulic stress (PHS),

introducing vegetation water potential modelled at the root, stem and leaf levels (Kennedy et al., 2019). In PHS, leaf water potential, instead of a soil metric, is the basis for stomatal conductance, and root water potential drives root water uptake instead of a transpiration partitioning function.

3.1.2. *Mortality in CLM-FATES*

Despite the fast development of CLM, the parameterization of vegetation mortality remains oversimplified. Plant mortality is assumed to be equivalent to 2% of individuals per year and is intended to represent the aggregate of processes such as insect attack, disease, wind throw, extreme temperatures, drought, and age-related decline in vigor (UCAR, 2020). Vegetation mortality is an important process, and although literature values of forest mortality rates indeed range from 0.7% to 3% of individuals per year, additional work is urgently required to better constrain this process in different climatic zones (Keller et al., 2004), for different species mixtures (Gomes et al., 2003) and for different size and age classes (Law et al., 2003). In CLM, all vegetation carbon and nitrogen pools are affected at a specific rate (fraction of the 2%) at each model timestep, and fluxes out of vegetation pools are deposited into litter pools.

In CLM-FATES, the simple parametrization of mortality of CLM is overwritten by the more complex set of mortality processes of FATES. In FATES, the total mortality is calculated as the sum of the background, carbon starvation, hydraulic failure, freezing, fire, disturbance impact and logging mortalities. The background (fixed at 1.4%), fire, logging and disturbance mortalities are not especially relevant to this thesis, but the hydraulic failure, freezing and carbon starvation mortality all take place during extreme winter events, or warm and cold winter pulses.

3.1.2.1. *Freezing mortality in FATES*

Freezing mortality in FATES is experienced when the daily mean vegetation temperature within a grid cell drops below the freezing tolerance temperature threshold of a PFT. The rate at which a PFT dies during a frost event is proportional to the difference between the vegetation temperature and the freezing tolerance threshold. In a cohort-based model, mortality is a based on a predictor variable, not a discrete event (as it might be in an individual-based model or in the real world). Thus, a scaling coefficient is required to generate cohort-wide loss of individuals from the freezing status predictor (Fisher et al. 2010). For freezing mortality, the delta is multiplied by a scalar which is set to 3.0 by default for all PFTs. Finally, a 5°C buffer is used, so that mortality starts at 0 % of individuals per year when vegetation temperature is 5°C above the tolerance threshold, and mortality linearly increases to 300 % of individuals per year as vegetation temperature approaches the freezing tolerance threshold. Whenever vegetation temperature is equal or below the tolerance threshold, mortality remains at 300 % of individuals per year. More information about the parametrization of frost mortality can be found in Albani et al. (2006), and the measurements of threshold temperatures for cold tolerance are reported in Sakai & Weiser (1973).

3.1.2.2. *Carbon starvation mortality in FATES*

In FATES, carbon starvation mortality (CS in % of individuals/year) is a function of the carbon storage (Cstor), leaf target storage (LTstor), and the maximum rate of trees in a landscape that will die when their carbon stores are exhausted (MaxCS). FATES implicitly assumes that there is a critical storage where mortality begins. Stored carbon is used for maintenance respiration. During maintained negative carbon balance, trees reduce maintenance respiration, but as a tradeoff experience carbon starvation. Due to the physiological basis for this process, heuristic functions are used to define carbon starvation. The target carbon storage (TCstor) pool is linearly related to the leaf target biomass

(LTstor) through a PFT-specific parameter. When plants can't achieve the TCstor because of a negative NPP, then the actual carbon storage (Cstor) pool will drop below TCstor.

$$CS = \begin{cases} MaxCS * \left(1 - \left(\frac{Cstor}{LTstor}\right)\right), if\ Cstor < LTstor \\ 0 \qquad\qquad\qquad\qquad , if\ Cstorage \geq Lstorage \end{cases} \qquad \text{(Eq. 1.1)}$$

3.1.2.3. Hydraulic failure mortality in FATES (without Hydro)

Due to its mechanistic complexity, a proxy is used to calculate hydraulic failure mortality in FATES. In the default FATES model, hydraulic failure mortality is triggered when the soil water potential falls below a PFT-dependent threshold value, such that the tolerance of low water potentials is a function of plant functional type. The threshold (10^{-6}) represents a state where the aggregation of soil moisture potential across the root zone is within 10^{-6} of the wilting point.

3.1.2.4. FATES-Hydro and hydraulic failure mortality

Hydro is a trait-based plant hydraulic model implemented in FATES as an option, and originally developed by Christoffersen et al. (2016). It follows the continuous porous media approach (Mirfenderesgi et al., 2016; Prévost, 1980), is based on a single mass balance equation to describe the coupled soil-plant system, and the relationship between plant water storage and plant water potential is explicitly expressed. Hydro consists of a discretization of the soil-plant-atmosphere continuum (SPAC) in a series of water storage compartments with variable heights, volumes, water retention and conducting properties. Tree and shrub PFTs are divided in 4 types of porous mediums (leaf, stem, transporting and absorbing roots). Each above-ground plant medium consists of a single storage pool, while roots are divided in vertical compartments by soil layer. The water pools are connected by pathways with defined lengths and conductances. The soil is divided in cylindrical "shells" around the absorbing roots (the rhizosphere), and hydraulic properties are constant across compartments within a given soil type.

The hydraulics in this scheme are governed by three main relationships: the relation between (1) water content and potential (pressure-volume or PV theory), (2) water potential and conductivity of plant tissues (P-K curve) and (3) leaf water potential and stomatal water stress factor. The first two relationships concern every pool within the plant–soil continuum and have specific equations for plant and soil porous media types. For the soil, the formulation of Clapp-Hornberger and Campbell describes the first two relationships (Campbell, 1974; Clapp & Hornberger, 1978). For the plant, the first relationship (PV curve) is described by two terms: a) the solute potential (<0 due to the presence of solutes), and b) the pressure potential (>=0 due to cell wall pressure) (Ding et al., 2014; Tyree & Hammel, 1972). The second relationship (linking plant water potential and conductivity) is calculated using the inverse polynomial of Manzoni et al. (2013) for the xylem vulnerability curve. The fraction loss of total conductance retrieved from this equation is defined at each compartment boundary and is used to calculate the maximum conductance of plant organs. The fraction of maximum stomatal conductance is then used to downregulate the non-water stressed stomatal conductance (calculated using Ball-Berry (1987) formulations). All parameters involved in these three relationships are biologically interpretable and measurable plant hydraulic traits. The numerical solution operates every half hour and updates water contents and potentials throughout the SPAC.

In contrast to the default FATES, in FATES-Hydro, hydraulic failure mortality (HFM) is based on the fraction loss of total conductance (*flc*) of plant tissues, a fixed threshold (*flcThreshold*) and a scalar to define the amplitude of mortality (Eq. 1.2). The default value for *flcThrshold* is 0.5 and for *MortScalar* 0.6. At each timestep, a value of *flc* is predicted for each plant organ (stem, leaf absorbing root and conducting root) depending on the water potential of organs. HFM is predicted when *flc*

becomes larger than *flcThreshold* and linearly increases until the maximum value of *flc*, which is 1. Although *flc* is predicted for each plant organ, the HFM of a PFT only accounts for the organ that shows the lowest *flc*.

$$HFM = \frac{flc - flcThreshold}{1 - flcThreshold} * MortScalar \qquad \text{(Eq. 1.2)}$$

3.1.3. *The hardening scheme*

The hardening model used in this study is based on the work by Rammig et al. (2010). In their model, the hardiness level (*HD*) is calculated on a daily basis using three functions: the target hardiness (*TH*), the hardening rate (*HR*), and the dehardening rate (*DR*) (Fig. 8).

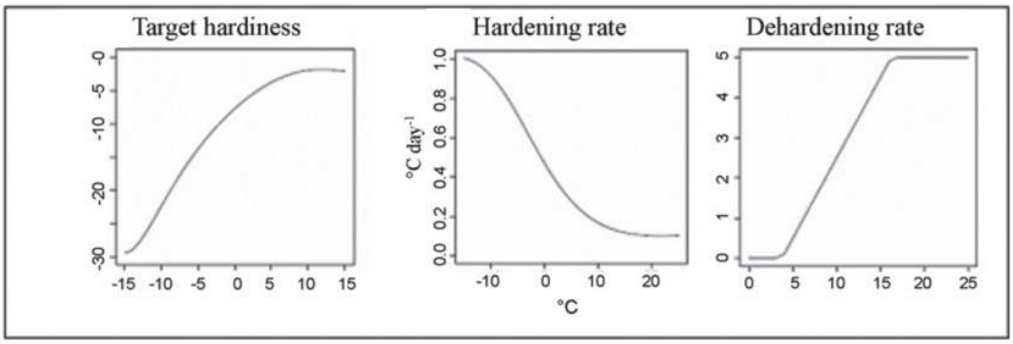

Figure 8: (a) the target hardiness (TH in °C), (b) the hardening rate (HR), and (c) the dehardening rate (DR) functions (in °C day−1) in relation to the ambient mean temperature corresponding to Norway Spruce in Farstanäs, Sweden (Rammig et al., 2010).

The scheme of Rammig et al. (2010) was conceived to fit the climate of central Sweden (Farstanäs) and measurements of Norway spruce (*Picea Abies*). The parameters required in the model of Rammig et al. (2010) are: the minimum hardiness level (H_{MIN}); −2°C, the maximum hardiness level (H_{MAX}); −30°C, *HR*; 0.1-1°C/day, *DR*; 0-5°C/day and several time dependent parameters used to define the seasons for hardening and dehardening. Parameters for the hardening scheme were retrieved from Kellomaki et al. (1995), Jönsson et al. (2004) and Bigras & Colombo (2013).

After a value has been assigned to *TH*, *HR* and *DR*, depending on the daily mean 2m air temperature, the model operates as follows: if *TH* is lower than the hardiness of the previous day (*HDP*), then *HR* is subtracted from *HDP*. By contrast, if *TH* is higher than *HDP*, then *DR* is added to *HDP* (Eq. 1.3).

$$\begin{cases} HD = HDP - HR & , \ if \ HDP > TH \\ HD = HDP + DR & , \ if \ HDP \leq TH \end{cases} \qquad \text{(Eq. 1.3)}$$

During winter (defined as Julian days 260 to 365), only hardening is possible, and to avoid mid-summer hardening, hardening is not possible before the start of autumn, and initiated when the 210th Julian day is passed and an accumulated degree day variable (*aggd5*, Eq. 1.4) exceeds 120°C (day of budburst in central Sweden (Hannerz, 1994)). During springtime, when the other conditions are not fulfilled, both hardening and dehardening are possible.

$$aggd5 = aggd5 + \max(0, Tmean - 5°C) \qquad \text{(Eq. 1.4)}$$

3.1.4. *Implementing the hardening scheme into CLM-FATES*

To make the hardening scheme of Rammig et al. (2010) applicable globally in CLM-FATES, we made H_{MAX} dependent on the temperature of a grid cell (*T5*) and on the freezing tolerance parameter of a PFT (*PFTFreezetol*). *T5* is the 5-year running mean of the minimum yearly temperature, and it is unique to each gridcell. *PFTFreezetol* is equal to 1.5°C for the least frost tolerant PFTs and goes down to −80°C for the most frost tolerant PFTs. In the control FATES model, *PFTFreezetol* serves to calculate freezing mortality, which takes place as soon as the temperature of vegetation gets below *PFTFreezetol*. Similar to the freezing mortality approach of the control FATES, in the hardening frost scheme, FR_{MORT} is the actual frost mortality in % of individuals/year, *FrostBuffer* is set to 5°C and *PFTcoldstress* equals 3% of individuals/year (Eq. 1.6). In contrast to the control FATES, *PFTFreezetol* only serves to calculate H_{MAX} and it is the minimum daily atmospheric temperature (T_{MIN}) and the hardiness level (*HD*) that are used to predict frost mortality (Fig. 10), as in Rammig et al. (2010).

$$H_{MAX} = \min(\max(PFTFreezetol, \max(T5, -60) - 10), H_{MIN}) \quad \text{(Eq. 1.5)}$$

$$FRmort = PFTcoldstress * \max\left(0, \min\left(1, \frac{-T_{MIN} + Hd}{FrostBuffer}\right)\right) \quad \text{(Eq. 1.6)}$$

As the H_{MAX} was made variable in time and space, the functions of *TH*, *HR* and *DR* (Fig. 8) had to be adapted accordingly. A low H_{MAX} would require a faster hardening and dehardening while a high H_{MAX} means the PFT can take more time to harden and deharden. The functions of *TH*, *HR* and *DR* were therefore made dependent on H_{MAX} itself. This, however, did not prevent the three functions to remain similar to those of Rammig et al. (2010) in Sweden for a PFT with a H_{MAX} of −30°C.

The use of Julian days to define the period where (i) hardening is not possible, (ii) only hardening is possible and (iii) both hardening and dehardening are possible, only works for central Sweden, where the specific Julian days correspond to phenological stages of Norway spruce. We removed the use of Julian days as time dependent parameters of the hardening scheme. Instead, we introduce a daylength threshold in seconds (*DaylThresh*, Eq. 1.7). *DaylThresh* depends on the yearly minimum temperature of the location (*T5*). When the daylength of a gridcell gets below *DaylThresh*, the hardening period starts, and dehardening is not allowed until days start getting longer again. This is important as it enables high latitude sites to start hardening at a longer daylength than at lower latitudes.

$$DaylThresh = 42000 + ((-30 - max(-60, min(0, T5)))/15) * 4500 \quad \text{(Eq. 1.7)}$$

Equation 1.7 is illustrated in figure 9 by three of the locations we used in paper II. At Spasskaya Pad, for example, T5 is approximately −65°C and corresponds to a *DaylThresh* of roughly 14 hours, which is the daylength obtained from the 3rd of September onwards and defines the start of the hardening period.

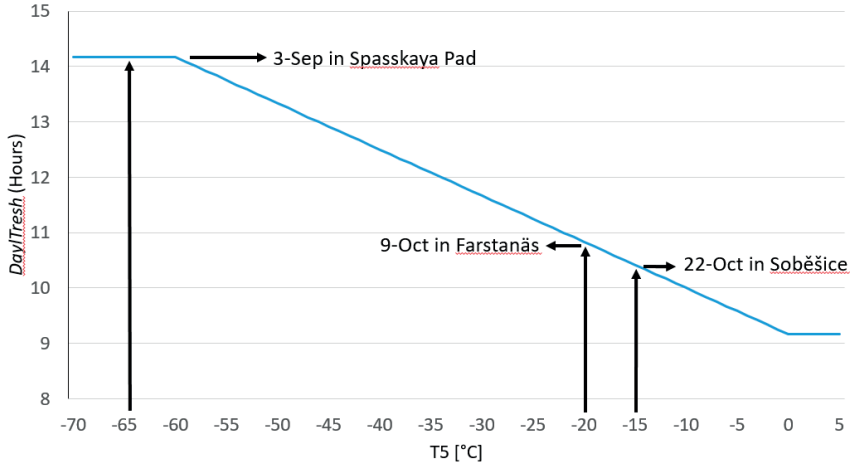

Figure 9: DaylTresh in hours as a function of T5 with corresponding day of the year for approximated values of T5 at the sites of Spasskaya Pad (Siberia), Farstanäs (Sweden) and Soběšice (Czech Republic).

In addition to mediating the occurrence of frost mortality, we used the 'hardening' state to simulate the impact of hardening on the hydraulic functioning of the plant, both in terms of the benefits of hardening (i.e. prevention of desiccation) and the physiological costs (reduced ability to conduct water and photosynthesize during the hardening and dehardening phases). We did this by modifying the maximum conductance between plant compartments (K_{MAX}), the intercept and slope of the stomatal model (*g0* & *g1)* and the hydraulic failure mortality scalar (Eq. 1.2) (Fig. 10). We then explore additional configurations of the scheme where hardening of plants led to changing PV curves, and a reduction of the carbon starvation mortality.

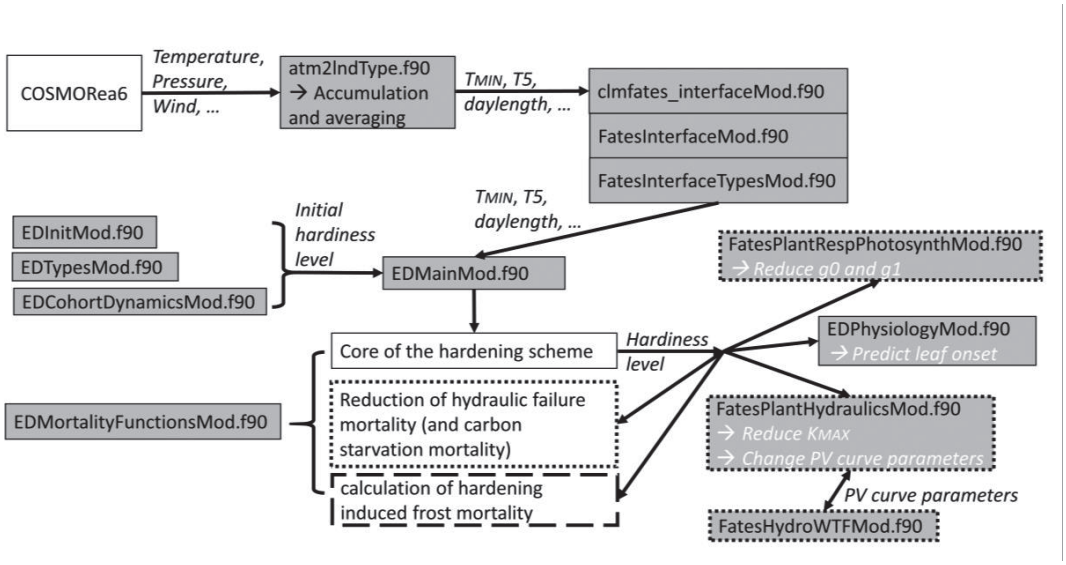

Figure 10: Diagram showing some of the major modifications made in CLM-FATES in order to represent the effects of hardening. Gray boxes represent the files of the model. In italics are written the variables that are passed from one file to another. Dotted boxes represent the developments that are unique to the hydraulic effects of hardening, while the dashed boxes are unique to the frost mortality effects of hardening.

Finally, the hardening schemes offers the opportunity to take the hardiness level of deciduous species into consideration when predicting the timing of leaf appearance in spring (Fig. 10 and Paper III) or shed in autumn (not tested in this thesis). In Paper III, we coupled the hardening scheme to the phenology of deciduous PFTs by allowing leaves to appear only after a PFT had dehardened by 50% of its maximum hardiness level (Fig. S2 of paper III). In the absence of coupling between hardening and leaf appearance, plants tended to still be in a hardy state at the time of leaf appearance, leading to a lack of stored carbon to safely trigger leaf onset.

More details about these adaptations of the hardening scheme are provided in the papers included in this thesis.

3.2. Atmospheric forcing datasets

All papers in this thesis involve offline land surface modelling, and hence, rely on atmospheric reanalysis data to control the boundary conditions of the land surface simulations. Without the constraint of the atmospheric forcing, variable estimates of land surface models can rapidly deviate from reality. Reanalyses consist of a blend of observational data and past short-range weather forecasts reprocessed over an extended historical period using a modern data assimilation system. Reanalyses strive to produce time-consistent datasets that can be used for meteorological and climatological studies. The most important reanalysis variables required as an input to the CLM model are surface temperature, precipitation (sometimes partitioned in rain and snow), pressure at sea level, wind speed, relative humidity, downward solar radiation, downward longwave radiation and observational height. Depending on the availability of variables, specific humidity or dew point temperature can be substituted to the relative humidity in CLM. Among the multitude of atmospheric reanalysis systems, some may give considerably different results for the same variable due to technical dissimilarities (model characteristics, horizontal and vertical resolution, physical parameterizations, assimilation scheme, etc.) or assimilated observation data (Fujiwara et al., 2017). The choice of a reanalysis dataset for a specific study depends on the performance of the reanalysis system in the studied area, the covered period, and the time and spatial resolutions of the gridded forcing data. In the following sub-sections, we shortly describe the ERA5-Land, GSWP3 and COSMO-REA6 reanalyses used for Papers I, II and III respectively.

3.2.1. *ERA5-Land*

The atmospheric forcing used to drive the simulations of Paper I was derived from ERA5-Land (ERA5L) (Sabater, 2019). ERA5L provides hourly global high resolution (9km) information on surface variables from January 1951 to present day, which makes it a valuable dataset for analysing the implementation of the hardening scheme into CLM5-FATES. We retrieved temperature at reference height, wind, humidity, surface pressure, precipitation, downward shortwave radiation, and downward longwave radiation at a 3-hourly resolution for the entire period. The high temporal and spatial resolutions of ERA5L makes this dataset very useful for all kinds of land surface applications such as flood or drought forecasting (Sabater, 2019). ERA5L was preferred to other reanalyses due to the accurate snow depths at the modelled locations of Paper I (i.e. inland Sweden and Siberia). The snow depth appeared to be a major driver of processes (e.g. plant hydraulics, vegetation growth, etc.) relevant to the implementation of the hardening scheme.

3.2.2. *GSWP3*

In Paper II, the atmospheric forcing to execute simulations was extracted from the Global Soil Wetness Project 3 version 1 (GSWP3v1) dataset (Dirmeyer et al., 2006). GSWP3v1 is a 3 hourly-resolution observed climate dataset on a global 0.5°×0.5° grid. The data set covers the period 1901 to 2015, which makes it a valuable dataset for assessing the evolution of frost events throughout the 20th century and beyond. For our study, we retrieved near-surface specific humidity, daily mean temperature, near-surface wind magnitude, downwelling longwave radiation, total precipitation, shortwave downwelling radiation and surface air pressure from 1921 to 2015. The main drawback of using GSWP3 in Paper II is that the coarse spatial resolution may underestimate the occurrence and magnitude of frost events through the smoothing of temperature extremes. We also found that CLM5-FATES forced by GSWP3 yielded larger snow depths than observations or other reanalysis (e.g. ERA5L) at some sites (e.g. Spasskaya Pad in Siberia). However, the accuracy of the snowpack was not particularly relevant to this specific study on frost mortality and the benefit of having a long timeseries enabled more robust conclusions on long-term patterns.

3.2.3. *COSMO-REA6*

The atmospheric forcing to drive the simulations of Paper III was derived from COSMO-REA6 (Bollmeyer et al., 2015). COSMO-REA6 provides hourly information at high resolution (6.2km) on surface variables from 1995 to August 2019 over Europe. The retrieved variables were temperature at reference height, wind, humidity, surface pressure, precipitation, downward shortwave radiation and downward longwave radiation for the entire period. In Paper III, the large scale frost drought event in the winter of 2013-2014 was analysed at several sites along the northern Norwegian coast for deciduous and evergreen shrubs. Modelling accurate snow depths was therefore of major importance. Although CLM5.0-FATES-Hydro driven by COSMO-REA6 overestimated snow depths at the coastal Norwegian sites of Paper III, COSMO-REA6 was preferred to ERA5-Land since this last one performed even worse at those sites. To reduce the snow depth bias of the model forced by COSMO-REA6 and observations of nearby weather stations, we shifted boundaries of the linear repartitioning of rain and snow (originally 0°C and 2°C) to −1°C (only snow below this limit) and 1°C (only rain above this limit). This shift, greatly improved the quality of the modelled snow depth at the sites, and made COSMO-REA6 a valuable dataset for the frost drought analysis (Fig. 1 and 3 of paper III).

4. Presentation of findings

4.1. Paper I: Inclusion of a cold hardening scheme to represent frost tolerance is essential to model realistic plant hydraulics in the Arctic-Boreal Zone in CLM5.0-FATES-Hydro.

Objectives

- Implement a hardening scheme based on the work from Rammig et al. (2010) into the ecosystem simulator (FATES) hosted in CTSM5.0.
- Adapt the scheme to make it performant in all climates/locations.
- Implement constraints of hardiness on plant hydraulic variables during winter in order to mimic the impacts of cold acclimation on plant hydraulics in the field.
- Assess the effects of hardiness on transpiration, root water fluxes, mortality, and vegetation productivity, and examine the sensitivity of variables and parameters involved in the hardening scheme.

Summary

FATES was recently improved with a new plant hydraulic scheme based on the porous media approach, which was initially developed for tropical locations. This means that the physiology of plant hydraulics in winter is lacking some important processes. In the default scheme, for example, stored plant water remains liquid even when temperature drops below zero. Thus, if soils freeze in winter, large water potential gradients between plants and soil can lead to root water release, desiccation, and ultimately death. To prevent excessive mid-winter root water loss, we propose a hydro-hardening scheme adapted for use within the context of plant hydrodynamic simulations, which can simulate the physiological costs and benefits of plant cold acclimation in terms of water movement and gas exchange. The hydro-hardening scheme is configured such that plants reduce conductances along the soil-plant-atmosphere continuum and the rate for hydraulic failure mortality. We explore additional configurations of the scheme where hardening of plants leads to changing pressure volume curves, and a reduction of carbon starvation mortality. The impact of the scheme on plant hydraulics, vegetation mortality and growth appears to be a promising improvement for the modelling of vegetation growth in cold environments. In this study, we present one parameterization of the hardening scheme, show how it performs at two sites with contrasting winter weather, and investigate the response of the scheme to variations of its key parameters (i.e. maximum hardiness level and temperature range for dehardening).

Main findings

- The hydraulic changes prescribed by the hardening scheme lead to more realistic vegetation biomass productivity at temperate and boreal sites. With the hardening scheme turned on, plants are able to grow at locations where the default FATES-Hydro model would not allow vegetation.
- By lowering plant conductance with hardening, we reduce mid-winter root water release and thereby notably prevent maximum and maintained mortality rates throughout the cold season.
- From our scheme emerges that hardening comes at a cost for photosynthesis (trade-off). In the experiments with an earlier dehardening or a higher maximum hardiness (closer to −2°C), for example, plant water fluxes are larger during winter and spring, enabling larger photosynthesis but also a higher risk for desiccation through roots if soils freeze.

Main conclusion

In this paper, we provide new insights into the modelling of plant hydraulics and their link to cold acclimation. The inclusion of cold hardiness is essential to model realistic plant hydraulics and vegetation dynamics in cold climates. Our work lays the foundation to use a hardening scheme to regulate frost damage and to study the link between different types of mortalities in terrestrial biosphere models in the arctic region.

4.2. Paper II: Integration of a frost mortality scheme into the demographic vegetation model FATES

Objectives

- Make the hardiness level of plants dependent on their capacity to acclimate to cold, so that the hardiness is not only location (grid-cell) dependent anymore, but also plant functional type dependent.
- Implement hardiness-dependent frost mortality into CLM5.0-FATES to study the impacts of frost on different vegetation types in temperate and boreal sites from 1950 to 2015.

Summary

Freezing is a major environmental stress, limiting the distribution of plants and causing large economic losses. To avoid this stress, temperate and boreal plants, through hardening, developed the ability to cope with low seasonal temperatures. Frost mortality typically takes place at northern latitudes following warm pulses and abrupt transitions from summer-like temperatures to typical winter conditions. During such events, the hardiness level of plants can be dramatically disturbed so that vegetation does not tolerate the return to freezing temperatures. In most land surface models, frost mortality is poorly represented or completely absent. In the FATES module of the Community Land Model (CLM), climate envelopes are represented by assigning a minimum temperature (between 2.5°C and –80°C) to each plant functional type. These thresholds determine which temperatures a plant can tolerate, so that plants with a freezing tolerance of 2.5°C are unlikely to survive in temperate and boreal regions, while plants that tolerate -80°C may never incur injury. In reality, the ability to withstand frost varies during the course of a year depending on temperature and photoperiod. In this study, we took advantage of the hardening scheme incorporated in Paper I, to include the hardiness level variable into the calculation of frost mortality. The static freezing tolerance thresholds, previously used to calculate freezing mortality directly, now dictate the calculation of the maximum hardiness level of PFTs. We then replaced the fixed freezing tolerance threshold in the original freezing mortality calculation of FATES with the time- and now also PFT-dependent hardiness level.

Main findings

- Frost mortality is now triggered by the hardiness level which is unique to each PFT and evolves dynamically as a function of the climate.
- During frost events, the hardening-frost scheme causes minor changes to total PFT biomass. However, at some locations, when biomass is low or during the model spin up, frost events modelled by the new scheme may result in large differences in biomass.
- Regarding the seasonality of frost events, we identified high autumn and spring frost mortality, especially at colder sites, and increasing mid-winter frost mortality due to global warming, especially at warmer sites.

Main conclusion

Due to the presence of fixed temperature thresholds, the previous freezing mortality approach of FATES did not account for climate variations and the resilience of vegetation to frost was independent of weather conditions. In this study, we introduce an alternative scheme that fulfils the same role of governing PFT distribution, but at the same time introduces more dynamic physiologically based mechanisms. The 'hardening-frost scheme' is a major step forward as it dynamically represents vegetation in ESMs by for the first time including a level of frost tolerance that is responding to the environment and (implicitly) includes cost and benefit. By linking hardening and frost mortality in a land surface model, we open new ways to explore the impact of frost events in the context of climate change.

4.3. Paper III: Modelled plant mortality due to an extreme winter event shows a divergent mortality for deciduous and evergreen species

Objectives

- Determine whether frost droughts can be represented realistically in CLM5.0-Fates-Hydro with the new hardening scheme.
- Explore whether the winter warm spells observed in 2013/14, described in several earlier studies, triggered excessive transpiration while the soil was still frozen, leading to acute frost desiccation and ultimately exceptionally larger amounts of hydraulic failure mortality.
- Establish whether needleleaf shrubs (which exhibit earlier dehardening) are more vulnerable to acute frost desiccation than deciduous shrubs.
- Finally, we wanted to investigate how the frost drought of 2013/14 impacted terrestrial carbon fluxes and land-atmosphere interactions.

Summary

Arctic-boreal winters are warming rapidly, which is accompanied by a steadily increasing frequency of extreme winter events. While extreme winter warming events are predicted to increase in the future, there are no ecosystem models that have studied the effects of acute frost desiccation on cold acclimated plants. Acute frost desiccation occurs when sudden atmospheric warming in winter causes leaf transpiration, while frozen soils prevent water uptake, triggering vegetation damage. In paper III, we use CLM5.0-FATES-Hydro with the hardening scheme developed in Paper I and II, driven by high-resolution atmospheric forcing (COSMO-REA6) to evaluate how a frost drought impacted mortality of coastal Norwegian deciduous and evergreen shrubs during a winter characterized by warm spells and dry conditions (i.e. the winter of 2013-2014). In this study, we coupled the hardening scheme to the phenology of deciduous PFTs by allowing leaves to appear only after a PFT had dehardened by at least 50% of its maximum hardiness level. Furthermore, as deciduous genotypes have been identified to acclimate faster than evergreens, and typically deacclimate later, we implemented different temperature ranges for dehardening of evergreens (between 2.5°C to 12.5°C) and deciduous (between 5°C and 15°C) PFTs.

Main findings

- The successive warm spells during the winter of 2013/14, are reflected by the hardening scheme, which shows strong dehardening of evergreen shrubs at our coastal locations. The modelled mortality resulting from those winter warm spells was confirmed by observations of damage at or in the vicinity of the three locations.
- The model is capable of representing acute frost desiccation, which took place at several occasions as evergreen shrubs lost their hardiness during winter warm spells or at the onset of spring.
- Reverse plant water flux through roots, as soils freeze in fall or after winter warm spells, can cause large rates of hydraulic failure mortality when plants are not sufficiently acclimated to cold. During the successive warm and cold spells of 2013/14, frost-based reversal was a major contributor to mid-winter tissue dehydration and mortality (in combination with acute frost desiccation)
- Due to the lower temperature requirements for dehardening, evergreen shrubs are more vulnerable than deciduous shrubs to extreme winter warming events.
- Due to the small percentage of hydraulic failure mortality in comparison to the total winter mortality, and the reduction of competition as a result of lower biomass, vegetation productivity was not significantly lower after the extreme winter of 2013/14.

Main conclusion

We demonstrate that the hardiness level of PFTs has a critical role in the amplitude and direction of plant water fluxes, and successfully modelled the higher vulnerability of evergreen shrubs. Although the hardiness level of vegetation appears to be a critical driver of winter desiccation, we establish a clear link between soil dryness and hydraulic failure mortality during the cold season.

4.4. Author contribution

I ran model simulations, analysed model output, downloaded and prepared input data (atmospheric forcing and surface datasets), and wrote the three manuscripts presented in the thesis. The supervisors: Hui Tang, Kjetil S. Aas, Frode Stordal and Frans-Jan W. Parmentier, contributed to the design of the work. All supervisors, and co-authors Rosie A. Fischer and Jarle W. Bjerke revised the three papers.

5. Discussion, outlook and concluding remarks

In this chapter, we discuss the scientific results of each paper in comparison to the objectives presented in Chapter 1.2. This concluding chapter aims to provide a more comprehensive understanding of the scientific findings of the thesis. Lastly, we discuss the potential directions for future research in relation to the findings.

5.1. Implementation and globalization of a hardening scheme into CTSM5-FATES

a) *Implement a globalized version of the hardening scheme based on the work from Rammig et al. (2010) into the ecosystem simulator (FATES) hosted in CTSM5.0.*
b) *Adapt the hardening scheme to make it performant in all climates/locations since the hardening scheme of Rammig et al (2010) was parametrized to be effective only in Farstanäs (Sweden).*
c) *Adapt the hardening scheme to all plant functional types (PFTs), since the version of Rammig et al. (2010) was parametrized to fit Norway spruce (Picea abies).*

Hardening schemes have been used in the past to predict the hardiness level of specific species through time, as a variable of temperature and photoperiod (Leinonen et al., 1997; Rammig et al., 2010). The output of these schemes is the hardiness level of plants, and although this variable has been described as crucial for predicting and controlling various physiological processes in overwintering vegetation, it is not included in most dynamic vegetation models (Uemura & Steponkus, 1997; Valentini et al., 1990; Wisniewski et al., 2018). To improve the representation of winter processes in CLM5.0-FATES, our first mission was to globalize, improve and generalize the hardiness scheme of Rammig et al. (2010).

In Paper I, we introduce a first version of the "hardening only" scheme. The first adaptation we brought to the scheme of Rammig et al. (2010) was to make the maximum hardiness parameter becomes site- and time- dependent (to function globally and to account for evolution associated to changes in climate). To do so, we made it depend on a new variable, i.e. the 5-year running mean of the minimum 2 m daily temperature (T5). A second adaptation was to make the target hardiness, the hardening rate and the dehardening rate (see methods) dependent on the maximum hardiness level so that vegetation can harden and deharden faster at colder than at warmer sites.

A second major modification concerned the timing of the year at which hardening is allowed to start. Rammig et al. (2010) defined the start of the hardening period as the 210th Julian day, which was calibrated for Norway spruce at a specific site in Sweden. Instead, we use a daylength threshold depending on the temperature index T5 of the corresponding site. The use of a temperature-dependent daylength threshold is essential since vegetation at colder sites must start to harden earlier, and the correlation between photoperiod and temperature is not the same at all locations (Fig. 9).

To tolerate freezing, plants undergo a set of physiological changes. The capacity to efficiently cold acclimate and survive frost depends on a plants' genome and the presence of performant cold tolerance traits. Therefore, different species may exhibit different maximum hardiness levels, hardening rates, dehardening rates and temperature ranges where hardening and dehardening occur (Mabaso et al., 2019; Oberschelp et al., 2020). In Paper II, we further develop the existing hardening scheme by considering the freezing tolerance threshold of PFTs in the calculation of the hardiness level, to make it PFT-dependent. The freezing tolerance thresholds of a PFT (between 2.5°C and −80°C in FATES) is from here on used as the maximum possible value for the maximum hardiness of the corresponding PFT. In terrestrial biosphere models, species are aggregated in groups based on

common functional characteristics criteria. Therefore, it is likely that the measured maximum freezing tolerance of some species that are within the same plant functional type category in the model, is variable in reality (Sakai, 1983). A PFT's maximum freezing tolerance (as well as most parameters of terrestrial biosphere models) is a rough approximation of what has been measured for species belonging to that PFT.

In Paper III, the differentiation of hardening for PFTs is further developed, although with a focus on the distinction between deciduous and evergreen genotypes. Since deciduous genotypes acclimate quicker than evergreens, and typically deacclimate later (Artlip et al., 1997; Kalberer et al., 2006), we implement a different temperature range for dehardening to take place. The dehardening rate of evergreens occurs between 2.5°C to 12.5°C, while deciduous PFTs were defined to deharden between 5°C and 15°C as in the original scheme of (Rammig et al., 2010).

5.2. Improve the representation of winter plant hydraulics by coupling it to the hardening scheme.

a) *Use the hardiness level of plants to constrain plant hydraulic variables during winter in order to mimic the impacts of cold acclimation on plant hydraulics in the field.*
b) *Assess the effects of hardiness on transpiration, root water fluxes, mortality, and vegetation productivity, and examine the sensitivity of variables involved in the hardening scheme*

The default version of the CLM5-FATES-Hydro allows water to freeze in soils but not in plants and it does not include a mechanism to prevent liquid plant water to flow from plants to soils when freezing strongly reduces soil water potential. We show that this results in a depletion of water in plant compartments and triggers large amounts of hydraulic failure and carbon starvation mortalities. In reality, the reduction in hydraulic conductivity of plant tissues inhibits or prevents water loss during freezing, depending on the atmospheric temperatures and amount of hardening of plants (Gusta et al., 2005; Smit-Spinks et al., 1984).

In Paper I, we used the hardiness level to modify the hydraulic functioning of evergreen and deciduous trees during cold acclimation. In the hydro-hardening scheme, the hardiness level of plants is used to reduce conductances at the intersection of plant tissues (K_{MAX}) and at the stomatal level (*g0* & *g1*), as well as the hydraulic failure mortality scalar (see methods). Our results show that the reduced conductance (K_{MAX}) during hardening is beneficial as it reduces root water release, and hence hydraulic failure mortality during freezing soil events, but comes at a cost as it temporarily reduces photosynthesis due to reduced transpiration.

Reducing g0 & g1 led to a slower decrease of leaf water potentials during late winter and spring, resulting in higher vegetation survival rates. We argue that the accompanying reduction in transpiration makes the model more realistic. Indeed, while photosynthesis is slightly influenced by cold in the default model, temperature is not taken into account in the calculation of transpiration, although literature has shown that g0 & g1 is lower in cold acclimated plants (Christoffersen et al., 2016; James et al., 2008).

The large rates of root water exudation simulated each year at cold sites in the default CLM5-FATES-Hydro systematically result in maximum HFM rates from late autumn until spring snow melt when soils finally thaw. In cold regions (such as Spasskaya Pad in Siberia), HFM during winter is so large that summer productivity cannot balance the high winter mortality. In reality, high latitude vegetation

is dormant in winter and the metabolism of plants is reduced or completely interrupted, meaning that the survival rates should be largely enhanced (Volaire, 2018). Our results show that the reduction of HFM with hardening can lead to large increases of biomass in areas with cold winters.

We also explored configurations of the scheme where hardening of plants led to changing pressure volume curves, and a reduction of the carbon starvation mortality. As the physiological changes induced by cold acclimation result in modifications of the osmotic potential at full turgor and the bulk elastic modulus (Mart et al., 2016; Scholz et al., 2012), i.e. two parameters that intervene in the calculation of the plant PV curves. In the changing PV curve simulation (see Paper I), lower winter root water exudation and transpiration fluxes were simulated. However, if K_{MAX} is not low enough at the location, larger root water uptake (especially in deeper layers that remain unfrozen longer in autumn) balances the decrease in plant water potential. While the PV curve modification should be a more realistic approach to model the impact of hardening on plant hydraulics, it has the undesirable effect to also cause larger HFM and lower biomass.

Finally, we assessed the sensitivity of the model to the parameters of the hardening scheme (maximum hardiness level and timing of dehardening). These, once more, highlight the considerable cost of hardening at cold sites where vegetation incurred frequent hydraulic failure mortality. The fact that hardening comes at a cost is well-known as previous field-based research has described the cost of hardening by showing that (1) cold acclimation causes a suppression of the rate of CO_2 uptake (Krivosheeva et al., 1996), (2) low temperatures lead to the inhibition of sucrose synthesis and photosynthesis (Savitch et al., 2002), and (3) photosynthesis stops when needles freeze (Havranek & Tranquillini, 1995).

To conclude, the hydro-hardening scheme is able to simulate the physiological costs and benefits of plant cold acclimation in terms of water movement and gas exchange, and its impact on plant hydraulics, vegetation mortality and growth appears to be a promising improvement for the modelling of vegetation growth in cold environments.

5.3. Improve the representation of frost mortality by coupling the freezing mortality parametrization with the hardening scheme.

a) Implement a frost scheme based upon the previously implemented hardening scheme. The frost scheme uses the varying hardiness level rather than a fixed tolerance threshold to calculate frost mortality.

b) Examine the trends, annual distribution and spatial patterns of the hardiness-dependent frost scheme and compare it to the previous frost scheme.

The original freezing mortality implementation in FATES (Albani et al., 2006) uses hard-coded temperature thresholds to constrain the distribution of vegetation across climate zones. Due to the presence of fixed temperature thresholds, this approach does not account for climate variations and the resilience of vegetation to frost is independent of weather conditions. In reality, variations in climate are major determinants of vegetation distribution across climate envelopes (Adams, 2009). The alternative scheme we introduce in Paper II also has the role of governing PFT distribution, but at the same time introduces more dynamic physiologically based mechanisms. As the new hardening-frost scheme relies on the hardiness level of plants to predict frost mortality, it has the capacity to simulate frost damage when plants are unprepared to withstand freezing. In the new hardening-frost model, the hardiness level of all PFTs ranges from –2 to –70°C. Mortality increases linearly from the

moment minimum temperature crosses the hardiness level to the moment they get 5°C lower than the hardiness level. In the original freezing mortality approach, mortality would start 5°C above the PFTfreezetol parameter (i.e. between 2.5 and –80°C). While a PFT tolerant to 2.5°C would start experiencing freezing mortality at 7.5°C in the old scheme, the same PFT will in the new scheme start experiencing frost mortality at –2°C.

The frost-hardening scheme implemented in Paper II is a major improvement since it enables the detection and prediction of the damaging effects of extreme winter events and late spring frost events. We show that at some locations (Soběšice and Farstanäs), and for some PFTs (broadleaf deciduous, needleleaf evergreen and needleleaf deciduous trees), the new hardening-frost scheme will cause minor changes to total PFT biomass, while at other sites (e.g. Spasskaya Pad), much lower amounts of biomass were simulated during the spin-up. We argue that such dynamics may have large impacts on competition in multiple PFT simulations, but more work with parameter estimation of high-latitude PFTs in FATES remains necessary before it can be run realistically in competition mode (Buotte et al., 2021).

Unless a PFT is intolerant to the temperatures of its site, damaging frost events are short lived in the new scheme. They rarely last more than a few days, and their amplitude is limited to 3% of individuals/year. Therefore, the potential impact of frost on vegetation is small in comparison to the parameterization of carbon starvation and hydraulic failure mortalities, which typically remain at high levels for several months during winter in northern regions (see Paper I). We did not modify the amplitude parameter due to a lack of observations to evaluate against, but we call for more quantitative observations on frost damage to achieve a precise parameterization of this process.

5.4. How are frost droughts represented in CLM5-FATES-Hydro with the hydro-hardening scheme?

a. Evaluate the capacity of FATES-hydro to accurately represent frost droughts in cases where the soil is still frozen but mild atmospheric conditions trigger excess transpiration.
b. Assess the vulnerability of deciduous versus evergreen shrubs (differentiated by their capacity to remain cold acclimated) during winter warming events.

If FATES-Hydro had been used without the hardening scheme, plants would systematically undergo strong frost-based reversal in cold locations such as Eastern Siberia (Paper I). Such frost-based reversal triggers extreme tissue dehydration and would result in hydraulic failure mortality systematically reaching its maximum amplitude each winter, until snow melt in spring. The hydro-hardening scheme (Paper I) greatly improved plant hydraulics in FATES-Hydro as it enables plants to remain partially hydrated during milder winters (without extreme early-winter soil freeze), thereby allowing for a better representation of excessive transpiration during winter warm spells.

In Paper III, for the first time, we demonstrate that CLM5.0-FATES-Hydro with hardening is able to represent acute frost desiccation. We show that the winter warm spells of 2013/14 had a strong impact on the modelled hardiness level of evergreen shrubs at the northern Norwegian sites where damage was reported, pulling them out of dormancy and resulting in both acute frost desiccation and frost-based reversal, i.e. results that are consistent with the damage reports of evergreen shrubs in the field. There is, however, still some degree of frost-based reversal in both evergreen and deciduous shrub simulations as dehardening during warm spells increases root conductivity. Despite the difficulty to

find literature on the subject, efficient reverse flow inhibition has been identified to be highly variable among species (Hafner et al., 2019), habitats, and even along the length of an individual root (Caldwell et al., 1998; Kim et al., 2018). At higher elevated sites with low enough temperatures, modelled evergreen species remained cold tolerant throughout the winter and avoided large mortality rates. In the field, those evergreens may have remained unharmed in 2014, due to the higher elevation of the sites.

Paper III also establishes that, due to their earlier dehardening, evergreen shrubs are more vulnerable than deciduous shrubs at the modelled locations. This is in agreement with experiments demonstrating that, relative to evergreens, deciduous shrubs start to accumulate cold-induced proteins earlier in autumn, and maintain them at higher levels until later in spring (Arora et al., 1992; Artlip et al., 1997). Due to the current design of the hardening scheme, similar hardiness levels are generated for both plant functional types in autumn, and it is only in spring that large differences are seen. The results provided in Paper III show that the winter warm spells of 2013/14 did not trigger the dehardening of deciduous shrubs at the northern Norwegian sites.

Despite the larger rates of hydraulic failure mortality for evergreens in 2013/14, and their lower biomass following the event, we did not identify a significant disturbance of vegetation productivity during the year following the event. We believe that the systematically large rates of carbon starvation occurring repeatedly winter after winter strongly reduce the signal provided by increased hydraulic failure mortality. Another hypothesis is that the slightly larger drop of biomass in 2014, would have led to a lower competition for resources (light and water) in the model. In reality, damaged plants also tend to show compensatory growth (Boege, 2005; McNaughton, 1983).

5.5. Concluding remarks and future research

Each of the papers resulted in an improvement of the representation and/or the understanding of winter processes undergone by temperate and boreal vegetation during the cold season in a terrestrial biosphere model (i.e. CTSM5-FATES). The inclusion of cold hardiness is essential to model realistic plant hydraulics, frost mortality, frost droughts and vegetation dynamics within cold climates.

While conducting this work, we identified some approximations and weaknesses in the methods. In this section we describe some of the main issues we encountered and propose some solutions or ideas that may need to be further explored to better represent winter processes in cold regions.

1. In Paper I, the solution of the Hydraulic scheme of FATES was calculated by the two-dimensional (2D) solver using Newton iterations. In this solution, the water potentials in plant and rhizosphere soils are solved together as prognostic variables. When running the model in locations such as Siberia, extremely low water potentials (−40 000 MPa) lead to extremely high matric water gradients and prevented the convergence towards a solution of the flow equations. To deal with these unrealistic values, we limited the calculation of supercooling in soils to −10°C and imposed −25MPa as a minimum value for water potential. These enabled the model to converge towards a realistic solution. To further improve the soil water dynamics and curves in the model, additional studies looking into the relationship between temperature and soil water potential at northern locations would be beneficial.

2. When the hydraulics of FATES are used in Siberia with the 2D Newton solver, large rates of water percolation and drainage from upper to deeper soil layers was modelled. Although Siberian soils are deeper, we prescribed soil depths of 1m as our focus was on the physiology of hardening and not on the supply and demand dynamics of soil moisture. Further work is needed to develop soil physics in terrestrial biosphere models, to prevent excessive drainage and unrealistically low water potentials

3. We show that even after the implementation of the hydro-hardening scheme, reverse flow through roots as soil freezes remains present, especially during shoulder seasons or during mid-winter dehardening. Quantifying reverse flow inhibition remains unknown and highly variable among species (Hafner et al., 2019), habitats, and even along the length of an individual root (Caldwell et al., 1998; Kim et al., 2018). More research is needed to further disentangle the root properties that may regulate or inhibit reverse flow, especially for boreal forests.

4. Further detailed studies are required to understand the large-scale impacts of frost-based reversal and excessive transpiration on net carbon exchange, gross ecosystem productivity, and water transfer through the soil–plant–atmosphere continuum. Research should not only focus on stomatal water losses during acute frost droughts but also try to assess to which extent reverse flow through roots is crucial to vegetation survival in temperate, boreal and arctic regions.

5. Stomatal conductance (gs) is important to improve model predictions of plant water use, carbon uptake and energy fluxes (Bauerle & Bowden, 2011; Berry et al., 2010; Franks et al., 2018). The Ball-Berry stomatal model describes gs as a function of, among others, a residual or intercept (g0) and a slope (g1). Reductions of both parameters were suggested during water stress, and inter- and intra-species differences are pointed out (Heroult et al., 2013; Miner & Bauerle, 2017; Zhou et al., 2013). Similarly, seasonal variations of Ball-Berry parameters have been investigated, and although results differ (Lai et al., 2000; Ono et al., 2013; Wolf et

al., 2006), research focusing on stomatal dynamics during freezing and hardening is lacking. Combining the current knowledge of the effects of hardening on conductance (Augustyniak et al., 2018; Göbel et al., 2019) and the effects of water stress on g0 and g1, however, justifies reducing those parameters with hardening. The amplitude at which stomatal parameters were reduced with hardiness, has been selected based on a sensitivity experiment that showed optimal growth but would greatly benefit from more quantitative observations.

6. In several model simulations, we struggled to minimize carbon starvation mortality and termination mortality (partial or total extinction of a PFT) during spring when leaves appear. Carbon starvation mortality resulted in large seasonal cycles at all temperate and boreal sites simulations we studied for deciduous and evergreen genotypes. As carbon storage pools diminish towards the end of the winter, there is no carbon left for leaves to appear and on several occasions large rates of termination mortality could not be avoid without having to tune the parameters of productivity. We suggest further work is needed to either calculate carbon and termination mortality in the model or to improve the accuracy of the parameters involved (e.g. storage pool size, Vcmax, allocation, root longevity).

7. Although the understanding of cold acclimation processes is expanding at an accelerating rate, there are still large knowledge gaps. For example, the range of processes triggered by cold acclimation are poorly known and we lack measurements to define the exact amplitude at which they are disturbed (R. Arora & Rowland, 2011; Chang et al., 2021; Shi et al., 2018; Shin et al., 2015).

7.1. Future research is needed to better assess the implications of cold acclimation on plant hydraulics, especially conductivity. Understanding these processes is hampered by the logistical and technical difficulties involved in the observation of cold systems. We call for more quantitative observations on frost damage to achieve a precise parameterization of this parameter.

7.2. Future research is needed to provide more quantitative observations on frost damage to improve the amplitude of frost. The amplitude of the freezing mortality parameter is 3% of individuals/year, and since damaging frost events are short lived in the new scheme, the potential of impact of frost on vegetation is small in comparison to the parameterization of carbon starvation and hydraulic failure mortalities, which typically remain at high levels for several months during winter in northern regions.

7.3. Quantifying and generalizing hardiness levels and rates inside the scheme itself are in some respects broad approximations which remain to be optimized further. Future developments should, for example, consider a larger influence of photoperiod and the inclusion of plant phenological states in the calculation of the hardiness level.

8. In this thesis, we developed tools that enable to increase our understanding of how climate influences vegetation dynamics through the occurrence of frost and drought events. We also used the tools we implemented to highlight that frost and drought events can have significant impacts on vegetation survival in cold regions of the world, ultimately leading to browning. Since browning is influenced by the temporal and spatial occurrence of extreme winter events, we emphasize the need to better understand the changes in occurrences of extreme winter events in the future to better evaluate their importance in arctic-boreal greening and browning.

References

Adams, J. (2009). *Vegetation-climate interaction: How plants make the global environment*. Springer Science & Business Media.

Adams, W. W., Zarter, C. R., Ebbert, V., & Demmig-Adams, B. (2004). Photoprotective strategies of overwintering evergreens. *Bioscience*, *54*(1), 41–49.

Albani, M., Medvigy, D., Hurtt, G. C., & Moorcroft, P. R. (2006). The contributions of land-use change, CO2 fertilization, and climate variability to the Eastern US carbon sink. *Global Change Biology*, *12*(12), 2370–2390.

Anchordoguy, T. J., Rudolph, A. S., Carpenter, J. F., & Crowe, J. H. (1987). Modes of interaction of cryoprotectants with membrane phospholipids during freezing. *Cryobiology*, *24*(4), 324–331.

Archaux, F., & Wolters, V. (2006). Impact of summer drought on forest biodiversity: What do we know? *Annals of Forest Science*, *63*(6), 645–652.

Arora, R., & Rowland, L. J. (2011). Physiological research on winter-hardiness: Deacclimation resistance, reacclimation ability, photoprotection strategies, and a cold acclimation protocol design. *HortScience*, *46*(8), 1070–1078.

Arora, R., Wisniewski, M. E., & Scorza, R. (1992). Cold acclimation in genetically related (sibling) deciduous and evergreen peach (Prunus persica [L.] Batsch) I. Seasonal changes in cold hardiness and polypeptides of bark and xylem tissues. *Plant Physiology*, *99*(4), 1562–1568.

Arora, V. K., & Boer, G. J. (2005). A parameterization of leaf phenology for the terrestrial ecosystem component of climate models. *Global Change Biology*, *11*(1), 39–59.

Artlip, T. S., Callahan, A. M., Bassett, C. L., & Wisniewski, M. E. (1997). Seasonal expression of a dehydrin gene in sibling deciduous and evergreen genotypes of peach (Prunus persica [L.] Batsch). *Plant Molecular Biology*, *33*(1), 61–70.

Asahina, E. (1956). The freezing process of plant cell. *Contributions from the Institute of Low Temperature Science*, *10*, 83–126.

Augspurger, C. K. (2013). Reconstructing patterns of temperature, phenology, and frost damage over 124 years: Spring damage risk is increasing. *Ecology*, *94*(1), 41–50.

Axelrod, D. I. (1952). A theory of angiosperm evolution. *Evolution*, 29–60.

Bala, G., Caldeira, K., Wickett, M., Phillips, T. J., Lobell, D. B., Delire, C., & Mirin, A. (2007). Combined climate and carbon-cycle effects of large-scale deforestation. *Proceedings of the National Academy of Sciences*, *104*(16), 6550–6555.

Barry, R. G., & Chorley, R. J. (2009). *Atmosphere, weather and climate*. Routledge.

Basler, D. (2016). Evaluating phenological models for the prediction of leaf-out dates in six temperate tree species across central Europe. *Agricultural and Forest Meteorology*, *217*, 10–21.

Beck, E. H., Heim, R., & Hansen, J. (2004). Plant resistance to cold stress: Mechanisms and environmental signals triggering frost hardening and dehardening. *Journal of Biosciences*, *29*(4), 449–459.

Bentrup, F.-W. (2017). Water ascent in trees and lianas: The cohesion-tension theory revisited in the wake of Otto Renner. *Protoplasma*, *254*(2), 627–633.

Berardi, D., Brzostek, E., Blanc-Betes, E., Davison, B., DeLucia, E. H., Hartman, M. D., Kent, J., Parton, W. J., Saha, D., & Hudiburg, T. W. (2020). 21st-century biogeochemical modeling: Challenges for Century-based models and where do we go from here? *GCB Bioenergy*, *12*(10), 774–788.

Berner, L. T., Massey, R., Jantz, P., Forbes, B. C., Macias-Fauria, M., Myers-Smith, I., Kumpula, T., Gauthier, G., Andreu-Hayles, L., & Gaglioti, B. V. (2020). Summer warming explains widespread but not uniform greening in the Arctic tundra biome. *Nature Communications*, *11*(1), 1–12.

Bi, J., Xu, L., Samanta, A., Zhu, Z., & Myneni, R. (2013). Divergent arctic-boreal vegetation changes between North America and Eurasia over the past 30 years. *Remote Sensing*, *5*(5), 2093–2112.

Bigras, F. J., & Colombo, S. J. (2013). *Conifer cold hardiness* (Vol. 1). Springer Science & Business Media.

Bisht, G., & Riley, W. J. (2019). Development and verification of a numerical library for solving global terrestrial multiphysics problems. *Journal of Advances in Modeling Earth Systems*, *11*(6), 1516–1542.

Bjerke, J. W., Karlsen, S. R., Høgda, K. A., Malnes, E., Jepsen, J. U., Lovibond, S., Vikhamar-Schuler, D., & Tømmervik, H. (2014). Record-low primary productivity and high plant damage in the Nordic Arctic Region in 2012 caused by multiple weather events and pest outbreaks. *Environmental Research Letters*, *9*(8), 084006.

Bjerke, J. W., Treharne, R., Vikhamar-Schuler, D., Karlsen, S. R., Ravolainen, V., Bokhorst, S., Phoenix, G. K., Bochenek, Z., & Tømmervik, H. (2017). Understanding the drivers of extensive plant damage in boreal and Arctic ecosystems: Insights from field surveys in the aftermath of damage. *Science of the Total Environment*, *599*, 1965–1976.

Boege, K. (2005). Influence of plant ontogeny on compensation to leaf damage. *American Journal of Botany*, *92*(10), 1632–1640.

Bohm, J. (1893). Capillarität und saftsteigen. *Ber. Dtsch. Bot. Ges.*, *11*, 203–212.

Bokhorst, S., Bjerke, J., Bowles, F., Melillo, J., Callaghan, T., & Phoenix, G. (2008). Impacts of extreme winter warming in the sub-Arctic: Growing season responses of dwarf shrub heathland. *Global Change Biology*, *14*(11), 2603–2612.

Bokhorst, S., Bjerke, J. W., Street, L., Callaghan, T. V., & Phoenix, G. K. (2011). Impacts of multiple extreme winter warming events on sub-Arctic heathland: Phenology, reproduction, growth, and CO2 flux responses. *Global Change Biology*, *17*(9), 2817–2830.

Bokhorst, S. F., Bjerke, J. W., Tømmervik, H., Callaghan, T. V., & Phoenix, G. K. (2009). Winter warming events damage sub-Arctic vegetation: Consistent evidence from an experimental manipulation and a natural event. *Journal of Ecology*, *97*(6), 1408–1415.

Bonan, G. (Ed.). (2019). Terrestrial Biosphere Models. In *Climate Change and Terrestrial Ecosystem Modeling* (pp. 1–24). Cambridge University Press. https://doi.org/10.1017/9781107339217.002

Bonan, G. B. (1996). A land surface model (LSM Version 1.0) for ecological, hydrological and atmospheric studies: Technical description and user's guide. NCAR Technical Note TN-417+ STR. *National Center for Atmospheric Research, Boulder, CO*, *150*.

Bonan, G. B., Williams, M., Fisher, R. A., & Oleson, K. W. (2014). Modeling stomatal conductance in the earth system: Linking leaf water-use efficiency and water transport along the soil–plant–atmosphere continuum. *Geoscientific Model Development*, *7*(5), 2193–2222.

Buotte, P. C., Koven, C. D., Xu, C., Shuman, J. K., Goulden, M. L., Levis, S., Katz, J., Ding, J., Ma, W., & Robbins, Z. (2021). Capturing functional strategies and compositional dynamics in vegetation demographic models. *Biogeosciences*, *18*(14), 4473–4490.

Burke, M. J., Gusta, L. V., Quamme, H. A., Weiser, C. J., & Li, P. H. (1976). Freezing and injury in plants. *Annual Review of Plant Physiology*, *27*(1), 507–528.

Carlsbecker, A., & Helariutta, Y. (2005). Phloem and xylem specification: Pieces of the puzzle emerge. *Current Opinion in Plant Biology*, *8*(5), 512–517.

Chang, C. Y.-Y., Bräutigam, K., Hüner, N. P., & Ensminger, I. (2021). Champions of winter survival: Cold acclimation and molecular regulation of cold hardiness in evergreen conifers. *New Phytologist*, *229*(2), 675–691.

Chen, H.-H., & Li, P. H. (1980). Characteristics of cold acclimation and deacclimation in tuber-bearing Solanum species. *Plant Physiology*, *65*(6), 1146–1148.

Christoffersen, B. O., Gloor, M., Fauset, S., Fyllas, N. M., Galbraith, D. R., Baker, T. R., Kruijt, B., Rowland, L., Fisher, R. A., Binks, O. J., & others. (2016). Linking hydraulic traits to tropical forest function in a size-structured and trait-driven model (TFS v. 1-Hydro). *Geoscientific Model Development*.

Clark, M. P., Kavetski, D., & Fenicia, F. (2011). Pursuing the method of multiple working hypotheses for hydrological modeling. *Water Resources Research*, *47*(9).

Close, T. J. (1997). Dehydrins: A commonalty in the response of plants to dehydration and low temperature. *Physiologia Plantarum*, *100*(2), 291–296.

Cochard, H. (2006). Cavitation in trees. *Comptes Rendus Physique*, *7*(9–10), 1018–1026.

Cochard, H. (2013). The basics of plant hydraulics in 3 minutes. *Journal of Sigmoidal Plant Hydraulics*, *1*, 3 p.

Cohen, E., Shapiro, B., Shalom, Y., & Klein, J. D. (1994). Water loss: A nondestructive indicator of enhanced cell membrane permeability of chilling-injured citrus fruit. *Journal of the American Society for Horticultural Science*, *119*(5), 983–986.

Cox, S. E., & Stushnoff, C. (2001). Temperature-related shifts in soluble carbohydrate content during dormancy and cold acclimation in Populus tremuloides. *Canadian Journal of Forest Research*, *31*(4), 730–737.

Crausbay, S. D., Ramirez, A. R., Carter, S. L., Cross, M. S., Hall, K. R., Bathke, D. J., Betancourt, J. L., Colt, S., Cravens, A. E., & Dalton, M. S. (2017). Defining ecological drought for the twenty-first century. *Bulletin of the American Meteorological Society*, *98*(12), 2543–2550.

Crosatti, C., Rizza, F., Badeck, F. W., Mazzucotelli, E., & Cattivelli, L. (2013). Harden the chloroplast to protect the plant. *Physiologia Plantarum*, *147*(1), 55–63.

Darcy, H. (1856). *Les fontaines publiques de la ville de Dijon: Exposition et application...* Victor Dalmont.

Das, K., & Roychoudhury, A. (2014). Reactive oxygen species (ROS) and response of antioxidants as ROS-scavengers during environmental stress in plants. *Frontiers in Environmental Science*, *2*, 53.

De Schepper, V., De Swaef, T., Bauweraerts, I., & Steppe, K. (2013). Phloem transport: A review of mechanisms and controls. *Journal of Experimental Botany*, *64*(16), 4839–4850.

Dickinson, R. E., Henderson-Sellers, A., Rosenzweig, C., & Sellers, P. J. (1991). Evapotranspiration models with canopy resistance for use in climate models, a review. *Agricultural and Forest Meteorology*, *54*(2–4), 373–388.

Diffenbaugh, N. S., Pal, J. S., Trapp, R. J., & Giorgi, F. (2005). Fine-scale processes regulate the response of extreme events to global climate change. *Proceedings of the National Academy of Sciences*, *102*(44), 15774–15778.

Dixon, H. H., & Joly, J. (1894). On the ascent of sap. *Proceedings of the Royal Society of London*, *57*, 3–5.

Dong, M. A., Farré, E. M., & Thomashow, M. F. (2011). Circadian clock-associated 1 and late elongated hypocotyl regulate expression of the C-repeat binding factor (CBF) pathway in Arabidopsis. *Proceedings of the National Academy of Sciences*, *108*(17), 7241–7246.

Duursma, R. A., & Medlyn, B. E. (2012). MAESPA: a model to study interactions between water limitation, environmental drivers and vegetation function at tree and stand levels, with an example application to [CO 2]× drought interactions. *Geoscientific Model Development*, *5*(4), 919–940.

Ebbert, V., Adams Iii, W. W., Mattoo, A. K., Sokolenko, A., & Demmig-Adams, B. (2005). Up-regulation of a photosystem II core protein phosphatase inhibitor and sustained D1 phosphorylation in zeaxanthin-retaining, photoinhibited needles of overwintering Douglas fir. *Plant, Cell & Environment*, *28*(2), 232–240.

Ebermayer, E. W. F. (1873). *Die physikalischen einwirkungen des waldes auf luft und boden und seine klimatologische und hygienische bedeutung: Begründet durch die beobachtungen der forst.-meteorolog. Stationen im königreich Bayern* (Vol. 1). C. Krebs.

Edwards, W. R. N., Jarvis, P. G., Landsberg, J. J., & Talbot, H. (1986). A dynamic model for studying flow of water in single trees. *Tree Physiology*, *1*(3), 309–324.

Egea, G., Verhoef, A., & Vidale, P. L. (2011). Towards an improved and more flexible representation of water stress in coupled photosynthesis–stomatal conductance models. *Agricultural and Forest Meteorology*, *151*(10), 1370–1384.

Ensminger, I., Berninger, F., & Streb, P. (2012). Response of Photosynthesis to low temperatures. In *Terrestiral Photosynthesis in a changing environment* (pp. 272–289). Cambridge University Press.

Ensminger, I., Sveshnikov, D., Campbell, D. A., Funk, C., Jansson, S., Lloyd, J., Shibistova, O., & Öquist, G. (2004). Intermittent low temperatures constrain spring recovery of photosynthesis in boreal Scots pine forests. *Global Change Biology*, *10*(6), 995–1008.

FATES Development Team. (2018). *Welcome to FATES's documentation! —FATES d2.0.1 documentation*. https://fates-users-guide.readthedocs.io/projects/tech-doc/en/stable/

Fatichi, S., Pappas, C., Zscheischler, J., & Leuzinger, S. (2019). Modelling carbon sources and sinks in terrestrial vegetation. *New Phytologist*, *221*(2), 652–668.

Ferguson, J. C., Tarara, J. M., Mills, L. J., Grove, G. G., & Keller, M. (2011). Dynamic thermal time model of cold hardiness for dormant grapevine buds. *Annals of Botany*, *107*(3), 389–396.

Ferranti, L., Corti, S., & Janousek, M. (2015). Flow-dependent verification of the ECMWF ensemble over the Euro-Atlantic sector. *Quarterly Journal of the Royal Meteorological Society*, *141*(688), 916–924.

Fisher, J. B., Huntzinger, D. N., Schwalm, C. R., & Sitch, S. (2014). Modeling the terrestrial biosphere. *Annual Review of Environment and Resources*, *39*, 91–123.

Fisher, R. A., & Koven, C. D. (2020). Perspectives on the future of land surface models and the challenges of representing complex terrestrial systems. *Journal of Advances in Modeling Earth Systems*, *12*(4), e2018MS001453.

Fisher, R. A., Koven, C. D., Anderegg, W. R., Christoffersen, B. O., Dietze, M. C., Farrior, C. E., Holm, J. A., Hurtt, G. C., Knox, R. G., & Lawrence, P. J. (2018). Vegetation demographics in Earth System Models: A review of progress and priorities. *Global Change Biology*, *24*(1), 35–54.

Fisher, R. A., Muszala, S., Verteinstein, M., Lawrence, P., Xu, C., McDowell, N. G., Knox, R. G., Koven, C., Holm, J., Rogers, B. M., & others. (2015). Taking off the training wheels: The properties of a dynamic vegetation model without climate envelopes, CLM4. 5 (ED). *Geoscientific Model Development*, *8*(11), 3593–3619.

Fisher, R. A., Wieder, W. R., Sanderson, B. M., Koven, C. D., Oleson, K. W., Xu, C., Fisher, J. B., Shi, M., Walker, A. P., & Lawrence, D. M. (2019). Parametric controls on vegetation responses to biogeochemical forcing in the CLM5. *Journal of Advances in Modeling Earth Systems*, *11*(9), 2879–2895.

Fisher, R. A., Williams, M., Da Costa, A. L., Malhi, Y., Da Costa, R. F., Almeida, S., & Meir, P. (2007). The response of an Eastern Amazonian rain forest to drought stress: Results and modelling analyses from a throughfall exclusion experiment. *Global Change Biology*, *13*(11), 2361–2378.

Fisher, R., McDowell, N., Purves, D., Moorcroft, P., Sitch, S., Cox, P., Huntingford, C., Meir, P., & Woodward, F. I. (2010). Assessing uncertainties in a second-generation dynamic vegetation model caused by ecological scale limitations. *New Phytologist*, *187*(3), 666–681.

Flato, G. M. (2011). Earth system models: An overview. *Wiley Interdisciplinary Reviews: Climate Change*, *2*(6), 783–800.

Francis, J. A., & Vavrus, S. J. (2012). Evidence linking Arctic amplification to extreme weather in mid-latitudes. *Geophysical Research Letters*, *39*(6).

Friedlingstein, P. (2015). Carbon cycle feedbacks and future climate change. *Philosophical Transactions of the Royal Society A: Mathematical, Physical and Engineering Sciences*, *373*(2054), 20140421.

Frost, G. V., Bhatt, U. S., Epstein, H. E., Walker, D. A., Raynolds, M. K., Berner, L. T., Bjerke, J. W., Breen, A. L., Forbes, B. C., Goetz, S. J., Iversen, C. M., Lara, M. J., M. J. Macander, Phoenix, G. K., Rocha, A. V., Salmon, V. G., Thornton, P. E., Tømmervik, H., & Wullschleger, S. D. (2019). Tundra Greenness. *Arctic Program*. https://arctic.noaa.gov/Report-Card/Report-Card-2019/ArtMID/7916/ArticleID/838/Tundra-Greenness

Frost, G. V., Macander, M. J., Bhatt, U. S., Berner, L. T., Bjerke, J. W., Epstein, H. E., Forbes, B. C., Goetz, S. J., Lara, M. J., & Park, T. (2021). *Tundra greenness*.

Fujiwara, M., Wright, J. S., Manney, G. L., Gray, L. J., Anstey, J., Birner, T., Davis, S., Gerber, E. P., Harvey, V. L., & Hegglin, M. I. (2017). Introduction to the SPARC Reanalysis Intercomparison Project (S-RIP) and overview of the reanalysis systems. *Atmospheric Chemistry and Physics*, *17*(2), 1417–1452.

Glerum, C. (1973). Annual trends in frost hardiness and electrical impedance for seven coniferous species. *Canadian Journal of Plant Science*, *53*(4), 881–889.

Gomes, E. P. C., Mantovani, W., & Kageyama, P. Y. (2003). Mortality and recruitment of trees in a secondary montane rain forest in southeastern Brazil. *Brazilian Journal of Biology*, *63*(1), 47–60.

Greenup, A. G., Sasani, S., Oliver, S. N., Walford, S. A., Millar, A. A., & Trevaskis, B. (2011). Transcriptome analysis of the vernalization response in barley (Hordeum vulgare) seedlings. *PLoS One*, *6*(3), e17900.

Guo, X., Liu, D., & Chong, K. (2018). Cold signaling in plants: Insights into mechanisms and regulation. *Journal of Integrative Plant Biology*, *60*(9), 745–756.

Gusta, L. V., Trischuk, R., & Weiser, C. J. (2005). Plant cold acclimation: The role of abscisic acid. *Journal of Plant Growth Regulation*, *24*(4), 308–318.

Hacke, U. G., Sperry, J. S., & Pittermann, J. (2004). Analysis of circular bordered pit function II. Gymnosperm tracheids with torus-margo pit membranes. *American Journal of Botany*, *91*(3), 386–400.

Hanin, M., Brini, F., Ebel, C., Toda, Y., Takeda, S., & Masmoudi, K. (2011). Plant dehydrins and stress tolerance: Versatile proteins for complex mechanisms. *Plant Signaling & Behavior*, *6*(10), 1503–1509.

Hannerz, M. (1994). *Predicting the risk of frost occurrence after budburst of Norway spruce in Sweden.*

Hänninen, H. (1995). Effects of climatic change on trees from cool and temperate regions: An ecophysiological approach to modelling of bud burst phenology. *Canadian Journal of Botany*, *73*(2), 183–199.

Hänninen, H. (2006). Climate warming and the risk of frost damage to boreal forest trees: Identification of critical ecophysiological traits. *Tree Physiology*, *26*(7), 889–898.

Hansen, B. B., Isaksen, K., Benestad, R. E., Kohler, J., Pedersen, Å. Ø., Loe, L. E., Coulson, S. J., Larsen, J. O., & Varpe, Ø. (2014). Warmer and wetter winters: Characteristics and implications of an extreme weather event in the High Arctic. *Environmental Research Letters*, *9*(11), 114021.

Hartley, I. P., Garnett, M. H., Sommerkorn, M., Hopkins, D. W., Fletcher, B. J., Sloan, V. L., Phoenix, G. K., & Wookey, P. A. (2012). A potential loss of carbon associated with greater plant growth in the European Arctic. *Nature Climate Change*, *2*(12), 875–879.

Hasselmann, K. (1976). Stochastic climate models part I. Theory. *Tellus*, *28*(6), 473–485.

Havranek, W. M., & Tranquillini, W. (1995). Physiological processes during winter dormancy and their ecological significance. In *Ecophysiology of coniferous forests* (pp. 95–124). Elsevier.

Holliday, J. A., Ralph, S. G., White, R., Bohlmann, J., & Aitken, S. N. (2008). Global monitoring of autumn gene expression within and among phenotypically divergent populations of Sitka spruce (Picea sitchensis). *New Phytologist*, *178*(1), 103–122.

Houghton, J. T. (1990). IPCC Scientific Assessment. *Climate Change*, *365*.

Hurtt, G. C., Moorcroft, P. R., And, S. W. P., & Levin, S. A. (1998). Terrestrial models and global change: Challenges for the future. *Global Change Biology*, *4*(5), 581–590.

James, A. T., Lawn, R. J., & Cooper, M. (2008). Genotypic variation for drought stress response traits in soybean. I. Variation in soybean and wild Glycine spp. For epidermal conductance, osmotic potential, and relative water content. *Australian Journal of Agricultural Research*, *59*(7), 656–669.

Janská, A., Maršík, P., Zelenková, S., & Ovesná, J. (2010). Cold stress and acclimation–what is important for metabolic adjustment? *Plant Biology*, *12*(3), 395–405.

Jansson, J. K., & Taş, N. (2014). The microbial ecology of permafrost. *Nature Reviews Microbiology*, *12*(6), 414–425.

Johansson, M., Ramos-Sánchez, J. M., Conde, D., Ibáñez, C., Takata, N., Allona, I., & Eriksson, M. E. (2015). Role of the circadian clock in cold acclimation and winter dormancy in perennial plants. In *Advances in plant dormancy* (pp. 51–74). Springer.

Johnson, D. M., McCulloh, K. A., Woodruff, D. R., & Meinzer, F. C. (2012). Hydraulic safety margins and embolism reversal in stems and leaves: Why are conifers and angiosperms so different? *Plant Science*, *195*, 48–53.

Jönsson, A. M., Linderson, M.-L., Stjernquist, I., Schlyter, P., & Bärring, L. (2004). Climate change and the effect of temperature backlashes causing frost damage in Picea abies. *Global and Planetary Change*, *44*(1–4), 195–207.

Kalberer, S. R., Wisniewski, M., & Arora, R. (2006). Deacclimation and reacclimation of cold-hardy plants: Current understanding and emerging concepts. *Plant Science*, *171*(1), 3–16.

Keenan, T. F., Baker, I., Barr, A., Ciais, P., Davis, K., Dietze, M., Dragoni, D., Gough, C. M., Grant, R., & Hollinger, D. (2012). Terrestrial biosphere model performance for inter-annual variability of land-atmosphere CO2 exchange. *Global Change Biology*, *18*(6), 1971–1987.

Keenan, T. F., Gray, J., Friedl, M. A., Toomey, M., Bohrer, G., Hollinger, D. Y., Munger, J. W., O'Keefe, J., Schmid, H. P., & Wing, I. S. (2014). Net carbon uptake has increased through warming-induced changes in temperate forest phenology. *Nature Climate Change*, *4*(7), 598–604.

Keller, M., Palace, M., Asner, G. P., Pereira Jr, R., & Silva, J. N. M. (2004). Coarse woody debris in undisturbed and logged forests in the eastern Brazilian Amazon. *Global Change Biology*, *10*(5), 784–795.

Kellomaki, S., Hanninen, H., & Kolstrom, M. (1995). Computations on frost damage to Scots pine under climatic warming in boreal conditions. *Ecological Applications*, *5*(1), 42–52.

Kennedy, D., Swenson, S., Oleson, K. W., Lawrence, D. M., Fisher, R., Lola da Costa, A. C., & Gentine, P. (2019). Implementing plant hydraulics in the community land model, version 5. *Journal of Advances in Modeling Earth Systems*, *11*(2), 485–513.

Kim, H. K., Park, J., & Hwang, I. (2014). Investigating water transport through the xylem network in vascular plants. *Journal of Experimental Botany*, *65*(7), 1895–1904.

King, R. W., & Heide, O. M. (2009). Seasonal flowering and evolution: The heritage from Charles Darwin. *Functional Plant Biology*, *36*(12), 1027–1036.

Koratkar, S. (2016, February 24). Cavitation and Embolism in Vascular Plants (With Diagram). *Biology Discussion*. https://www.biologydiscussion.com/plants/cavitation-and-embolism-in-vascular-plants-with-diagram/22732

Koven, C. (2019). *FATES Parameters and Output for Parameter Sensitivity at the Panama Barro Colorado Island Testbed*. Next-Generation Ecosystem Experiments Tropics; Lawrence Berkeley National ….

Kreyling, J., Thiel, D., Nagy, L., Jentsch, A., Huber, G., Konnert, M., & Beierkuhnlein, C. (2012). Late frost sensitivity of juvenile Fagus sylvatica L. differs between southern Germany and

Bulgaria and depends on preceding air temperature. *European Journal of Forest Research*, *131*(3), 717–725.

Krinner, G., Viovy, N., de Noblet-Ducoudré, N., Ogée, J., Polcher, J., Friedlingstein, P., Ciais, P., Sitch, S., & Prentice, I. C. (2005). A dynamic global vegetation model for studies of the coupled atmosphere-biosphere system. *Global Biogeochemical Cycles*, *19*(1).

Krivosheeva, A., Tao, D.-L., Ottander, C., Wingsle, G., Dube, S. L., & Öquist, G. (1996). Cold acclimation and photoinhibition of photosynthesis in Scots pine. *Planta*, *200*(3), 296–305.

Lang, G. A. (1987). Endo-, para-and ecodormancy: Physiological terminology and classification for dormancy research. *Hortic. Sci.*, *22*, 271–277.

Larcher, W. (2003). *Physiological plant ecology: Ecophysiology and stress physiology of functional groups*. Springer Science & Business Media.

Larcher, W., & Siegwolf, R. (1985). Development of acute frost drought in Rhododendron ferrugineum at the alpine timberline. *Oecologia*, *67*(2), 298–300.

Law, B. E., Falge, E., Gu, L. v, Baldocchi, D. D., Bakwin, P., Berbigier, P., Davis, K., Dolman, A. J., Falk, M., & Fuentes, J. D. (2002). Environmental controls over carbon dioxide and water vapor exchange of terrestrial vegetation. *Agricultural and Forest Meteorology*, *113*(1–4), 97–120.

Law, B. E., Sun, O. J., Campbell, J., Van Tuyl, S., & Thornton, P. E. (2003). Changes in carbon storage and fluxes in a chronosequence of ponderosa pine. *Global Change Biology*, *9*(4), 510–524.

Lawrence, D. M., Fisher, R. A., Koven, C. D., Oleson, K. W., Swenson, S. C., Bonan, G., Collier, N., Ghimire, B., van Kampenhout, L., Kennedy, D., & others. (2019). The Community Land Model version 5: Description of new features, benchmarking, and impact of forcing uncertainty. *Journal of Advances in Modeling Earth Systems*, *11*(12), 4245–4287.

Le Quéré, C., Andrew, R. M., Friedlingstein, P., Sitch, S., Hauck, J., Pongratz, J., Pickers, P. A., Korsbakken, J. I., Peters, G. P., & Canadell, J. G. (2018). Global carbon budget 2018. *Earth System Science Data*, *10*(4), 2141–2194.

Leinonen, I., Repo, T., & Hänninen, H. (1997). Changing environmental effects on frost hardiness of Scots pine during dehardening. *Annals of Botany*, *79*(2), 133–138.

Levitt, J. (1972). *Responses of plants to environmental stresses*.

Levitt, J. (1980). *Responses of Plants to Environmental Stress, Volume 1: Chilling, Freezing, and High Temperature Stresses.* Academic Press.

Loranty, M. M., Goetz, S. J., & Beck, P. S. (2011). Tundra vegetation effects on pan-Arctic albedo. *Environmental Research Letters*, *6*(2), 024014.

Lyons, J. M. (1973). Chilling injury in plants. *Annual Review of Plant Physiology*, *24*(1), 445–466.

Mabaso, F., Ham, H., & Nel, A. (2019). Frost tolerance of various Pinus pure species and hybrids. *Southern Forests: A Journal of Forest Science*, *81*(3), 273–280.

MacDougall, A. H., Avis, C. A., & Weaver, A. J. (2012). Significant contribution to climate warming from the permafrost carbon feedback. *Nature Geoscience*, *5*(10), 719–721.

Manabe, S. (1969). Climate and the ocean circulation: I. The atmospheric circulation and the hydrology of the earth's surface. *Monthly Weather Review*, *97*(11), 739–774.

Mart, K. B., Veneklaas, E. J., & Bramley, H. (2016). Osmotic potential at full turgor: An easily measurable trait to help breeders select for drought tolerance in wheat. *Plant Breeding*, *135*(3), 279–285.

McGuire, A. D., Anderson, L. G., Christensen, T. R., Dallimore, S., Guo, L., Hayes, D. J., Heimann, M., Lorenson, T. D., Macdonald, R. W., & Roulet, N. (2009). Sensitivity of the carbon cycle in the Arctic to climate change. *Ecological Monographs*, *79*(4), 523–555.

McNaughton, S. J. (1983). Compensatory plant growth as a response to herbivory. *Oikos*, 329–336.

Meinzer, F. C. (1993). Stomatal control of transpiration. *Trends in Ecology & Evolution*, *8*(8), 289–294.

Mirfenderesgi, G., Bohrer, G., Matheny, A. M., Fatichi, S., de Moraes Frasson, R. P., & Schäfer, K. V. (2016). Tree level hydrodynamic approach for resolving aboveground water storage and stomatal conductance and modeling the effects of tree hydraulic strategy. *Journal of Geophysical Research: Biogeosciences*, *121*(7), 1792–1813.

MODLIBOWSKA, I., & Rogers, W. S. (1955). Freezing of Plant Tissues3. *Journal of Experimental Botany*, *6*(3), 384–391.

Moorcroft, P. R., Hurtt, G. C., & Pacala, S. W. (2001). A method for scaling vegetation dynamics: The ecosystem demography model (ED). *Ecological Monographs*, *71*(4), 557–586.

Murray, M. B., Cannell, M. G. R., & Smith, R. I. (1989). Date of budburst of fifteen tree species in Britain following climatic warming. *Journal of Applied Ecology*, 693–700.

Nadezhdina, N., David, T. S., David, J. S., Ferreira, M. I., Dohnal, M., Tesař, M., Gartner, K., Leitgeb, E., Nadezhdin, V., Cermak, J., & others. (2010). Trees never rest: The multiple facets of hydraulic redistribution. *Ecohydrology*, *3*(4), 431–444.

Nauta, A. L., Heijmans, M. M., Blok, D., Limpens, J., Elberling, B., Gallagher, A., Li, B., Petrov, R. E., Maximov, T. C., & Van Huissteden, J. (2015). Permafrost collapse after shrub removal shifts tundra ecosystem to a methane source. *Nature Climate Change*, *5*(1), 67–70.

Neger, F. (1915). Rauchwirkung, Spätfrost und Frosttrocknis und ihre Diagnostik. *Thar. Forstl. Jb*, *66*, 195–212.

Nizinski, J. J., & Saugier, B. (1988). A model of leaf budding and development for a mature Quercus forest. *Journal of Applied Ecology*, 643–652.

North, G. B., & Nobel, P. S. (1997). Root-soil contact for the desert succulent Agave deserti in wet and drying soil. *New Phytologist*, *135*(1), 21–29.

Oberschelp, G. P. J., Guarnaschelli, A. B., Teson, N., Harrand, L., Podestá, F. E., & Margarit, E. (2020). Cold acclimation and freezing tolerance in three Eucalyptus species: A metabolomic and proteomic approach. *Plant Physiology and Biochemistry*, *154*, 316–327.

Oliveira, R. S., Dawson, T. E., Burgess, S. S., & Nepstad, D. C. (2005). Hydraulic redistribution in three Amazonian trees. *Oecologia*, *145*(3), 354–363.

Örvar, B. L., Sangwan, V., Omann, F., & Dhindsa, R. S. (2000). Early steps in cold sensing by plant cells: The role of actin cytoskeleton and membrane fluidity. *The Plant Journal*, *23*(6), 785–794.

Ostle, N. J., Smith, P., Fisher, R., Ian Woodward, F., Fisher, J. B., Smith, J. U., Galbraith, D., Levy, P., Meir, P., & McNamara, N. P. (2009). Integrating plant–soil interactions into global carbon cycle models. *Journal of Ecology*, *97*(5), 851–863.

Ottander, C., Campbell, D., & Öquist, G. (1995). Seasonal changes in photosystem II organisation and pigment composition in Pinus sylvestris. *Planta*, *197*(1), 176–183.

Pagter, M., & Arora, R. (2013). Winter survival and deacclimation of perennials under warming climate: Physiological perspectives. *Physiologia Plantarum*, *147*(1), 75–87.

Pagter, M., Hausman, J.-F., & Arora, R. (2011). Deacclimation kinetics and carbohydrate changes in stem tissues of Hydrangea in response to an experimental warm spell. *Plant Science*, *180*(1), 140–148.

Papendick, R., & Campbell, G. S. (1981). Theory and measurement of water potential. *Water Potential Relations in Soil Microbiology*, *9*, 1–22.

Parmentier, F.-J. W., Rasse, D. P., Lund, M., Bjerke, J. W., Drake, B. G., Weldon, S., Tømmervik, H., & Hansen, G. H. (2018). Vulnerability and resilience of the carbon exchange of a subarctic peatland to an extreme winter event. *Environmental Research Letters*, *13*(6), 065009.

Pearson, R. G., Phillips, S. J., Loranty, M. M., Beck, P. S., Damoulas, T., Knight, S. J., & Goetz, S. J. (2013). Shifts in Arctic vegetation and associated feedbacks under climate change. *Nature Climate Change*, *3*(7), 673–677.

Pelletier, J. D. (1997). Analysis and modeling of the natural variability of climate. *Journal of Climate*, *10*(6), 1331–1342.

Peñuelas, J., & Staudt, M. (2010). BVOCs and global change. *Trends in Plant Science*, *15*(3), 133–144.

Phoenix, G. K., & Bjerke, J. W. (2016). Arctic browning: Extreme events and trends reversing arctic greening. *Global Change Biology*, *22*, 2960–2962.

Pickard, W. F. (1981). The ascent of sap in plants. *Progress in Biophysics and Molecular Biology*, *37*, 181–229.

Powell, T. L., Galbraith, D. R., Christoffersen, B. O., Harper, A., Imbuzeiro, H. M., Rowland, L., Almeida, S., Brando, P. M., da Costa, A. C. L., & Costa, M. H. (2013). Confronting model

predictions of carbon fluxes with measurements of Amazon forests subjected to experimental drought. *New Phytologist*, *200*(2), 350–365.

Prentice, I. C., Bondeau, A., Cramer, W., Harrison, S. P., Hickler, T., Lucht, W., Sitch, S., Smith, B., & Sykes, M. T. (2007). Terrestrial ecosystems in a changing world. *Terrestrial Ecosystems in a Changing World. Springer, Berlin*, 175–192.

Preston, J. C., & Sandve, S. R. (2013). Adaptation to seasonality and the winter freeze. *Frontiers in Plant Science*, *4*, 167.

Prévost, J. H. (1980). Mechanics of continuous porous media. *International Journal of Engineering Science*, *18*(6), 787–800.

Prieto, I., Armas, C., & Pugnaire, F. I. (2012). Water release through plant roots: New insights into its consequences at the plant and ecosystem level. *New Phytologist*, *193*(4), 830–841.

Rammig, A., Jönsson, A. M., Hickler, T., Smith, B., Bärring, L., & Sykes, M. T. (2010). Impacts of changing frost regimes on Swedish forests: Incorporating cold hardiness in a regional ecosystem model. *Ecological Modelling*, *221*(2), 303–313.

Rantanen, M., Karpechko, A., Lipponen, A., Nordling, K., Hyvärinen, O., Ruosteenoja, K., Vihma, T., & Laaksonen, A. (2021). *The Arctic has warmed four times faster than the globe since 1980*.

Repo, T. (1991). *Rehardening potential of Scots pine seedlings during dehardening.*

Richardson, A. D., Anderson, R. S., Arain, M. A., Barr, A. G., Bohrer, G., Chen, G., Chen, J. M., Ciais, P., Davis, K. J., & Desai, A. R. (2012). Terrestrial biosphere models need better representation of vegetation phenology: Results from the N orth A merican C arbon P rogram S ite S ynthesis. *Global Change Biology*, *18*(2), 566–584.

Richardson, A. D., Andy Black, T., Ciais, P., Delbart, N., Friedl, M. A., Gobron, N., Hollinger, D. Y., Kutsch, W. L., Longdoz, B., & Luyssaert, S. (2010). Influence of spring and autumn phenological transitions on forest ecosystem productivity. *Philosophical Transactions of the Royal Society B: Biological Sciences*, *365*(1555), 3227–3246.

Richardson, A. D., Keenan, T. F., Migliavacca, M., Ryu, Y., Sonnentag, O., & Toomey, M. (2013). Climate change, phenology, and phenological control of vegetation feedbacks to the climate system. *Agricultural and Forest Meteorology*, *169*, 156–173.

Rinne, P. L., Kaikuranta, P. M., & Van Der Schoot, C. (2001). The shoot apical meristem restores its symplasmic organization during chilling-induced release from dormancy. *The Plant Journal*, *26*(3), 249–264.

Rinne, P., Welling, A., & Kaikuranta, P. (1998). Onset of freezing tolerance in birch (Betula pubescens Ehrh.) involves LEA proteins and osmoregulation and is impaired in an ABA-deficient genotype. *Plant, Cell & Environment*, *21*(6), 601–611.

Roberts, M. J., Vidale, P. L., Senior, C., Hewitt, H. T., Bates, C., Berthou, S., Chang, P., Christensen, H. M., Danilov, S., & Demory, M.-E. (2018). The benefits of global high resolution for climate simulation: Process understanding and the enabling of stakeholder decisions at the regional scale. *Bulletin of the American Meteorological Society*, *99*(11), 2341–2359.

Ruelland, E., Vaultier, M.-N., Zachowski, A., & Hurry, V. (2009). Cold signalling and cold acclimation in plants. *Advances in Botanical Research*, *49*, 35–150.

Sabater, M. (2019). *ERA5-Land Monthly Averaged from 1981 to Present*. Copernicus Climate Change Service (C3S) Climate Data Store (CDS).

Sakai, A. (1983). Comparative study on freezing resistance of conifers with special reference to cold adaptation and its evolutive aspects. *Canadian Journal of Botany*, *61*(9), 2323–2332.

Sakai, A., & Larcher, W. (1987). Low temperature and frost as environmental factors. In *Frost Survival of Plants* (pp. 1–20). Springer.

Sandve, S. R., & Fjellheim, S. (2010). Did gene family expansions during the Eocene–Oligocene boundary climate cooling play a role in Pooideae adaptation to cool climates? *Molecular Ecology*, *19*(10), 2075–2088.

Sangwan, V., Foulds, I., Singh, J., & Dhindsa, R. S. (2001). Cold-activation of Brassica napus BN115 promoter is mediated by structural changes in membranes and cytoskeleton, and requires Ca2+ influx. *The Plant Journal*, *27*(1), 1–12.

Savitch, L. V., Leonardos, E. D., Krol, M., Jansson, S., Grodzinski, B., Huner, N. P. A., & Öquist, G. (2002). Two different strategies for light utilization in photosynthesis in relation to growth and cold acclimation. *Plant, Cell & Environment*, *25*(6), 761–771.

Saxe, H., Cannell, M. G., Johnsen, Ø., Ryan, M. G., & Vourlitis, G. (2001). Tree and forest functioning in response to global warming. *New Phytologist*, *149*(3), 369–399.

Schluter, D. (2016). Speciation, Ecological Opportunity, and Latitude: (American Society of Naturalists Address). *The American Naturalist*, *187*(1), 1–18.

Scholz, F. G., Bucci, S. J., Arias, N., Meinzer, F. C., & Goldstein, G. (2012). Osmotic and elastic adjustments in cold desert shrubs differing in rooting depth: Coping with drought and subzero temperatures. *Oecologia*, *170*(4), 885–897.

Schuur, E. A., & Mack, M. C. (2018). Ecological response to permafrost thaw and consequences for local and global ecosystem services. *Annual Review of Ecology, Evolution, and Systematics*, *49*(1).

Screen, J. A., Deser, C., & Sun, L. (2015). Projected changes in regional climate extremes arising from Arctic sea ice loss. *Environmental Research Letters*, *10*(8), 084006.

Sellers, P. J., Mintz, Y., Sud, Y. e al, & Dalcher, A. (1986). A simple biosphere model (SiB) for use within general circulation models. *Journal of the Atmospheric Sciences*, *43*(6), 505–531.

Serreze, M. C., & Barry, R. G. (2011). Processes and impacts of Arctic amplification: A research synthesis. *Global and Planetary Change*, *77*(1–2), 85–96.

Serreze, M. C., & Francis, J. A. (2006). The Arctic amplification debate. *Climatic Change*, *76*(3), 241–264.

Shi, Y., Ding, Y., & Yang, S. (2018). Molecular regulation of CBF signaling in cold acclimation. *Trends in Plant Science*, *23*(7), 623–637.

Shin, H., Oh, Y., & Kim, D. (2015). Differences in cold hardiness, carbohydrates, dehydrins and related gene expressions under an experimental deacclimation and reacclimation in Prunus persica. *Physiologia Plantarum*, *154*(4), 485–499. https://doi.org/10.1111/ppl.12293

Sitch, S., Smith, B., Prentice, I. C., Arneth, A., Bondeau, A., Cramer, W., Kaplan, J. O., Levis, S., Lucht, W., & Sykes, M. T. (2003). Evaluation of ecosystem dynamics, plant geography and

terrestrial carbon cycling in the LPJ dynamic global vegetation model. *Global Change Biology*, *9*(2), 161–185.

Smit-Spinks, B., Swanson, B. T., & Markhart, A. I. (1984). Changes in water relations, water flux, and root exudate abscisic acid content with cold acclimation of Pinus sylvestris L. *Functional Plant Biology*, *11*(5), 431–441.

Speed, J. D., Woodin, S. J., Tømmervik, H., & Van der Wal, R. (2010). Extrapolating herbivore-induced carbon loss across an arctic landscape. *Polar Biology*, *33*(6), 789–797.

Sperry, J., Adler, F., Campbell, G., & Comstock, J. (1998). Limitation of plant water use by rhizosphere and xylem conductance: Results from a model. *Plant, Cell & Environment*, *21*(4), 347–359.

Sperry, J. S., Venturas, M. D., Anderegg, W. R., Mencuccini, M., Mackay, D. S., Wang, Y., & Love, D. M. (2017). Predicting stomatal responses to the environment from the optimization of photosynthetic gain and hydraulic cost. *Plant, Cell & Environment*, *40*(6), 816–830.

Sperry, J., & Tyree, M. (1990). Water-stress-induced xylem embolism in three species of conifers. *Plant, Cell & Environment*, *13*(5), 427–436.

Steponkus, P. L. (1984). Role of the plasma membrane in freezing injury and cold acclimation. *Annual Review of Plant Physiology*, *35*(1), 543–584.

Steponkus, P. L. (1993). A contrast of the cryostability of the plasma membrane of winter rye and spring oat-two species that widely differ in their freezing tolerance and plasma membrane lipid composition. *Advances in Low Temperature Biology*, *3*, 211–312.

Steudle, E. (2001). The cohesion-tension mechanism and the acquisition of water by plant roots. *Annual Review of Plant Biology*, *52*(1), 847–875.

Stevenson, R. K. (1994). *Dormancy and acclimation in dogwood clonal ecotypes*. University of Saskatchewan.

Stickley, C. E., St John, K., Koç, N., Jordan, R. W., Passchier, S., Pearce, R. B., & Kearns, L. E. (2009). Evidence for middle Eocene Arctic sea ice from diatoms and ice-rafted debris. *Nature*, *460*(7253), 376–379.

Stocker, T. (2011). *Introduction to climate modelling*. Springer Science & Business Media.

Strauss, G., & Hauser, H. (1986). Stabilization of lipid bilayer vesicles by sucrose during freezing. *Proceedings of the National Academy of Sciences*, *83*(8), 2422–2426.

Swann, A. L., Fung, I. Y., Levis, S., Bonan, G. B., & Doney, S. C. (2010). Changes in Arctic vegetation amplify high-latitude warming through the greenhouse effect. *Proceedings of the National Academy of Sciences*, *107*(4), 1295–1300.

Tai, H. H., Williams, M., Iyengar, A., Yeates, J., & Beardmore, T. (2007). Regulation of the β-hydroxyacyl ACP dehydratase gene of Picea mariana by alternative splicing. *Plant Cell Reports*, *26*(1), 105–113.

Teutonico, R. A., & Osborn, T. C. (1995). Mapping loci controlling vernalization requirement in Brassica rapa. *Theoretical and Applied Genetics*, *91*(8), 1279–1283.

Thomashow, M. F. (1999). Plant cold acclimation: Freezing tolerance genes and regulatory mechanisms. *Annual Review of Plant Biology*, *50*(1), 571–599.

Tranquillini, W. (1980). Winter desiccation as the cause for alpine timberline. *NZFS FRI Technical Paper*, *70*, 263–267.

Tranquillini, W. (1982). Frost-drought and its ecological significance. In *Physiological plant ecology II* (pp. 379–400). Springer.

Treharne, R., Bjerke, J. W., Tømmervik, H., & Phoenix, G. K. (2020). Extreme event impacts on CO2 fluxes across a range of high latitude, shrub-dominated ecosystems. *Environmental Research Letters*, *15*(10), 104084.

Tyree, M. T., & Sperry, J. S. (1989). Vulnerability of xylem to cavitation and embolism. *Annual Review of Plant Biology*, *40*(1), 19–36.

Tyree, M. T., & Zimmermann, M. H. (2002). Xylem dysfunction: When cohesion breaks down. In *Xylem structure and the ascent of sap* (pp. 89–141). Springer.

UCAR. (2020). *1. CLM5.0 User's Guide—Ctsm release-clm5.0 documentation*. https://escomp.github.io/ctsm-docs/versions/release-clm5.0/html/users_guide/index.html

Uemura, M., & Steponkus, P. L. (1997). Effect of cold acclimation on membrane lipid composition and freeze-induced membrane destablization. In *Plant cold hardiness* (pp. 171–179). Springer.

Ueno, S., Klopp, C., Leplé, J. C., Derory, J., Noirot, C., Léger, V., Prince, E., Kremer, A., Plomion, C., & Le Provost, G. (2013). Transcriptional profiling of bud dormancy induction and release in oak by next-generation sequencing. *BMC Genomics*, *14*(1), 1–15.

Ukkola, A. M., De Kauwe, M. G., Pitman, A. J., Best, M. J., Abramowitz, G., Haverd, V., Decker, M., & Haughton, N. (2016). Land surface models systematically overestimate the intensity, duration and magnitude of seasonal-scale evaporative droughts. *Environmental Research Letters*, *11*(10), 104012.

Umezawa, T., Nakashima, K., Miyakawa, T., Kuromori, T., Tanokura, M., Shinozaki, K., & Yamaguchi-Shinozaki, K. (2010). Molecular basis of the core regulatory network in ABA responses: Sensing, signaling and transport. *Plant and Cell Physiology*, *51*(11), 1821–1839.

Valentini, R., Mugnozza, G. S., Giordano, E., & Kuzminsky, E. (1990). Influence of cold hardening on water relations of three Eucalyptus species. *Tree Physiology*, *6*(1), 1–10.

Verhoef, A., & Egea, G. (2014). Modeling plant transpiration under limited soil water: Comparison of different plant and soil hydraulic parameterizations and preliminary implications for their use in land surface models. *Agricultural and Forest Meteorology*, *191*, 22–32.

Vikhamar-Schuler, D., Isaksen, K., Haugen, J. E., Tømmervik, H., Luks, B., Schuler, T. V., & Bjerke, J. W. (2016). Changes in winter warming events in the Nordic Arctic Region. *Journal of Climate*, *29*(17), 6223–6244.

Volaire, F. (2018). A unified framework of plant adaptive strategies to drought: Crossing scales and disciplines. *Global Change Biology*, *24*(7), 2929–2938.

Vyse, K., Pagter, M., Zuther, E., & Hincha, D. K. (2019). Deacclimation after cold acclimation—A crucial, but widely neglected part of plant winter survival. *Journal of Experimental Botany*, *70*(18), 4595–4604.

Walter, H. (1929). Die osmotischen Werte und die Kälteschäden unserer wintergrünen Pflanzen während der Winterperiode 1929. *Ber. Dtsch. Bot. Ges.*, *47*, 338–348.

Walter, H., & Thren, R. (1934). Die Berechnung des osmotischen Wertes auf Grund von kryoskopischen Messungen und der Vergleich mit Saugkraftbestimmungen. *Jahrbuch F\Hur Wissenschaft Der Botanik*, *80*, 20–35.

Wang, C. Y., & Wallace, H. A. (2004). Chilling and freezing injury. *The Commercial Storage of Fruits, Vegetables, and Florist and Nursery Stocks. Agriculture Handbook*, *66*.

Weckwerth, P., Ehlert, B., & Romeis, T. (2015). Zm CPK 1, a calcium-independent kinase member of the Z ea mays CDPK gene family, functions as a negative regulator in cold stress signalling. *Plant, Cell & Environment*, *38*(3), 544–558.

Weiser, C. J. (1970). Cold resistance and injury in woody plants: Knowledge of hardy plant adaptations to freezing stress may help us to reduce winter damage. *Science*, *169*(3952), 1269–1278.

Welling, A., Kaikuranta, P., & Rinne, P. (1997). Photoperiodic induction of dormancy and freezing tolerance in Betula pubescens. Involvement of ABA and dehydrins. *Physiologia Plantarum*, *100*(1), 119–125.

Welling, A., Moritz, T., Palva, E. T., & Junttila, O. (2002). Independent activation of cold acclimation by low temperature and short photoperiod in hybrid aspen. *Plant Physiology*, *129*(4), 1633–1641.

Welling, A., & Palva, E. T. (2006). Molecular control of cold acclimation in trees. *Physiologia Plantarum*, *127*(2), 167–181.

Welling, A., Rinne, P., Viherä-Aarnio, A., Kontunen-Soppela, S., Heino, P., & Palva, E. T. (2004). Photoperiod and temperature differentially regulate the expression of two dehydrin genes during overwintering of birch (Betula pubescens Ehrh.). *Journal of Experimental Botany*, *55*(396), 507–516.

Westhoff, M., Zimmermann, D., Schneider, H., Wegner, L. H., Geßner, P., Jakob, P., Bamberg, E., Shirley, S., Bentrup, F.-W., & Zimmermann, U. (2009). Evidence for discontinuous water columns in the xylem conduit of tall birch trees. *Plant Biology*, *11*(3), 307–327.

Wieder, W. R., Bonan, G. B., & Allison, S. D. (2013). Global soil carbon projections are improved by modelling microbial processes. *Nature Climate Change*, *3*(10), 909–912.

Wilhite, D. A., & Glantz, M. H. (1985). Understanding: The drought phenomenon: The role of definitions. *Water International*, *10*(3), 111–120.

Williams, M., Bond, B. J., & Ryan, M. G. (2001). Evaluating different soil and plant hydraulic constraints on tree function using a model and sap flow data from ponderosa pine. *Plant, Cell & Environment*, *24*(7), 679–690.

Williams, M., Malhi, Y., Nobre, A. D., Rastetter, E. B., Grace, J., & Pereira, M. G. (1998). Seasonal variation in net carbon exchange and evapotranspiration in a Brazilian rain forest: A modelling analysis. *Plant, Cell & Environment*, *21*(10), 953–968.

Wisniewski, M., Bassett, C., & Gusta, L. V. (2003). An overview of cold hardiness in woody plants: Seeing the forest through the trees. *HortScience*, *38*(5), 952–959.

Wisniewski, M., Nassuth, A., & Arora, R. (2018). Cold Hardiness in Trees: A Mini-Review. *Frontiers in Plant Science*, *9*, 1394. https://doi.org/10.3389/fpls.2018.01394

Wistuba, N., Reich, R., Wagner, H.-J., Zhu, J. J., Schneider, H., Bentrup, F.-W., Haase, A., & Zimmermann, U. (2000). Xylem flow and its driving forces in a tropical liana: Concomitant flow-sensitive NMR imaging and pressure probe measurements. *Plant Biology*, *2*(06), 579–582.

Wu, W., Lynch, A. H., & Rivers, A. (2005). Estimating the uncertainty in a regional climate model related to initial and lateral boundary conditions. *Journal of Climate*, *18*(7), 917–933.

Xu, X., Medvigy, D., Powers, J. S., Becknell, J. M., & Guan, K. (2016). Diversity in plant hydraulic traits explains seasonal and inter-annual variations of vegetation dynamics in seasonally dry tropical forests. *New Phytologist*, *212*(1), 80–95.

Yi, S., Woo, M., & Arain, M. A. (2007). Impacts of peat and vegetation on permafrost degradation under climate warming. *Geophysical Research Letters*, *34*(16).

Yue, C., Ciais, P., Luyssaert, S., Li, W., McGrath, M. J., Chang, J., & Peng, S. (2018). Representing anthropogenic gross land use change, wood harvest, and forest age dynamics in a global vegetation model ORCHIDEE-MICT v8. 4.2. *Geoscientific Model Development*, *11*(1), 409–428.

Zachos, J., Pagani, M., Sloan, L., Thomas, E., & Billups, K. (2001). Trends, rhythms, and aberrations in global climate 65 Ma to present. *Science*, *292*(5517), 686–693.

Zimmermann, U., Bitter, R., Marchiori, P. E. R., Rüger, S., Ehrenberger, W., Sukhorukov, V. L., Schüttler, A., & Ribeiro, R. V. (2013). A non-invasive plant-based probe for continuous monitoring of water stress in real time: A new tool for irrigation scheduling and deeper insight into drought and salinity stress physiology. *Theoretical and Experimental Plant Physiology*, *25*(1), 2–11.

Zimmermann, U., Schneider, H., Wegner, L. H., & Haase, A. (2004). Water ascent in tall trees: Does evolution of land plants rely on a highly metastable state? *New Phytologist*, *162*(3), 575–615.

Part II: Papers

I

Paper I: Inclusion of a cold hardening scheme to represent frost tolerance is essential to model realistic plant hydraulics in the Arctic-Boreal Zone in CLM5.0-FATES-Hydro

Marius S. A. Lambert, Hui Tang, Kjetil S. Aas, Frode Stordal, Rosie A. Fisher, Yilin Fang, Junyan Ding and Frans-Jan W. Parmentier

https://doi.org/10.5194/gmd-2022-136

Inclusion of a cold hardening scheme to represent frost tolerance is essential to model realistic plant hydraulics in the Arctic-Boreal Zone in CLM5.0-FATES-Hydro

Marius S. A. Lambert[1], Hui Tang[2,3,7], Kjetil S. Aas[2,4], Frode Stordal[2], Rosie A. Fisher[4], Yilin Fang[5], Junyan Ding[5] and Frans-Jan W. Parmentier[1,6]

[1]Centre for Biogeochemistry in the Anthropocene, Department of Geosciences, University of Oslo, 0315 Oslo, Norway
[2]Department of Geosciences, University of Oslo, 0315 Oslo, Norway
[3]Geo-Ecology Research Group, Natural History Museum, University of Oslo, 0562 Oslo, Norway
[4]CICERO - Center for International Climate Research, 0318 Oslo, Norway
[5]Pacific Northwest National Laboratory, Richland, WA, USA
[6]Department of Physical Geography and Ecosystem Science, Lund University, 223 62 Lund, Sweden
[7]Finnish Meteorological Institute (FMI), Climate System Research, Helsinki, Finland

Correspondence to: Marius S. A. Lambert (marius.lambert@geo.uio.no)

Abstract. As temperatures decrease in autumn, vegetation of temperate and boreal ecosystems increases its tolerance to freezing. This process, known as hardening, results in a set of physiological changes at the molecular level that initiate modifications of cell membrane composition and the synthesis of anti-freeze proteins. Together with the freezing of extracellular water, anti-freeze proteins reduce plant water potentials and xylem conductivity. To represent the responses of vegetation to climate change, land surface schemes increasingly employ 'hydrodynamic' models that represent the explicit fluxes of water from soil and through plants. The functioning of such schemes under frozen soil conditions, however, is poorly understood. Nonetheless, hydraulic processes are of major importance in the dynamics of these systems, which can suffer from e.g. winter 'frost drought' events.

In this study, we implement a scheme that represents hardening into CLM5.0-FATES-Hydro. FATES-Hydro is a plant hydrodynamics module in FATES, a cohort model of vegetation physiology, growth and dynamics hosted in CLM5.0. We find that, in frozen systems, it is necessary to introduce reductions in plant water loss associated with hardening to prevent winter desiccation. This work makes it possible to use CLM5.0-FATES-Hydro to model realistic impacts from frost droughts on vegetation growth and photosynthesis, leading to more reliable projections of how northern ecosystems respond to climate change.

1 Introduction

In the arctic-boreal region, winters are dark, typically last over 6 months, and average temperatures are low (generally around -20°C). To survive the harsh winters of this region, cold-adapted vegetation goes through a set of physiological and structural changes to avoid desiccation and frost mortality (Bansal et al., 2016; Chang et al., 2021). This capacity of plants to withstand freezing can be highly variable throughout the year – depending on the species and environmental factors such as light and temperature. In summer, the tolerance to freezing is low, but it slowly increases when exposed to a decrease in photoperiod and temperature (Beck et al., 2004)— a process known as cold acclimation (Li et al., 2004; Wisniewski et al., 2018). Cold-acclimation triggers multiple physiological and biochemical responses which enable plants to i) tolerate extracellular ice formation and the resulting cellular dehydration (Levitt, 1980; Janská et al., 2010), ii) avoid the formation of interstitial ice crystals by keeping tissues isolated from the cold and/or by regulating nucleation. Ice nucleation can be suppressed down to -38°C if biological antifreeze proteins such as dehydrins and flavonoids are synthetized (Hanin et al., 2011) – a process called supercooling. Between -20°C and -30°C, the formation of intracellular glass (vitrification) further enables cold acclimated woody plants to develop a resistance to much lower temperatures. Trees in northern latitudes have evolved resistance to naturally occurring temperatures as low as -70°C (Sakai, 1983), whereas herbaceous plants can rarely tolerate < -25°C. Experiments have demonstrated that trees can resist the temperature of liquid nitrogen (-196°C) when regulating ice nucleation (Rinne et al., 1998).

Plants exposed to temperatures below their tolerance threshold (which varies as a function of time and environmental conditions) suffer from 1) mechanical stress, due to the intercellular ice crystallization and fragility of the tissues, and 2) osmotic dehydration due to the freezing of intercellular water. Therefore, the increased survival of plant cells and tissues is the evolutionary benefit of cold acclimation. The two strategies of tolerance and avoidance are often found simultaneously in the same plant. Cold acclimation strategies, rates and ranges involve complex species-dependent physiological and gene expression changes (Chinnusamy et al., 2006; Welling and Palva, 2006).

The physiological adaptations induced by cold acclimation have a large impact on the hydraulics of plants. Apoplastic ice formation and the increased viscosity of protein-bound water particles are known to reduce water flow (Dowgert and Steponkus, 1984; Gusta et al., 2005; Smit-Spinks et al., 1984). In addition, water stress resulting from deeply frozen soils with low soil water potentials triggers slow developmental changes in the root structure to increase their impermeability and reduce water loss (Beck et al., 2007; Kreszies et al., 2019; North and Nobel, 1995). Other strategies include the creation of an air gap during root shrinkage (Carminati et al., 2009; North and Nobel, 1997) and the inhibition of conducting channels (Knipfer et al., 2011; Lee et al., 2005; Ye and Steudle, 2006). Since water transport is prohibited in cold-acclimatized tissues, growth is also affected and it is important that plants de-acclimate rapidly in spring to re-activate their metabolism.

Plant hydraulics, apart from its critical role in the survival of plants during droughts, is also a major driver of species distribution (Fontes, 2019; Lopez-Iglesias et al., 2014; Navarro et al., 2019; Rasztovits et al., 2014). Species distribution is shaped by mortality and recruitment, and the ability of species to survive under periods of low water availability depends on

their hydraulic traits (Greenwood et al., 2017). Tolerance to and delay of desiccation, for example, involve traits such as greater resistance to embolism (i.e. interruption of water flow through plant conductive vessels), the ability of cells to remain alive at low water levels and the reduction of water loss (Kursar et al., 2009; Tyree et al., 2003).

Despite its importance, terrestrial biosphere models typically rely on simple approaches to represent plant hydraulics, involving an extension of Darcy's law. Darcy stated that the flux of water anywhere in the soil plant continuum was proportional to the hydraulic conductivity and the water potential gradient (Darcy, 1856). One of the simplest implementations of this is to model soil-root conductance as a function of soil moisture (Jarvis and Morison, 1981; Bonan et al., 2014). In more complex models, variable xylem conductance and water potential are added (Williams et al., 2001; Duursma and Medlyn, 2012). One of the most advanced approaches is the continuous porous media approach (Edwards et al., 1986; Sperry et al., 1998; Christoffersen et al., 2016; Mirfenderesgi et al., 2016) which extends the water mass balance in the soil-plant-atmosphere continuum by relating changes in water content directly to water potential and vice-versa. Analogous to the retention curves in soil physics, the model uses the explicit relationship between water content and potential in plant xylem (pressure-volume curves). The use of plant traits to parameterize such models, as well as their ability to predict measurable features of plant water relations (leaf water potential, sap flow) makes these models attractive from the perspective of both realism and connection to data. Furthermore, such models enable bidirectional water flow through root tissue. Reverse flow from roots to soil is an important process for hydraulic redistribution and tissue dehydration in case of extreme drought (Oliveira et al., 2005; Nadezhdina et al., 2010; Prieto et al., 2012). A hydraulic model incorporating these advanced mechanisms has recently been included in the Functionally Assembled Terrestrial Ecosystem Simulator (FATES).

FATES is a size and age-structured representation of vegetation dynamics which can be coupled to a land surface model or an Earth system model (Christoffersen et al., 2016). CLM (Lawrence et al., 2019) and the Energy Exascale Earth System Model (E3SM), have both been coupled to FATES and it is used by numerous scientists across the globe to simulate land surface processes (Koven, 2019).

The new plant hydraulics scheme in FATES was initially developed for specific sites in the tropics, and to our knowledge, porous-media hydraulics models have not been applied extensively, if at all, in high latitude or cold systems. Thus, the physiology of plant hydraulics in winter is generally not well represented in such schemes. The default scheme, for example, stored plant water remains liquid even when temperatures drop below zero and plant gas exchange can continue in the event of frozen soils. In the cold regions of the world, extreme winters can cause soils to freeze to temperatures well below -20°C. Such cases lead to extremely low water potentials in the soil compared to the plant, while the model assumes that water remains liquid inside the plant. Due to this difference in water potential, soils tend to pull water from vegetation, depleting plant storage pools and incurring large amounts of hydraulic failure mortality in the model.

In this study, we investigate how a model can represent the processes that lead to cold acclimation by implementing a hardening scheme into the CLM5-FATES-Hydro demographic land surface model. The scheme that represents hardening is configured such that cold-acclimated plants reduce conductances along the soil-plant-atmosphere continuum and the rate for hydraulic failure mortality. We explore additional configurations of the scheme where hardening of plants led to changing pressure

volume curves, and a reduction of the carbon starvation mortality. The modification of these parameters is intended to mimic the physiological changes plants go through when acclimating to cold and the reduction in their metabolic and water transport capacities. Finally, we assess the sensitivity of the model to the parameters of the hardening scheme (maximum hardiness level and timing of dehardening). We hypothesize that the changes prescribed by the hardening scheme (a) are necessary to model realistic vegetation growth in cold climates, and (b) make it possible to use CLM5-FATES-Hydro to model realistic impacts from frost droughts on vegetation growth and photosynthesis, leading to more reliable projections of how northern ecosystems respond to climate change.

2 Methods

2.1 The model

CLM5.0-FATES-Hydro stands for the fifth version of the Community Land Model, coupled to the Functionally Assembled Ecosystem Simulator (FATES) with the modified trait based hydraulic scheme (Hydro-TFS). In this context, CLM5.0 represents the biogeophysical aspects of the land surface, including the energy balance, soil hydrology, biophysics and cryospheric processes, as well as soil biogeochemistry and other land surface types (lakes, urban, glaciers, crops) (Lawrence et al., 2019).

2.1.1 FATES

FATES (Fisher et al., 2015; Koven, 2019) is a cohort-based vegetation demographic model. It has been integrated into CLM5.0 to represent vegetation processes and dynamics wile tracking the vertical (in terms of plant height), spatial (in terms of successional age) and biological (in terms of plant functional type) heterogeneity of terrestrial ecosystems. When coupled to the CLM5.0 FATES handles all processes related to live vegetation (inclusive of photosynthesis, stomatal conductance, respiration, growth, and plant recruitment and mortality) as well as fire and litter dynamics.

2.1.2 Hydro

The 'Hydro' configuration of FATES is a plant hydrodynamic model. Originally developed by Christoffersen et al. (2016), it follows a continuous porous media approach based on the soil-plant-atmosphere continuum described by Sperry et al. (1998). A single mass balance equation describes the coupled soil-plant system, and the relationship between plant water storage and plant water potential is explicitly described. It consists of a discretization of the soil-plant continuum in a series of water storage compartments with variable heights, volumes, water retention and conducting properties (Fig. 1).

Trees are divided into 4 types of porous media (leaf, stem, transporting and absorbing roots). Each above ground plant medium and transporting roots consists of a single storage pool, while absorbing roots are divided in vertical compartments by soil layer. The water pools are connected by pathways with defined lengths and conductances. The soil is divided in cylindrical

"shells" around the absorbing roots (the rhizosphere), and hydraulic properties are constant across compartments within a given soil type.

The hydraulics in this scheme are governed by the relationships between content, potential and conductivity of plant tissues. The model requires parameterization of: (1) tissue water content vs. potential (the pressure-volume or PV curve), (2) water potential vs. conductivity of plant tissues and (3) leaf water potential vs. stomatal conductance stress factor. The first two relationships concern every pool within the plant–soil continuum and follow specific equations for plant and soil porous media types. For the soil, we used the formulation of Clapp-Hornberger and Campbell to describe the first two relationships (Campbell, 1974; Clapp and Hornberger, 1978). For the plant, the first relationship (PV curve) is described by two terms: a) the solute potential (<0 due to the presence of solutes), and b) the pressure potential (>=0 due to cell wall turgor) (Ding et al., 2014; Tyree and Hammel, 1972). The cell wall turgor pressure is the hydrostatic force that pushes the membrane against the cell wall in excess of ambient atmospheric pressure (Fricke, 2017). The equations to calculate the solute and pressure potentials depend on parameters such as the osmotic potential at full turgor (pinot) and the elastic bulk modulus (epsil). The second relationship (linking plant water potential and conductivity) is calculated using the inverse polynomial of Manzoni et al. (2013) for the xylem vulnerability curve. The fractional loss of total conductance retrieved from this equation is defined at each compartment boundary (Fig. 1) and used to calculate the maximum conductance, K_{MAX}. This parameter depends on plant architectural properties and maximum xylem-specific conductivity, and it relates to the maximum attainable flow of water through the xylem. The fraction of maximum stomatal conductance is used to down-regulate the non-water stressed stomatal conductance (calculated using Ball-Berry (1987) formulations).

All parameters involved in these relationships are biologically interpretable and measurable plant hydraulic traits. The numerical solution operates every half hour (time-step) and updates water contents and potentials throughout the plant soil continuum.

2.1.3 The 2D solver

A crucial component of the porous media hydrodynamics model is the solver used at each time step to find a solution for cohort level water fluxes. The first solver implemented in FATES was a tri-diagonal and 1-dimensional (series of compartments) matrix solver solving the water transport in the plant and rhizosphere soil a layer at a time. Since the solver was not capable of quickly finding a solution during extreme winter conditions, a more efficient two-dimensional (2D) solver using Newton iterations, has been implemented as a replacement. In this solution, the water potentials in plant and rhizosphere soils are solved together as prognostic variables. Although the new solver improves the quality of the solution and reduces errors, we ran into numerous solver errors when running simulations in Siberia. In very cold soils, extremely low water potentials (-40 000 MPa) lead to extremely high matric water gradients and prevent successful solution of the flow equations (despite increases of the time resolution and number of iterations). In the frozen soil scheme of CLM5, liquid water becomes absent when soils freeze, leading to infinitely small water potentials. Our solution to this problem was twofold:

1) The calculation of supercooling in soils is limited to -10°C since soil temperature can decrease to -40°C in the uppermost soil layers at extremely cold locations, i.e., East Siberia. This solution yields higher water potential values at all times.

2) We imposed a minimum value on the calculation of soil matric potential from liquid water content of -25 Mpa and a linear interpolation was used from -25 MPa to -35 Mpa. This implementation allows the solver to efficiently find a solution.

Large rates of water percolation and drainage from upper to deeper soil layers has been reported in earlier modelling simulations in Siberia (Sato et al., 2010). Our focus is on the physiology of hardening and not on the supply and demand dynamics of soil moisture, hence we prescribed a depth to bedrock of 1m in all simulations.

2.2 The hardening scheme

The temporal dynamics of plant hardiness implemented in this study are based on the work by Rammig et al. (2010). In their model, the hardiness level (*HD*, in °C) is calculated on a daily basis using three functions: the target hardiness (*TH*, in °C), the hardening rate (*HR*, in °C day^{-1}), and the dehardening rate (*DR*, in °C day^{-1}) (Fig. 2). In this context, *HD* is variable throughout the year and represents the minimum temperature plants can withstand without incurring injury.

Once a value has been assigned to *TH*, *HR* and *DR*, depending on the daily mean 2m air temperature, the model operates as follows: if *TH* is lower than the HD of the previous day (*HDP*), then *HR* is removed from *HDP*. By contrast, if *TH* is higher than *HDP*, *DR* is added to *HDP* (Eq. 1). To illustrate Eq. (1) and the interrelation between *HDP* and *HD*, figure S14 shows the temporal evolution of *TH* and *HD* during two random years.

$$HD = \begin{cases} HDP - HR\,, & if\ HDP > TH \\ HDP + DR\,, & if\ HDP \leq TH \end{cases} \quad (1)$$

The parameters required for the hardening Scheme by Rammig et al. (2010) are: the minimum hardiness level (H_{MIN}); -2°C, the maximum hardiness level (H_{MAX}); -30°C, *HR*; 0.1-1°C day^{-1}, *DR*; 0-5°C day^{-1} and several time dependent parameters used to define the seasons for hardening and dehardening. This scheme was developed to fit the climate of central Sweden (Farstanäs) and measurements of Norway spruce (Picea Abies). Parameters for the hardening scheme (Table S1) were retrieved from Kellomaki et al. (1995), Jönsson et al. (2004) and Bigras & Colombo (2013).

Due to the large climatic differences between Sweden and East Siberia, it is unlikely that the original scheme from Rammig et al. will perform well at Spasskaya Pad. To deal with this, in our adaptation of the hardening model, H_{MAX} becomes site- and time- dependent (to function globally and account for evolution associated to changes in climate), and varies with the 5 year running mean of the annual minimum of daily mean air temperature at 2m height (*T5*). An exception is made during the first five simulation years. During the first year, H_{MAX} is based on the minimum temperature of the current year, while from the second to fifth years, it is based on the mean of the minimum temperature of the preceding years. H_{MAX} can be anywhere between H_{MIN} (-2°C) and a maximum of -70°C (typical in the Arctic and East Siberia) (Sakai, 1983). The functions used to calculate *TH* (Eq. 2), *HR* (Eq. 3) and *DR* (Eq. 4) were made dependent of H_{MAX} so that vegetation can harden and deharden faster at colder sites where H_{MAX} is lower (Fig. 2 shows the functions for H_{MAX} = -70°C).

1) Target hardiness (*TH*)

$$TH = \begin{cases} H_{MAX} & , \ if\ T \le \frac{H_{MAX}}{1.5} \\ H_{MIN} & , \ if\ T \ge 6 - \frac{H_{MAX}}{6} \\ -sin\left(\pi * \left(0.5 + \frac{T - \frac{H_{MAX}}{1.5}}{-\frac{Hmax}{1.5} + \left(6 - \frac{H_{MAX}}{6}\right)}\right)\right) * \frac{H_{MIN} - H_{MAX}}{2} - \frac{H_{MIN} - H_{MAX}}{2} + H_{MIN} & , \ if\ \frac{H_{MAX}}{1.5} \le T \le 6 - \frac{H_{MAX}}{6} \end{cases} \quad (2)$$

2) Hardening rate (*HR*)

$$HR = \begin{cases} \frac{H_{MAX} - H_{MIN}}{-31.11} + 0.1 & , \ if\ T \le \frac{H_{MAX}}{2} \\ 0.1 & , \ if\ T \ge 20 \\ \sin\left(\pi * \left(0.5 + \frac{T - \frac{H_{MAX}}{2}}{-\frac{H_{MAX}}{2} + 20}\right)\right) * \left(\frac{H_{MAX} - H_{MIN}}{-62.22}\right) + \left(\left(\frac{H_{MAX} - H_{MIN}}{-62.22}\right) + 0.1\right) & , \ if\ \frac{H_{MAX}}{2} \le T \le 20 \end{cases} \quad (3)$$

3) Dehardening rate (*DR*)

$$DR = \begin{cases} 0 & , \ if\ T \le 2.5 \\ 5 * \frac{H_{MAX} - H_{MIN}}{-31.11} & , \ if\ T \ge 12.5 \\ (T - 2.5) * \left(\frac{H_{MAX} - H_{MIN}}{-62.22}\right) & , \ if\ 2.5 \le T \le 12.5 \end{cases} \quad (4)$$

In Rammig et al. (2010), the hardening period is prevented until the 210th Julian day and a growing degree day threshold is reached. We instead use a site specific daylength threshold (*DaylThresh*) depending on the temperature index T5 of the corresponding site (Eqs. 5, 6). A site dependent value for *DaylThresh* is essential since vegetation at colder sites must start to harden earlier, and the correlation between photoperiod and temperature is not the same at all locations. Finally, to avoid dehardening in autumn, we keep *HD* fixed during the hardening-only period of the year in cases where *TH* is not below *HDP* (Eq. 6). In our version of the hardening scheme, if the requirements of Eq. (6) are met, the value given to *HD* in Eq. (1) will be overwritten.

$$DaylThresh = 42000 + ((-30 - max(-60, min(0, T5)))/15) * 4500 \quad (5)$$

$$HD = \begin{cases} HDP - HR\ , if\ daylength \le DaylThresh, daylength\ decreases\ and\ HDP > TH \\ HDP\ \ \ \ \ \ , if\ daylength \le DaylThresh, daylength\ decreases\ and\ HDP \le TH \end{cases} \quad (6)$$

At the end of the time-step, values of *HD* outside of the range between H_{MIN} and H_{MAX} will be redefined within these extremes according to Eq. (7).

$$HD = \begin{cases} H_{MIN}, \ if\ HD > H_{MIN} \\ H_{MAX}, \ if\ HD < H_{MAX} \end{cases} \quad (7)$$

2.3 Physiological impacts of hardening state on plants

Rammig et al. (2010) used the prognostic hardening state to directly modulate the degree to which frost damages plants. In this study, to enhance the mechanistic basis of the simulations, we used the 'hardening' state to simulate the impact of hardening on the hydraulic functioning of the plant, both in terms of the benefits of hardening (i.e. prevention of desiccation) and the physiological costs (reduced ability to conduct water and photosynthesize during the hardening and dehardening phases). We did this by modifying K_{MAX}, *g0* & *g1* and the hydraulic failure mortality scalar (see "version zero" simulation in

Table 1). We then explore additional configurations of the scheme where hardening of plants led to changing PV curves, and a reduction of the carbon starvation mortality.

2.3.1 Maximum conductance between plant compartments (K_{MAX})

In FATES-hydro, K_{MAX} is calculated on the upstream (towards the soil) and downstream (towards the atmosphere) sides of each water compartment connection along the soil-plant continuum. The water potential of the system impacts the direction of the flow and thereby the applicable root radial conductance.

During hardening and water stress, apoplastic ice formation, increased viscosity of protein-bound plant water particles, the increased impermeability of root structures and the inhibition of conducting channels reduce water flow (Dowgert and Steponkus, 1984; Gusta et al., 2005; Smit-Spinks et al., 1984). Therefore, when the hardening scheme is turned on and the hardening level of plants (*HD*) is lower than -3°C (-2°C plus -1°C as margin), the level of hardening is used to exponentially reduce each of the calculated K_{MAX} values along the soil-plant continuum. In "version zero" (Table 1), K_{MAX} was reduced by $10^{\left(\frac{HD+3}{11}\right)}$ (Eq. 7).

$$K_{MAX} = K_{MAX} * 10^{\left(\frac{HD+3}{11}\right)},\ if\ HD < -3 \quad (7)$$

2.3.2 Stomatal conductance (g0 and g1)

The calculation of stomatal conductance in this version of FATES-hydro is based on the Ball-Berry stomatal conductance model. This scheme is typically applied globally, and its parameters and function are not responsive to plant hardening status by default. This means that in winter, when soils are frozen, water loss can still deplete tissue water contents. To prevent desiccation in our scheme, we modify the parameters of the stomatal conductance model as a function of hardening status. The stomatal model has two parameters, the 'minimum' conductance, *g0* which is the stomatal conductance when photosynthesis reaches zero. In the default setup, *g0* is fixed at $10\,000\ \frac{\mu mol}{m^2 * s}$ for both evergreen needleleaf and deciduous broadleaf trees. The second parameter, *g1* is the slope of the Ball-Berry stomatal conductance model and is fixed at 8 for all C3 PFTs in the default setup. In our simulations, if *HD* is lower than -3°C, *HD* reduces *g0* and *g1* in a similar way as the reduction of K_{MAX} (Eqs. 8, 9). In the version zero simulation we reduced *g0* and *g1* by $10^{\left(\frac{HD+3}{40}\right)}$ (Eqs. 8, 9) (Table 1).

$$g0 = g0 * 10^{\left(\frac{HD+3}{40}\right)},\ if\ HD < -3 \quad (8)$$

$$g1 = g1 * 10^{\left(\frac{HD+3}{40}\right)},\ if\ HD < -3 \quad (9)$$

2.3.3 Hydraulic failure mortality (HFM)

In the default version of FATES-Hydro, HFM (the hydraulic failure mortality) is triggered when the fractional loss of conductivity (*flc*) is larger than a predetermined threshold (*flcThreshold*, set at 0.5). The fractional loss of conductivity is multiplied by a scalar (*MortScalar*, 0.6 in default FATES) that converts the proximal cause of mortality (conductance loss)

into a cohort-specific rate of mortality (fraction /year) (Eq. 10). As shown in the result section, the default parametrization of HFM used at these cold climate sites, leads to systematic, large and uninterrupted mortality rates throughout the winter on account of desiccation. Since cold acclimated plants are typically dormant (Chang et al., 2021), and dormant plants are known to have a slower or interrupted metabolism, we tested a scenario where we reduced HFM with H_{RATE}. H_{RATE} is a version of *HD* normalized to the value of H_{MAX} (Eq. 11). H_{RATE} was preferred to *HD* in the reduction of HFM so that if *HD* is equal to H_{MAX}, the reduction of HFM is at a maximum. In the control hardening simulation we reduced HFM by up to 50% at *HD* equal H_{MAX} Eq. (12). In the two sensitivity experiments conducted on HFM, we modified the occurrences of 50% in Eq. (12) to obtain a reduction reaching 100% and 0% respectively (Table 1).

$$HFM = \frac{flc - flcThreshold}{1 - flcThreshold} * MortScalar \quad (10)$$

$$H_{RATE} = \frac{HD - H_{MAX}}{H_{MIN} - H_{MAX}} \quad (11)$$

$$MortScalar = MortScalar * (Hrate * 50\% + 50\%),\ if\ HD < -3 \quad (12)$$

2.3.4 Pressure volume curve

PV curves describe the relationship between total water potential and relative water content in the soil and the plant compartments. The formulation of the plant compartment PV curves in FATES-Hydro relies on a set of parameters: osmotic water potential at full turgor/saturation (pinot), bulk elastic modulus (epsil), saturation volumetric water content, residual volumetric water content, capillary region parameters and relative water content at full turgor (see description of FATES-Hydro in the model description subsection of the methods). Among these parameters, literature has shown that pinot and epsil are highly variable, depending on water deficiency. Stressors that induce water deficiency (e.g. drought, cold and frost) trigger similar responses at the cellular and molecular level. To maintain turgor during stress (Beck et al., 2007) or during hardening (Valentini et al., 1990), plant organs increase their solute concentration which decreases pinot and they increase the elasticity of their cell walls which corresponds to a decrease in epsil (Bartlett et al., 2012; Kuprian et al., 2018). While research on desert shrubs has shown that epsil increased by roughly 10 Mpa during winter (Scholz et al., 2012), literature reveals that pinot easily decreases by 0.5 MPa with hardening and during drought stress (Mart et al., 2016; Valentini et al., 1990).

In this section we describe how we made the PV curves for plant mediums vary throughout the year depending on *HD* (Fig. 3). We lowered the PV curves while daily updating the osmotic potential at full turgor and the elastic bulk modulus (Eqs. 13, 14). At an *HD* of -70°C, we lower the default pinot values for leaves (-1.465984), stems (-1.22807) transporting roots (-1.22807) and absorbing roots (-1.043478) by 0.5 Mpa. The default epsil values (for leaves: 12, stems: 10, absorbing roots: 10 and transporting roots: 8) are increased by 10 MPa at an *HD* of -70°C. Unless *HD* gets below -3°C, the default Hydro PV curve is used, while at its lowest (-70°C), the PV curves are maximally modified. The changes to pinot and epsil modify the shape of the PV curve so that a given water content is linked to a lower water potential.

$$Pinot = DefaultPinot - \left(1 - \frac{HD+70}{67}\right) * 0.5 \quad (13)$$

$$Epsil = DefaultEpsil + \left(1 - \frac{HD+70}{67}\right) * 10 \quad (14)$$

2.3.5 Carbon starvation mortality (CSM)

Similarly to HFM, CSM (the carbon starvation mortality) is triggered when the carbon stored in the leaves is below a target level, and the fraction of carbon is multiplied by a fixed scalar (set at 0.6 for all plant functional types). CSM is incurred each winter creating an annual cycle for living biomass of evergreen trees in temperate and boreal regions. In the version zero simulation, CSM is not reduced (Table 1). In the sensitivity experiments, CSM was reduced following the same method as for HFM (Eq. 12).

2.4 Experimental setup

Simulations were carried out using CLM5.0-FATES-Hydro, with fully prognostic state variables for vegetation, litter, and soil. The atmospheric forcing to drive the model simulations was derived from ERA5-Land data (ERA5L) (ERA5-Land Monthly Averaged from 1981 to Present). ERA5L provides hourly global high resolution (9km) information on surface variables from January 1981 to present day, which makes it a valuable dataset for our hardening scheme analysis. In this study, we retrieved temperature at reference height, wind, humidity, surface pressure, precipitation, downward shortwave radiation and downward longwave radiation for the entire period. Each simulation was run for 90 years in which the atmospheric forcing from the 30-year period between 1981 and 2011 was repeated three times. These three periods are depicted as the years 1921 to 2011 for convenience.

2.4.1 Site descriptions

We conducted site-specific simulations for Farstanäs (in Sweden), and near Spasskaya Pad (in Russia). These locations were selected to verify and illustrate the behavior of the hardening scheme in distinctly different climates.

1) Spasskaya Pad is a scientific research station in the taiga near Yakutsk, Russia (62°N and 129°E), the coldest large city in the world, with an annual average temperature of roughly -9°C. Spasskaya Pad has never recorded a temperature above freezing between the 10th of November and the 14th of March and the average winter temperature is below -20°C. However, the warm summers (with a July average and highest daily mean temperatures of ~20°C and ~25°C respectively) place Spasskaya Pad far south from the tree line. The total yearly precipitation is around 280 mm, and the snow depth typically reaches 40 cm. Spasskaya Pad is in the center of Yakutia, the largest republic of the Russian Federation, which is mostly covered by boreal vegetation (74%) (Isaev et al., 2010). The forests are mainly composed of Larch (deciduous needleleaf), patches of Scots pine (evergreen needleleaf) on sandy soil (Sugimoto et al., 2002), dwarf Siberian pine (*Pinus pumila*) and to a lesser extent Siberian spruce (*Picea omorika*), and small stands of birch (*Betula*), fir (*Abies*) and aspen (*Populus*).

2) Farstanäs (59°N and 17°E) is slightly south of Stockholm and presents a cold temperate climate. The mean yearly temperature is around 5.5°C and the total yearly precipitation is around 800 mm. The vegetation at Farstanäs is a mixed forest with, among others, spruce, pine, beech, oak, elm, ash, and maple.

2.4.2 Plant functional type

To remove species competition and better understand the impacts of hardening on vegetation growth, we performed each simulation with only one plant functional type. We tested the scheme on two plant functional types: extratropical evergreen needleleaf trees and cold-deciduous broadleaf trees. Although evergreen needleleaf trees are not the dominant plant type at Spasskaya Pad (Petrov et al., 2011; Tatarinova et al., 2017; Hamada et al., 2004), we selected this location since it is one of the most extreme (cold and dry) climates where pine trees still exist. Therefore, we expect that the benefit from introducing a cold hardening scheme may be particularly apparent at this location. Results from broadleaf deciduous simulations are included in the supplemental (Fig. S3). Note that soil conditions, including matric potential, are similar in deciduous and evergreen simulations (Fig. 4).

2.4.3 Main simulations

In the first part of our results we compare the implementation of the new hardening scheme (version zero) into CLM5-FATES-Hydro to the default version of the model. In the version zero of the hardening scheme, cold-acclimated plants reduce I) the maximum conductance between plant tissues, and between roots and soil (K_{MAX}), II) both the intercept and the slope of the stomatal conductance model, and III) the rate for hydraulic failure mortality (HFM) (Table 1). For the version zero simulation, the values for the reductions of K_{MAX}, *g0* and *g1*, *DR* and H_{MAX} were selected based on preliminary testing to minimize winter water losses and to maximize vegetation biomass at Spasskaya Pad and Farstanäs. In the version zero hardening simulation, dehardening (*DR*) is described by a linear function that increases from 2.5°C to 12.5°C for evergreen trees (Eq. 4). For reasons discussed further down, the PV modifications were not selected in the version zero.

2.4.4 Sensitivity experiments

To test the sensitivity of vegetation growth to the amplitude at which K_{MAX}, *g0* & *g1* and HFM are modified by hardening, we tested individual modifications for each of these parameters (Table 2). Compared to the magnitude of the reductions selected in the version zero simulation, we selected both stronger and weaker reductions for the sensitivity experiments. Additional simulations were run to assess the impact of g0 and g1 independently from each other. We further tested extra implications which cold acclimation may have on processes in FATES-Hydro, such as the modification of PV curves and the reduction of CSM with hardening (Table 2). For CSM, the reductions with hardiness follow the same method as for HFM (Eq. 12). In contrast to the other CSM experiments, the one called “50% all year” does not depend on the hardiness level but directly on H_{MAX} instead. Two additional sensitivity experiments were performed on the temperature range of the dehardening rate (*DR*) and on the maximum hardiness level (H_{MAX}) – parameters involved in the calculation of the hardiness level (Table 2). To

evaluate the sensitivity of the hardening scheme to *DR*, we ran an experiment where the *DR* function increases between 0° and 10°C and an experiment where *DR* increases between 5°C and 15°C (Table 2). While H_{MAX} is defined as T5 minus 10°C in the version zero simulation, we ran experiments where H_{MAX} was defined by T5 minus 5°C and T5 minus 15°C.

3 Results

3.1 Hardening to survive in the arctic

At full spin-up, the default CLM5.0-FATES-Hydro model, without hardening, yielded evergreen tree biomass of ~40 MgC ha^{-1} at Farstanäs and only ~0.2 MgC ha^{-1} at Spasskaya Pad (Fig. 4a and b). After inclusion of the hardening scheme, larger biomass levels are simulated in Spasskaya Pad (~4.5 MgC ha^{-1}), and similar levels at Farstanäs (~42 MgC ha^{-1}).

In Spasskaya Pad, the temperature of the top soil layers drops below -20°C each winter (Fig. 5d). The resulting low liquid water content of the soil leads to such low matric potentials that the default model systematically simulates a release of water from the plant to the frozen soil (Fig. 6d). The root water release is strongest in autumn when soils start to freeze, but it can continue deep into the winter as long as plants still have stored water and the soil matric potential decreases further. If the top soil temperature remains higher than -25 °C, our results show that winter dehydration typically leads to plant matric potentials higher than -15 MPa (Fig. 7b). During extreme years with top soil temperatures below -25 °C, the matric potential in plant tissues can sometimes get as low as -28 MPa. The repetition of long lasting low soil matric potentials one winter after the other, resulted in large HFM rates (> 55 % individuals $year^{-1}$) (Fig. 8a and b). The sum of HFM, CSM and other minor mortalities, outweighs the summer productivity of needleleaf trees in Spasskaya Pad (Figs. 4b and S4b).

When the hardening model is employed in FATES-hydro, low winter temperatures at Spasskaya Pad mean that *HD* quickly reaches the fixed limit of -70°C (Fig. 10). This results in a strong reduction of I) K_{MAX}, II) *g0* & *g1* and III) HFM (See methods above and sensitivity sections below). The reduction of K_{MAX} between tissues, and especially between absorbing roots and the first rhizosphere, greatly reduces the amplitude of reverse water flow through the roots when soils are frozen (Fig. 5c and d).

The temporal dynamics of the hardening model allow for cold-induced damage. For example, if temperatures drop abruptly below freezing in autumn, plants won't have acclimated yet and the amplitude of the reverse water flux will therefore be similar to the default model. However, as plants start acclimating, the resistance to water flux increases and root water exudation is inhibited by the hardening scheme. The second implication of hardening in our hydraulically-adapted hardening scheme plants is the reduction of *g0* & *g1*. This reduces transpiration in spring and enables leaves to maintain their water potential while plants are still cold acclimated. The reduction of the conductances ($K_{MAX,}$ *g0* and *g1*) results in larger amounts of stored plant water (Fig. 6f). Levels of stored plant water are ~2.4 Kg KgC^{-1} during summer, decrease to around ~1.75 Kg KgC^{-1} during warmer winters and reach as low as ~1.1 Kg KgC^{-1} during extremely cold winters. In the default model, stored water drops to ~0.6 Kg KgC^{-1} without major variation between years. By keeping larger amounts of water in hardened plants, the fractional loss of total conductance (flc) remains lower than in default simulations. The hardening scheme greatly reduces hydraulic failure mortality (HFM) at Spasskaya Pad (Fig 8b), since HFM is a function of flc (Eq. 10), and an additional direct

reduction of HFM was applied during cold acclimation (Fig S12b). The contribution of hardiness to the reduction of K_{MAX}, *g0* and *g1*, and HFM, can be seen by comparing Fig. 8b and Fig. S12. The changes imposed through hardening favors vegetation growth in northern regions while the default model simulates almost nonexistent and declining vegetation (Fig. 4b).

At Farstanäs, temperatures in the top soil layers usually remain between 0 and -5°C during winter (Fig. 5c). This means that the water potential in plant compartments rarely drops below -3 MPa during typical winters. During cold winters, plant water potentials remain above -6 MPa in both the default and the hardening versions of the model (Fig. 7a). Therefore, the rate of HFM is lower at Farstanäs than at Spasskaya Pad, and episodes of mortality are shorter (Fig. 8a). In the simulations with hardening, plants have higher water potentials, reflective of the lower rates of water loss from winter root water exudation and stomatal transpiration. The main reason why the changes induced by hardening are small in Farstanäs – compared to Spasskaya Pad – is that changes are proportional to *HD*, which does not decrease much at Farstanäs (Fig. 10), and therefore the reductions applied to the conductance and mortality are smaller.

The simulations at Spasskaya Pad and Farstanäs, both feature years with notably large drops in living biomass (Fig. 4a and b). These are related to low soil water potentials during winter (Fig. 7a and b). The unusually low soil matric potentials in these years contribute to an increase in dehydration and lead to higher mortality rates (Fig. 8). Our results show that a stronger reduction of K_{MAX} with hardening, a lower H_{MAX}, or a stronger reduction in HFM led to larger survival rates. At Spasskaya Pad, none of the sensitivity simulations prevented the strong mortality rates during extreme years (Fig. 11). While an even stronger reduction of K_{MAX} and a later dehardening slightly helped survival, all simulations went through approximatively 50% less mortality during the dry years. Figs. S2b and 4b illustrate that during these extreme years, the total precipitation was low and the snow layer was thin. The water stored in plants and the matric potential of plants recovered only in the middle of the following summer (Fig. 6f, 7b).

3.2 Sensitivity experiments

3.2.1 Dehardening rate (DR)

At both sites (Farstanäs and Spasskaya Pad) the earlier dehardening starts, the better it is for vegetation growth (Figs. 11 and 12). There seem to be limited benefits in delaying hardening in autumn. At Spasskaya Pad, the modification of dehardening has little influence in the middle of the winter because of the extremely low hardiness levels (*HD*) (Fig. 10b). However, the "early dehardening simulation", in which hardening decreases later and increases earlier (*DR* between 0° and 10°C) shows root water efflux at the beginning and at the end of the winter season (Fig. S4d). This results in lower stored plant water and thereby higher hydraulic failure mortality (Figs. S4f and S5b). Interestingly, this results in a trade-off with carbon starvation mortality, since plant metabolism is activated earlier, reducing CSM (Fig. 9) and increasing gross primary productivity (Fig. S6).

At Farstanäs, soils are rarely frozen in autumn and spring, and when they freeze it is never as much as in Spasskaya Pad (Fig. 5). This, combined with the shorter cold seasons and the higher hardiness levels during winter, results in a reduced occurrence

of hydraulic failure mortality compared to Spasskaya Pad (Fig. S5). The 30-year atmospheric forcing period is too short and variable to show the trade-off between hydraulic failure mortality and carbon starvation mortality or even gross primary productivity.

3.2.2 Maximum hardiness level (H_{MAX})

At Spasskaya Pad, the H_{MAX} sensitivity simulations (where H_{MAX} is predicted by T5 minus variable Celsius degrees, see Table 1) are close to the hardening limit of -70°C (Fig. 10b), which means that they yield similar results (Fig. 11).

At Farstanäs, lowering H_{MAX} had large impacts on the total biomass (Fig. 12) because it increases survival during years with low soil water potentials and strong mid-winter root water release (Fig. S5). Conversely, it reduces productivity during years with higher soil water potentials (Figs. S4 and 12).

In our model, a reduction in H_{MAX} lowers conductivity, introducing a cost to plants in the form of decreased transpiration and photosynthesis (Fig. S4). Our results show the increase in CSM and decrease in HFM due to the lowering of Hmax at Spasskaya Pad (Fig. S7).

3.2.3 Pressure volume (PV) curve

PV curves were produced by making two of their parameters dependent on the hardening status *HD* (see method section). Our implementation results in a shift in the PV curves when plants cold acclimate, and associates a lower matric potential with a given volumetric water content when they are hardened (Fig. 3). By decreasing the water potential in the plant, we effectively decrease the water gradient between freezing surface soil layers (generally surface layers). However, we simultaneously increase the water gradient between deep roots and unfrozen, usually deeper, soil layers. Since plants tend to establish equilibrium with the soil, stronger water uptake in deep roots decelerates the decrease in plant water potential.

Comparing Farstanäs and Spasskaya Pad reveals that the level of reduction of K_{MAX} is crucial to the effective functioning of the dynamic PV curves. At Farstanäs (Fig. S8a), deep layers of the soil rarely freeze, and the weak reduction of K_{MAX} enables water uptake, thereby offsetting the direct effect of *HD* on the PV curves. In Spasskaya Pad (Fig. S8b), the strong reduction in K_{MAX} and the resulting prevention of water fluxes between roots and soil enabled lower water potential in the plant compartments. This led to slightly larger HFM rates and lower vegetation biomass (Fig. 11). We note that the higher leaf water potential in the dynamic PV simulation in Farstanäs in 2003 (Fig. S8a), is only due to differences in snow depths, and changes to soil temperatures resulting from different biomasses between both PV sensitivity simulations.

3.2.4 Maximum conductance between plant compartments (K_{MAX})

In this section, we show how sensitive evergreen trees are to the rate at which *HD* reduces K_{MAX} (Eq. 7). In Farstanäs, weaker reductions of K_{MAX} were favourable to vegetation productivity during “mild” winters, while stronger reductions became beneficial during “cold” winters (Fig. 12). During a cold year (e.g. first year of Fig. S9 a, c and e), the simulation with strong reduction in K_{MAX} allows plants to lose less water to root exudation. Since trees hold on to more water, a larger exchange of

water and carbon for photosynthesis is possible during early spring. By contrast, during a "mild" year (e.g. second year of Fig. S9 a, c and e), the strong reduction in K_{MAX} does not provide an advantage for the plant since soil water potentials remains high and strong root water exudation is absent even in the default model run (Fig. 12). Again, our model captures here the costs and benefits of hardening. Overall, it seems like the medium reduction of K_{MAX} yields the highest biomass in Farstanäs (Fig. 12). At Spasskaya Pad, large reductions in K_{MAX} are always necessary to allow persistence of living biomass in our simulations (Fig. 11). Moreover, the simulations with the largest reductions of K_{MAX} have the highest vegetation biomass.

3.2.5 Minimum stomatal conductance (g0 and g1)

Lowering g0 & g1 with hardening greatly reduces transpiration during winter (Fig. S10). This allows leaf water potentials (Fig. S11) to be maintained at values that do not trigger mortality. Reducing g0 and g1 also appears to lead to higher leaf water potentials during summer, especially at Farstanäs, potentially due to lower rates of transpiration resulting in larger water availability in the soil during summer (Fig S10e and f). Overall, the reduction of g0 and g1 has a positive impact on the living biomass at both sites (Fig. 11 and 12).

Reducing only g0 leads to water loss when light levels increase the stomatal response, and reducing only g1 still allows substantial transpiration to occur when stomata are shut. Both need to be reduced to avoid a loss of internal plant water stores during wintertime (Fig. S11 a and b).

3.2.6 Hydraulic failure mortality

If the rate scalar of HFM is not modified by the hardening scheme, high mortality rates are simulated for extended periods during winter at Spasskaya Pad (red line in Fig. S12b). When the rate of HFM is reduced by 50% and 100% at H_{MAX} (green and (light) blue lines respectively in Fig. S12), this results in a large increase in vegetation biomass (Fig. 11). A 50% reduction of HFM leads to almost a doubling of the biomass, and a 100% reduction (not realistic but included as an edge case) to almost a quadrupling.

On the other hand, the larger amounts of living biomass generated by the reduction of mortality, imply that larger amounts of water are transpired and there is more competition for soil liquid water. During extreme years, it appears that vegetation in simulations with reduced HFM, suffers from larger rates of CSM, which does not completely disappear during the following summer (Fig. S12d). In addition, while there was no HFM in the unchanged HFM simulation in spring, plants in reduced HFM simulations incur small amounts of HFM until later into the following summer (Fig. S12d).

3.2.7 Carbon starvation mortality

Implications of changing the rate of CSM are minor compared to HFM, although both scaling factors are identical (0.6 is the maximum mortality rate). HFM is parametrized in such a way that it quickly reaches 0.6 during strong water stress, while CSM remains at ~0.3, even during the more extreme years (Fig.S13a and b). The biomass response of a reduction in CSM is similar at both sites: vegetation thrives best with reduced CSM (Fig. 11 and 12).

4 Discussion

Much of the recent development of vegetation dynamics in land surface models has focused on representing advanced plant hydrodynamics (Christoffersen et al., 2016; Kennedy et al., 2019; Sperry et al., 2017; Xu et al., 2016). Usage of schemes that simulate the internal dynamics of plant moisture, however, have rarely been tested in cold systems – if at all, to our knowledge. By integrating a model of plant hardening with a porous media approach to plant hydrodynamics, we integrate a set of mechanisms that are both necessary for plants to avoid winter desiccation and capture the costs (in terms of reduced growth in spring) and benefits (in terms of reduced mortality rates) of winter 'hardening'. Our analyses further highlight trade-offs between avoidance of 'frost drought' mortality via hardening and avoidance of carbon starvation mortality via early season photosynthesis.

The default version of the CLM5-FATES-Hydro model used here, allows water to freeze in soils but not in plants. It does not include a mechanism to prevent liquid plant water to flow from plants to soils when freezing strongly reduces soil water potential. We show that this results in a depletion of water in plant compartments and triggers large amounts of hydraulic failure and carbon starvation mortalities.

The hydraulically-mediated hardening scheme we propose in this paper, consists of three modifications. The first being a reduction in the hydraulic conductivities of plant tissues which inhibits or prevents water loss during freezing depending on the atmospheric temperatures and amount of hardening by the plants (Gusta et al., 2005; Smit-Spinks et al., 1984; Steponkus, 1984). While the benefit of hardening is the reduced hydraulic failure mortality during freezing soil events, its cost is a temporary reduction of photosynthesis due to reduced transpiration. The sensitivity experiments on the timing of dehardening (DR) and on the maximum hardiness level (H_{MAX}) of this study, highlight the considerable cost of hardening in cold sites which incur frequent hydraulic failure mortality (Fig. 9, S6, S7). Previous field-based research has described the cost of hardening by showing that (1) cold acclimation causes a suppression of the rate of CO_2 uptake (Krivosheeva et al., 1996), (2) low temperatures lead to the inhibition of sucrose synthesis and photosynthesis (Savitch et al., 2002; Stitt and Hurry, 2002), and (3) photosynthesis stops when needles freeze (Havranek and Tranquillini, 1995). In addition, growth cessation, dormancy and cold acclimation are closely related to each other (Chang et al., 2021).

The second modification is to the stomatal model of Ball and Berry (1987). Reducing g0 & g1 led to a slower decrease of leaf water potentials during late winter and spring, resulting in higher vegetation survival rates. We argue that the accompanying reduction in transpiration makes the model more realistic. Indeed, while photosynthesis is slightly influenced by cold in the default model, temperature is not taken into account in the calculation of transpiration, although literature has shown that g0 & g1 is lower in cold acclimated plants (Christersson, 1972; Duursma et al., 2019; James et al., 2008). A partial but not full reduction of g0 and g1 allows for some transpiration, and thereby maintaining the capacity of the advanced hydraulic model to represent winter droughts. In contrast to summer droughts, typically caused by the absence of rainfall in summer, winter droughts or frost droughts are caused by the unavailability of water in frozen soils, preventing the replacement of transpired water during warm winter days.

The third modification that comprises our hardening scheme is the reduction in the rate of HFM. While the default formulation of HFM might be realistic when simulating summer droughts, it is not adapted to boreal and arctic regions where winter droughts would cause extended periods of mortality (i.e. lasting until snow melt in spring). At cold sites, the default CLM5-FATES-Hydro simulates a frost drought each winter due to root water exudation which systematically results in maximum HFM rates from late autumn until spring snow melt when soils finally thaw. The current parameterization of HFM in cold regions is such that summer productivity cannot balance the high winter mortality. In reality, high latitude vegetation is dormant in winter and the metabolism of plants is reduced or completely interrupted (Volaire, 2018). When dormant, plants reduce or stop meristem activity to make it insensitive to growth and promote signals in order to enhance survival during seasons with life threatening environmental conditions (Volaire, 2018). To quote Volaire (2018), "knowing when not to grow does not confer drought resistance but may well enhance drought survival". Our results show that the reduction of HFM with hardening can lead to large increases of biomass in areas with cold winters. The large amounts of biomass, however, appear to be a limiting factor during dry years, when plants must compete for water. The larger amount of biomass caused by reduced HFM rates resulted in higher CSM rates, highlighting another trade-off emerging from the hardening scheme.

To tolerate freezing, plants undergo a set of physiological changes. The capacity to efficiently cold acclimate and survive frost depends on a plants' genome and the presence of performant cold tolerance traits. Therefore, in reality different species, may exhibit different maximum hardiness levels (H_{MAX}), hardening rates (*HR*), dehardening rates (*DR*) and temperature ranges where hardening and dehardening occur (Mabaso et al., 2019; Oberschelp et al., 2020). In terrestrial biosphere models, species are aggregated in groups based on common functional characteristics criteria. Therefore, it is likely that the measured maximum freezing tolerance of some species that are within the same plant functional type category in the model, is variable in reality. (Sakai, 1983). A PFTs maximum freezing tolerance (as well as most parameters of terrestrial biosphere models) is a rough approximation of what has been measured for species belonging to that PFT. Common garden are generally used to identify the genetic variations among populations in their ability to cope with stresses (Bansal et al., 2016; de Villemereuil et al., 2016). As the expression of physiological/morphological traits associated with stress tolerance is also dependent on the environmental conditions of a common garden, several gardens are required to quantify the relative influence of environment and genetics on the expression of stress tolerance traits (Greer and Warrington, 1982). Earlier studies used a H_{MAX} of -30°C and a *DR* initiated at 5°C to model the hardiness of *Norway spruce* in Farstanäs (Bigras and Colombo, 2013; Jönsson et al., 2004; Rammig et al., 2010). However, *Pinus sylvestris* seedlings in Finland start dehardening already at temperatures as low as 3°C (Repo and Pelkonen, 1986). Our hydraulically-mediated hardening scheme captures both the costs and benefits of hardening, which in simulations with dynamic vegetation would likely lead to different competitive outcomes for plants with alternative hardening thresholds. Finer discretization of plant strategies along the axis of cold tolerance would provide an interesting extension to this study.

The physiological changes induced by cold acclimation result in modifications of the osmotic potential at full turgor and the bulk elastic modulus (Mart et al., 2016; Scholz et al., 2012; Valentini et al., 1990), i.e. two parameters that intervene in the calculation of the plant PV curves. In the changing PV curve simulation (see methods for more details), lower winter root

water exudation and transpiration fluxes were simulated. If K_{MAX} is not low enough, larger root water uptake (especially in deeper layers that remain unfrozen longer in autumn) balances the decrease in plant water potential. While the PV curve modification should be a more realistic approach to model plant hydraulics, it also results in larger HFM and lower biomass.

Our study illustrated the potential for a trade-off between the avoidance of HFM in the spring and the avoidance of CSM triggered by low photosynthesis rates resulting from a long hardening season. This trade-off mirrors the one originally proposed by McDowell et al. (2008) for summer droughts (whereby stomatal closure avoids HFM but predicates CSM). Mature trees store large amounts of mobile carbon, which decrease under water stress, but evidence to support this hypothesis is lacking (Hartmann, 2015; Sala, 2009). While HFM can be assessed by the percent loss of total conductance, CSM is much harder to infer. The limited understanding of the roles of non-structural carbohydrates suggests a link between CSM and HFM as sugars not only are a source of energy, but also regulate osmotic pressure and embolism repair following drought (McDowell & Sevanto, 2010). Our results show that changes in CSM result in relatively small changes of biomass compared to HFM reductions. This is mainly due to the fact that droughts typically cause larger HFM than CSM episodes.

5 Conclusions

In this study, we propose a hardening scheme adapted for use within the context of plant hydrodynamic simulations, which can simulate the physiological costs and benefits of plant cold acclimation in terms of water movement and gas exchange. Its impact on plant hydraulics and vegetation mortality and growth appears to be a promising improvement for the modelling of vegetation growth in cold environments. We present here one parameterization of the hardening scheme, show how it performs at two sites with contrasting winter weather, and investigate the response of the scheme to variations to its key parameters. Although the understanding about cold acclimation processes is expanding at an accelerating rate, there are still large knowledge gaps. For example, the range of processes triggered by cold acclimation are poorly understood and we lack measurements to define the exact amplitude at which they are disturbed (Arora and Rowland, 2011; Chang et al., 2021; Shi et al., 2018; Shin et al., 2015). In addition, quantifying and generalizing hardiness levels and rates inside the scheme itself are in some respects broad approximations which remain to be optimized further. Future developments might, for example, consider a larger influence of photoperiod and the inclusion of plant phenological states in the calculation of the hardiness level. In this study, we primarily aim at discussing the role and impacts of major parameters and potential impacts of cold acclimation as a framework for further implementation in dynamic vegetation models with advanced plant hydraulics. We show that this framework 1) leads to more realistic vegetation biomass productivity at temperate and boreal sites, 2) influences winter root water release and mortality rates by lowering plant conductance, and 3) that hardening comes at a cost for photosynthesis (trade-off of hardening emerges from our scheme).

Recent observations of increasing vegetation mortality appear to be a result of climate change, in particular the increase in intensity and frequency of droughts caused by extreme weather conditions (Allen et al., 2010). This highlights the urgency to improve our understanding of plant survival and mortality mechanisms. To date, there are large gaps in our knowledge on

plant hydraulics and their link to mortality rates. In this paper, we hope to provide new insights into modelling of plant hydraulics and their link to cold acclimation.

Future research is needed to better assess the implications of cold acclimation on plant hydraulics, especially conductivity. Understanding these processes in hampered by the logistical and technical difficulties involved in the observation of cold systems. Our work lays the foundation to use a hardening scheme to regulate frost damage and to study the link between different types of mortalities in terrestrial biosphere models in the Arctic region. The inclusion of cold hardiness is essential to model realistic plant hydraulics and vegetation dynamics within cold climates.

Data availability

The modelling data that supports the findings of this study is available at https://doi.org/10.11582/2022.00028. The code of CTSM5.0 can be found at https://zenodo.org/badge/latestdoi/493596086, and the code of FATES at https://zenodo.org/badge/latestdoi/493596262.

Acknowledgements

This work is a contribution to the Strategic Research Initiative 'Land Atmosphere Interactions in Cold Environments' (LATICE) of the University of Oslo. We gratefully acknowledge the support of the Research Council of Norway for the WINTERPROOF (project no. 274711), the Swedish Research Council under registration no. 2017-05268, the EMERALD (project no. 294948), and the Center for Biogeochemistry in the Anthropocene at the Faculty of Mathematics and Natural Sciences at UiO. We would also like to thank the ECMWF for the ERA5L reanalysis product. Finally, we would like to acknowledge our colleagues at NCAR and Berkeley lab for their precious help during model setup and manuscript preparation. RF acknowledges the support of the US Dept of Energy 'Next Generation Ecosystem Experiment in the Tropics' project, and RF and KSA the support of the EUH2020 4C project. YF acknowledges the support of the Energy Exascale Earth System Model (E3SM) project, funded by the U.S. Department of Energy, Office of Science Biological and Environmental Research, through the Earth System Model Development program area. The Pacific Northwest National Laboratory is operated for DOE by Battelle Memorial Institute under contract DE-AC06-76RL01830. The simulations were performed on the FRAM supercomputer operated by Sigma2 (project number NN2806K).

Author Contribution

MSAL, HT, KJA, FS, RAF and FJWP designed the work; MSAL performed experiments and data analyses; MSAL drafted the manuscript; HT, KSA, FS, JWB, RAF, YF, JD and FJWP revised the manuscript. All authors approved the final version of the manuscript for publication. The authors declare that they have no conflict of interest.

References

Allen, C. D., Macalady, A., Chenchouni, H., Bachelet, D., McDowell, N., Vennetier, M., Gonzales, P., Hogg, T., Rigling, A., and Breshears, D.: Climate-induced forest mortality: a global overview of emerging risks, Forest Ecology and Management, 259, 660–684, 2010.

Arora, R. and Rowland, L. J.: Physiological research on winter-hardiness: deacclimation resistance, reacclimation ability, photoprotection strategies, and a cold acclimation protocol design, HortScience, 46, 1070–1078, 2011.

Ball, J. T., Woodrow, I. E., and Berry, J. A.: A model predicting stomatal conductance and its contribution to the control of photosynthesis under different environmental conditions, in: Progress in photosynthesis research, Springer, 221–224, 1987.

Bansal, S., Harrington, C. A., and St. Clair, J. B.: Tolerance to multiple climate stressors: A case study of Douglas-fir drought and cold hardiness, Ecology and Evolution, 6, 2074–2083, 2016.

Bartlett, M. K., Scoffoni, C., and Sack, L.: The determinants of leaf turgor loss point and prediction of drought tolerance of species and biomes: a global meta-analysis, Ecology letters, 15, 393–405, 2012.

Beck, E. H., Heim, R., and Hansen, J.: Plant resistance to cold stress: mechanisms and environmental signals triggering frost hardening and dehardening, Journal of biosciences, 29, 449–459, 2004.

Beck, E. H., Fettig, S., Knake, C., Hartig, K., and Bhattarai, T.: Specific and unspecific responses of plants to cold and drought stress, Journal of biosciences, 32, 501–510, 2007.

Bigras, F. J. and Colombo, S. J.: Conifer cold hardiness, Springer Science & Business Media, 2013.

Bonan, G. B., Williams, M., Fisher, R. A., and Oleson, K. W.: Modeling stomatal conductance in the earth system: linking leaf water-use efficiency and water transport along the soil–plant–atmosphere continuum, Geoscientific Model Development, 7, 2193–2222, 2014.

Campbell, G. S.: A simple method for determining unsaturated conductivity from moisture retention data, Soil science, 117, 311–314, 1974.

Carminati, A., Vetterlein, D., Weller, U., Vogel, H.-J., and Oswald, S. E.: When roots lose contact, Vadose Zone Journal, 8, 805–809, 2009.

Chang, C. Y.-Y., Bräutigam, K., Hüner, N. P., and Ensminger, I.: Champions of winter survival: cold acclimation and molecular regulation of cold hardiness in evergreen conifers, New Phytologist, 229, 675–691, 2021.

Chinnusamy, V., Zhu, J., and Zhu, J.-K.: Gene regulation during cold acclimation in plants, Physiologia Plantarum, 126, 52–61, 2006.

Christersson, L.: The transpiration rate of unhardened, hardened, and dehardened seedlings of spruce and pine, Physiologia Plantarum, 26, 258–263, 1972.

Christoffersen, B. O., Gloor, M., Fauset, S., Fyllas, N. M., Galbraith, D. R., Baker, T. R., Kruijt, B., Rowland, L., Fisher, R. A., Binks, O. J., and others: Linking hydraulic traits to tropical forest function in a size-structured and trait-driven model (TFS v. 1-Hydro), Geoscientific Model Development, 2016.

Clapp, R. B. and Hornberger, G. M.: Empirical equations for some soil hydraulic properties, Water resources research, 14, 601–604, 1978.

Darcy, H.: Les fontaines publiques de la ville de Dijon: exposition et application..., Victor Dalmont, 1856.

Ding, Y., Zhang, Y., Zheng, Q.-S., and Tyree, M. T.: Pressure–volume curves: revisiting the impact of negative turgor during cell collapse by literature review and simulations of cell micromechanics, New Phytologist, 203, 378–387, 2014.

Dowgert, M. F. and Steponkus, P. L.: Behavior of the plasma membrane of isolated protoplasts during a freeze-thaw cycle, Plant physiology, 75, 1139–1151, 1984.

Duursma, R. A. and Medlyn, B. E.: MAESPA: a model to study interactions between water limitation, environmental drivers and vegetation function at tree and stand levels, with an example application to [CO 2]× drought interactions, Geoscientific Model Development, 5, 919–940, 2012.

Duursma, R. A., Blackman, C. J., Lopéz, R., Martin-StPaul, N. K., Cochard, H., and Medlyn, B. E.: On the minimum leaf conductance: its role in models of plant water use, and ecological and environmental controls, New Phytologist, 221, 693–705, 2019.

Edwards, W. R. N., Jarvis, P. G., Landsberg, J. J., and Talbot, H.: A dynamic model for studying flow of water in single trees, Tree Physiology, 1, 309–324, 1986.

Fisher, R. A., Muszala, S., Verteinstein, M., Lawrence, P., Xu, C., McDowell, N. G., Knox, R. G., Koven, C., Holm, J., and Rogers, B. M.: Taking off the training wheels: the properties of a dynamic vegetation model without climate envelopes, CLM4. 5 (ED), Geoscientific Model Development, 8, 3593–3619, 2015.

Fontes, C.: Tropical plant hydraulics in a changing climate: importance for species distribution and vulnerability to drought, University of California, Berkeley, 2019.

Fricke, W.: Turgor pressure, eLS, 1–6, 2017.

Greenwood, S., Ruiz-Benito, P., Martínez-Vilalta, J., Lloret, F., Kitzberger, T., Allen, C. D., Fensham, R., Laughlin, D. C., Kattge, J., and Bönisch, G.: Tree mortality across biomes is promoted by drought intensity, lower wood density and higher specific leaf area, Ecology letters, 20, 539–553, 2017.

Greer, D. H. and Warrington, I. J.: Effect of photoperiod, night temperature, and frost incidence on development of frost hardiness in Pinus radiata, Functional Plant Biology, 9, 333–342, 1982.

Gusta, L. V., Trischuk, R., and Weiser, C. J.: Plant cold acclimation: the role of abscisic acid, Journal of Plant Growth Regulation, 24, 308–318, 2005.

Hamada, S., Ohta, T., Hiyama, T., Kuwada, T., Takahashi, A., and Maximov, T. C.: Hydrometeorological behaviour of pine and larch forests in eastern Siberia, Hydrological Processes, 18, 23–39, 2004.

Hanin, M., Brini, F., Ebel, C., Toda, Y., Takeda, S., and Masmoudi, K.: Plant dehydrins and stress tolerance: versatile proteins for complex mechanisms, Plant signaling & behavior, 6, 1503–1509, 2011.

Hartmann, H.: Carbon starvation during drought-induced tree mortality–are we chasing a myth?, Journal of Plant Hydraulics, 2, e005, 2015.

Havranek, W. M. and Tranquillini, W.: Physiological processes during winter dormancy and their ecological significance, in: Ecophysiology of coniferous forests, Elsevier, 95–124, 1995.

Isaev, A. P., Protopopov, A. V., Protopopova, V. V., Egorova, A. A., Timofeyev, P. A., Nikolaev, A. N., Shurduk, I. F., Lytkina, L. P., Ermakov, N. B., and Nikitina, N. V.: Vegetation of Yakutia: elements of ecology and plant sociology, in: The Far North, Springer, 143–260, 2010.

James, A. T., Lawn, R. J., and Cooper, M.: Genotypic variation for drought stress response traits in soybean. I. Variation in soybean and wild Glycine spp. for epidermal conductance, osmotic potential, and relative water content, Australian Journal of Agricultural Research, 59, 656–669, 2008.

Janská, A., Maršík, P., Zelenková, S., and Ovesná, J.: Cold stress and acclimation–what is important for metabolic adjustment?, Plant Biology, 12, 395–405, 2010.

Jarvis, P. G. and Morison, J. I. L.: The control of transpiration and photosynthesis by the stomata, in: Stomatal physiology, vol. 8, Cambridge University Press Cambridge, 247–279, 1981.

Jönsson, A. M., Linderson, M.-L., Stjernquist, I., Schlyter, P., and Bärring, L.: Climate change and the effect of temperature backlashes causing frost damage in Picea abies, Global and Planetary Change, 44, 195–207, 2004.

Kellomaki, S., Hanninen, H., and Kolstrom, M.: Computations on frost damage to Scots pine under climatic warming in boreal conditions, Ecological Applications, 5, 42–52, 1995.

Kennedy, D., Swenson, S., Oleson, K. W., Lawrence, D. M., Fisher, R., Lola da Costa, A. C., and Gentine, P.: Implementing plant hydraulics in the community land model, version 5, Journal of Advances in Modeling Earth Systems, 11, 485–513, 2019.

Knipfer, T., Besse, M., Verdeil, J.-L., and Fricke, W.: Aquaporin-facilitated water uptake in barley (Hordeum vulgare L.) roots, Journal of Experimental Botany, 62, 4115–4126, 2011.

Koven, C.: FATES Parameters and Output for Parameter Sensitivity at the Panama Barro Colorado Island Testbed, Next-Generation Ecosystem Experiments Tropics; Lawrence Berkeley National …, 2019.

Kreszies, T., Shellakkutti, N., Osthoff, A., Yu, P., Baldauf, J. A., Zeisler-Diehl, V. V., Ranathunge, K., Hochholdinger, F., and Schreiber, L.: Osmotic stress enhances suberization of apoplastic barriers in barley seminal roots: analysis of chemical, transcriptomic and physiological responses, New Phytologist, 221, 180–194, 2019.

Krivosheeva, A., Tao, D.-L., Ottander, C., Wingsle, G., Dube, S. L., and Öquist, G.: Cold acclimation and photoinhibition of photosynthesis in Scots pine, Planta, 200, 296–305, 1996.

Kuprian, E., Koch, S., Munkler, C., Resnyak, A., Buchner, O., Oberhammer, M., and Neuner, G.: Does winter desiccation account for seasonal increases in supercooling capacity of Norway spruce bud primordia?, Tree physiology, 38, 591–601, 2018.

Kursar, T. A., Engelbrecht, B. M., Burke, A., Tyree, M. T., EI Omari, B., and Giraldo, J. P.: Tolerance to low leaf water status of tropical tree seedlings is related to drought performance and distribution, Functional Ecology, 23, 93–102, 2009.

Lawrence, D. M., Fisher, R. A., Koven, C. D., Oleson, K. W., Swenson, S. C., Bonan, G., Collier, N., Ghimire, B., van Kampenhout, L., Kennedy, D., and others: The Community Land Model version 5: Description of new features, benchmarking, and impact of forcing uncertainty, Journal of Advances in Modeling Earth Systems, 11, 4245–4287, 2019.

Lee, S., Chung, G. C., and Steudle, E.: Low temperature and mechanical stresses differently gate aquaporins of root cortical cells of chilling-sensitive cucumber and-resistant figleaf gourd, Plant, Cell & Environment, 28, 1191–1202, 2005.

Levitt, J.: Responses of Plants to Environmental Stress, Volume 1: Chilling, Freezing, and High Temperature Stresses., Academic Press., 1980.

Li, C., Junttila, O., and Palva, E. T.: Environmental regulation and physiological basis of freezing tolerance in woody plants, Acta Physiologiae Plantarum, 26, 213–222, 2004.

Lopez-Iglesias, B., Villar, R., and Poorter, L.: Functional traits predict drought performance and distribution of Mediterranean woody species, Acta Oecologica, 56, 10–18, 2014.

Mabaso, F., Ham, H., and Nel, A.: Frost tolerance of various Pinus pure species and hybrids, Southern Forests: A Journal of Forest Science, 81, 273–280, 2019.

Manzoni, S., Vico, G., Katul, G., Palmroth, S., Jackson, R. B., and Porporato, A.: Hydraulic limits on maximum plant transpiration and the emergence of the safety–efficiency trade-off, New Phytologist, 198, 169–178, 2013.

Mart, K. B., Veneklaas, E. J., and Bramley, H.: Osmotic potential at full turgor: an easily measurable trait to help breeders select for drought tolerance in wheat, Plant Breeding, 135, 279–285, 2016.

McDowell, N., Pockman, W. T., Allen, C. D., Breshears, D. D., Cobb, N., Kolb, T., Plaut, J., Sperry, J., West, A., Williams, D. G., and others: Mechanisms of plant survival and mortality during drought: why do some plants survive while others succumb to drought?, New phytologist, 178, 719–739, 2008.

McDowell, N. G. and Sevanto, S.: The mechanisms of carbon starvation: how, when, or does it even occur at all?, New Phytologist, 186, 264–266, 2010.

Mirfenderesgi, G., Bohrer, G., Matheny, A. M., Fatichi, S., de Moraes Frasson, R. P., and Schäfer, K. V.: Tree level hydrodynamic approach for resolving aboveground water storage and stomatal conductance and modeling the effects of tree hydraulic strategy, Journal of Geophysical Research: Biogeosciences, 121, 1792–1813, 2016.

Nadezhdina, N., David, T. S., David, J. S., Ferreira, M. I., Dohnal, M., Tesař, M., Gartner, K., Leitgeb, E., Nadezhdin, V., Cermak, J., and others: Trees never rest: the multiple facets of hydraulic redistribution, Ecohydrology, 3, 431–444, 2010.

Navarro, M. Á. P., Sapes, G., Batllori, E., Serra-Diaz, J. M., Esteve, M. A., and Lloret, F.: Climatic suitability derived from species distribution models captures community responses to an extreme drought episode, Ecosystems, 22, 77–90, 2019.

North, G. B. and Nobel, P. S.: Hydraulic conductivity of concentric root tissues of Agave deserti Engelm. under wet and drying conditions, New Phytologist, 130, 47–57, 1995.

North, G. B. and Nobel, P. S.: Root-soil contact for the desert succulent Agave deserti in wet and drying soil, New Phytologist, 135, 21–29, 1997.

Oberschelp, G. P. J., Guarnaschelli, A. B., Teson, N., Harrand, L., Podestá, F. E., and Margarit, E.: Cold acclimation and freezing tolerance in three Eucalyptus species: A metabolomic and proteomic approach, Plant Physiology and Biochemistry, 154, 316–327, 2020.

Oliveira, R. S., Dawson, T. E., Burgess, S. S., and Nepstad, D. C.: Hydraulic redistribution in three Amazonian trees, Oecologia, 145, 354–363, 2005.

Petrov, K. A., Sofronova, V. E., Bubyakina, V. V., Perk, A. A., Tatarinova, T. D., Ponomarev, A. G., Chepalov, V. A., Okhlopkova, Z. M., Vasilieva, I. V., and Maximov, T. C.: Woody plants of Yakutia and low-temperature stress, Russian Journal of Plant Physiology, 58, 1011–1019, 2011.

Prieto, I., Armas, C., and Pugnaire, F. I.: Water release through plant roots: new insights into its consequences at the plant and ecosystem level, New Phytologist, 193, 830–841, 2012.

Rammig, A., Jönsson, A. M., Hickler, T., Smith, B., Bärring, L., and Sykes, M. T.: Impacts of changing frost regimes on Swedish forests: incorporating cold hardiness in a regional ecosystem model, Ecological Modelling, 221, 303–313, 2010.

Rasztovits, E., Berki, I., Mátyás, C., Czimber, K., Pötzelsberger, E., and Móricz, N.: The incorporation of extreme drought events improves models for beech persistence at its distribution limit, Annals of forest science, 71, 201–210, 2014.

Repo, T. and Pelkonen, P.: Temperature step response of dehardening in Pinus sylvestris seedlings, Scandinavian Journal of Forest Research, 1, 271–284, 1986.

Rinne, P., Welling, A., and Kaikuranta, P.: Onset of freezing tolerance in birch (Betula pubescens Ehrh.) involves LEA proteins and osmoregulation and is impaired in an ABA-deficient genotype, Plant, Cell & Environment, 21, 601–611, 1998.

ERA5-Land Monthly Averaged from 1981 to Present:

Sakai, A.: Comparative study on freezing resistance of conifers with special reference to cold adaptation and its evolutive aspects, Canadian Journal of Botany, 61, 2323–2332, 1983.

Sala, A.: Lack of direct evidence for the carbon-starvation hypothesis to explain drought-induced mortality in trees, Proceedings of the National Academy of Sciences, 106, E68–E68, 2009.

Sato, H., Kobayashi, H., and Delbart, N.: Simulation study of the vegetation structure and function in eastern Siberian larch forests using the individual-based vegetation model SEIB-DGVM, Forest ecology and management, 259, 301–311, 2010.

Savitch, L. V., Leonardos, E. D., Krol, M., Jansson, S., Grodzinski, B., Huner, N. P. A., and Öquist, G.: Two different strategies for light utilization in photosynthesis in relation to growth and cold acclimation, Plant, Cell & Environment, 25, 761–771, 2002.

Scholz, F. G., Bucci, S. J., Arias, N., Meinzer, F. C., and Goldstein, G.: Osmotic and elastic adjustments in cold desert shrubs differing in rooting depth: coping with drought and subzero temperatures, Oecologia, 170, 885–897, 2012.

Shi, Y., Ding, Y., and Yang, S.: Molecular regulation of CBF signaling in cold acclimation, Trends in plant science, 23, 623–637, 2018.

Shin, H., Oh, Y., and Kim, D.: Differences in cold hardiness, carbohydrates, dehydrins and related gene expressions under an experimental deacclimation and reacclimation in Prunus persica, Physiologia Plantarum, 154, 485–499, https://doi.org/10.1111/ppl.12293, 2015.

Smit-Spinks, B., Swanson, B. T., and Markhart, A. I.: Changes in water relations, water flux, and root exudate abscisic acid content with cold acclimation of Pinus sylvestris L, Functional Plant Biology, 11, 431–441, 1984.

Sperry, J., Adler, F., Campbell, G., and Comstock, J.: Limitation of plant water use by rhizosphere and xylem conductance: results from a model, Plant, Cell & Environment, 21, 347–359, 1998.

Sperry, J. S., Venturas, M. D., Anderegg, W. R., Mencuccini, M., Mackay, D. S., Wang, Y., and Love, D. M.: Predicting stomatal responses to the environment from the optimization of photosynthetic gain and hydraulic cost, Plant, cell & environment, 40, 816–830, 2017.

Steponkus, P. L.: Role of the plasma membrane in freezing injury and cold acclimation, Annual Review of Plant Physiology, 35, 543–584, 1984.

Stitt, M. and Hurry, V.: A plant for all seasons: alterations in photosynthetic carbon metabolism during cold acclimation in Arabidopsis, Current opinion in plant biology, 5, 199–206, 2002.

Sugimoto, A., Yanagisawa, N., Naito, D., Fujita, N., and Maximov, T. C.: Importance of permafrost as a source of water for plants in east Siberian taiga, Ecological Research, 17, 493–503, 2002.

Tatarinova, T. D., Perk, A. A., Bubyakina, V. V., Vasilieva, I. V., Ponomarev, A. G., and Maximov, T. C.: Dehydrin stress proteins in Pinus sylvestris L. needles under conditions of extreme climate of Yakutia, in: Doklady Biochemistry and Biophysics, 98–101, 2017.

Tyree, M. T. and Hammel, H. T.: The measurement of the turgor pressure and the water relations of plants by the pressure-bomb technique, Journal of experimental Botany, 23, 267–282, 1972.

Tyree, M. T., Engelbrecht, B. M., Vargas, G., and Kursar, T. A.: Desiccation tolerance of five tropical seedlings in Panama. Relationship to a field assessment of drought performance, Plant physiology, 132, 1439–1447, 2003.

Valentini, R., Mugnozza, G. S., Giordano, E., and Kuzminsky, E.: Influence of cold hardening on water relations of three Eucalyptus species, Tree physiology, 6, 1–10, 1990.

de Villemereuil, P., Gaggiotti, O. E., Mouterde, M., and Till-Bottraud, I.: Common garden experiments in the genomic era: new perspectives and opportunities, Heredity, 116, 249–254, 2016.

Volaire, F.: A unified framework of plant adaptive strategies to drought: crossing scales and disciplines, Global change biology, 24, 2929–2938, 2018.

Welling, A. and Palva, E. T.: Molecular control of cold acclimation in trees, Physiologia Plantarum, 127, 167–181, 2006.

Williams, M., Bond, B. J., and Ryan, M. G.: Evaluating different soil and plant hydraulic constraints on tree function using a model and sap flow data from ponderosa pine, Plant, Cell & Environment, 24, 679–690, 2001.

Wisniewski, M., Nassuth, A., and Arora, R.: Cold Hardiness in Trees: A Mini-Review, Frontiers in Plant Science, 9, 1394, https://doi.org/10.3389/fpls.2018.01394, 2018.

Xu, C., Christoffersen, B., Knox, R., Wolfe, B., Wei, L., Chitra-Tarak, R., Slot, M., Fisher, R., Kueppers, L. M., and Chambers, J.: The Importance of Hydraulic Traits to Tropical Forest Dynamics, in: AGU Fall Meeting Abstracts, B127-05, 2020.

Xu, X., Medvigy, D., Powers, J. S., Becknell, J. M., and Guan, K.: Diversity in plant hydraulic traits explains seasonal and inter-annual variations of vegetation dynamics in seasonally dry tropical forests, New Phytologist, 212, 80–95, 2016.

Ye, Q. and Steudle, E.: Oxidative gating of water channels (aquaporins) in corn roots, Plant, Cell & Environment, 29, 459–470, 2006.

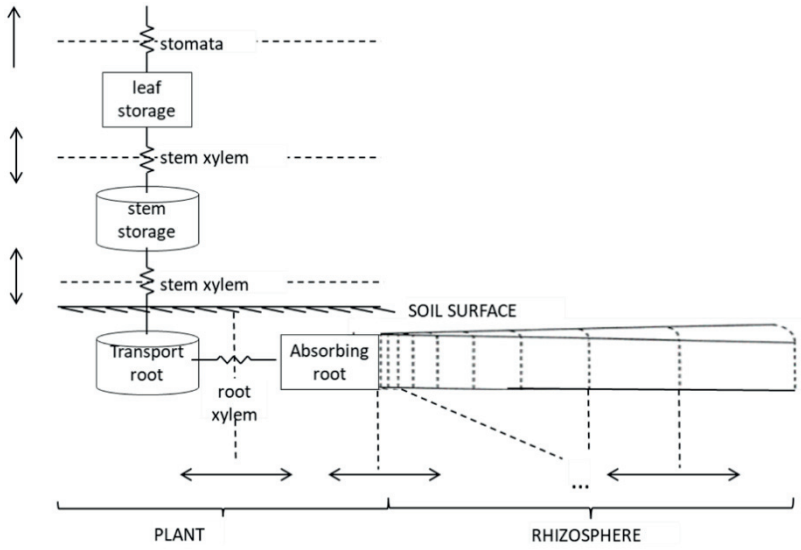

Figure 1: Structure of the FATES-Hydro model (Xu et al., 2020).

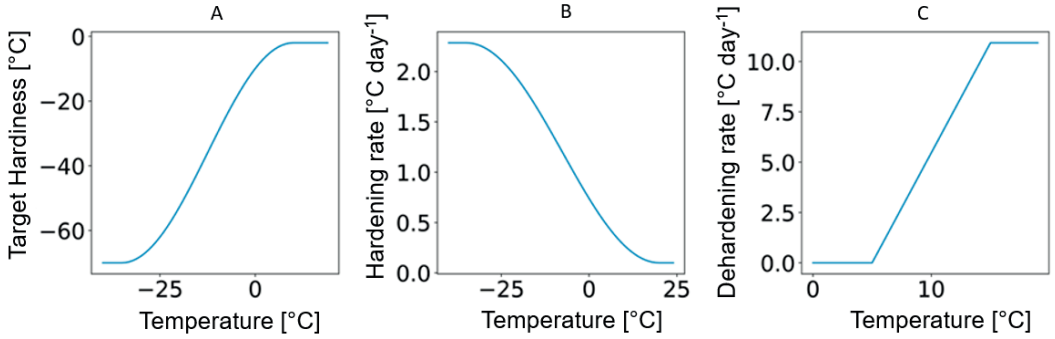

Figure 2: Example of (a) the target hardiness (TH), (b) the hardening rate (HR, in °C day−1), and (c) the dehardening rate (DR) functions (in °C day−1) in relation to the ambient mean temperature corresponding to a site and a plant functional type with a maximum hardiness level (H_{MAX}) of -70°C.

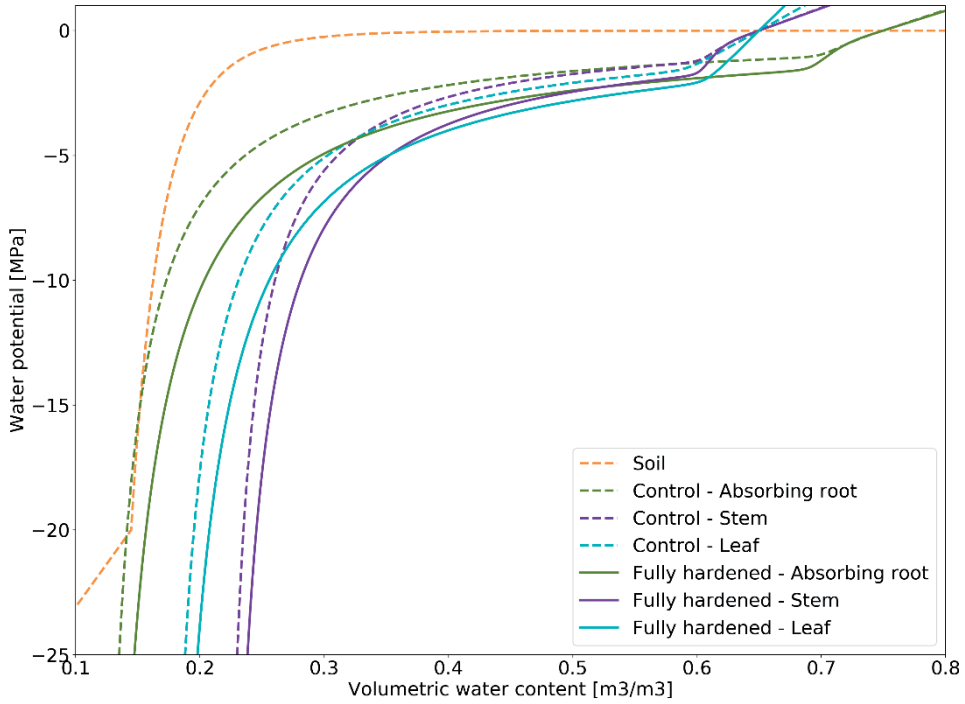

Figure 3: Pressure volume curves for soil (orange) and plant compartments. The PV curves used by the default CLM5-FATES-Hydro and non-hardened plants are the dashed lines, while the PV curves used by plants acclimated to -70°C are the full lines.

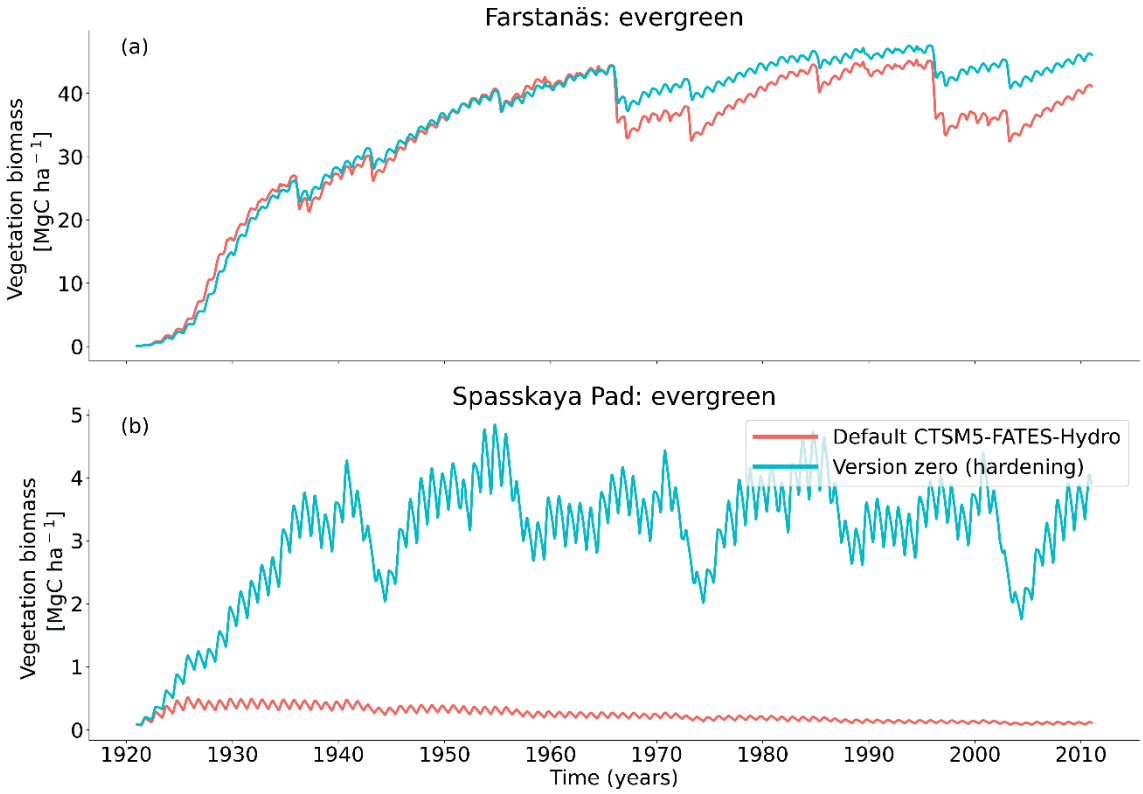

Figure 4: Living biomass for needleleaf evergreen trees at the sites of a) Farstanäs, and b) Spasskaya Pad, during the period 1921-2011 (atmospheric forcing: 3*[1981-2011]). The default simulation is shown in red, and the hardening simulation is shown in blue.

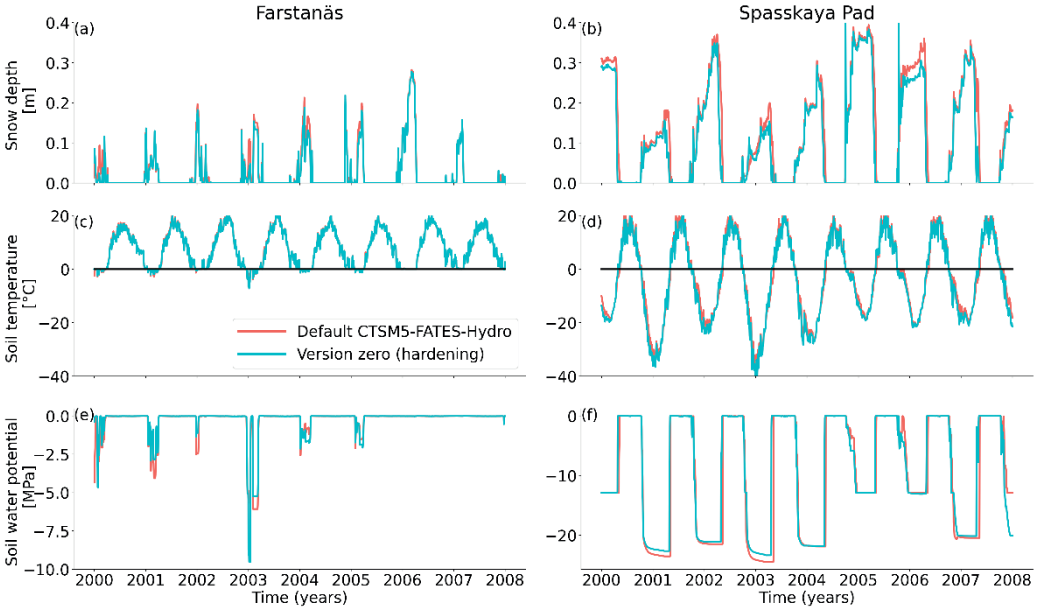

Figure 5: Soil conditions for needleleaf evergreen trees at the sites of: Left) Farstanäs, and Right) Spasskaya Pad, during the period 2000-2008. Top: transpiration, middle: root water uptake, and bottom: stored plant water. The default simulation is shown in red, and the hardening simulation is shown in blue.

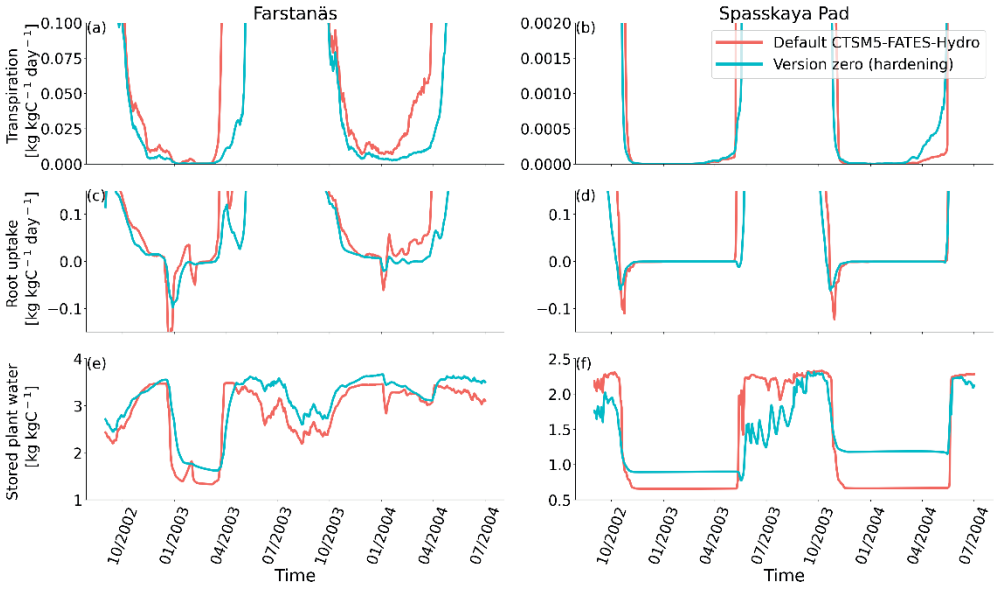

Figure 6: Plant water fluxes for needleleaf evergreen trees at the sites of: Left) Farstanäs, and Right) Spasskaya Pad, during the period 2002/09-2004/07. Top: transpiration, middle: root water uptake, and bottom: stored plant water. The default simulation is shown in red, and the hardening simulation is shown in blue.

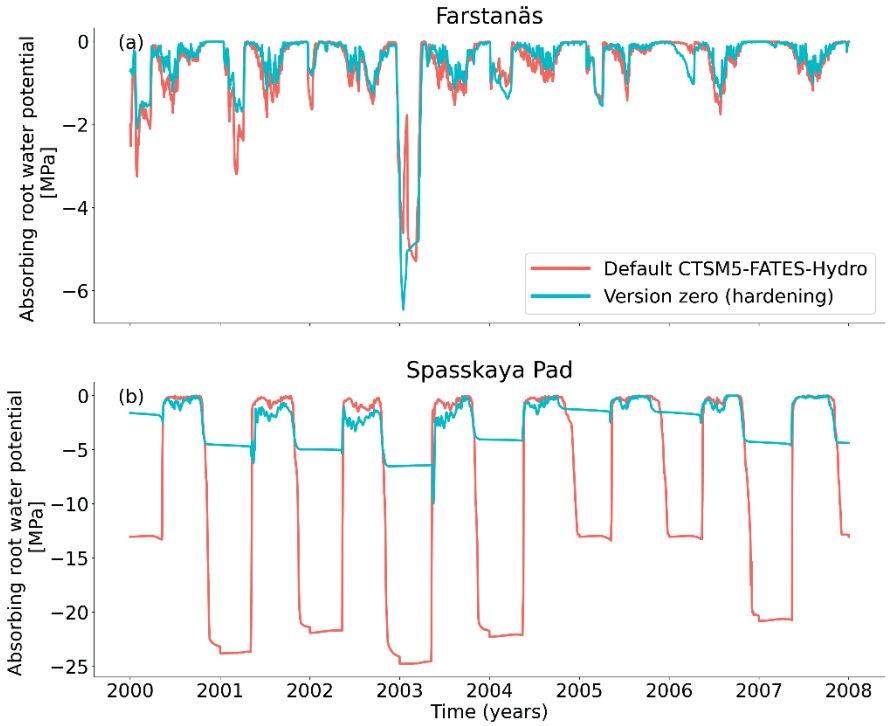

Figure 7: Absorbing root water potential for needleleaf evergreen trees at the sites of a) Farstanäs, and b) Spasskaya Pad, during the period 2000-2008. The default simulation is shown in red, and the hardening simulation is shown in blue.

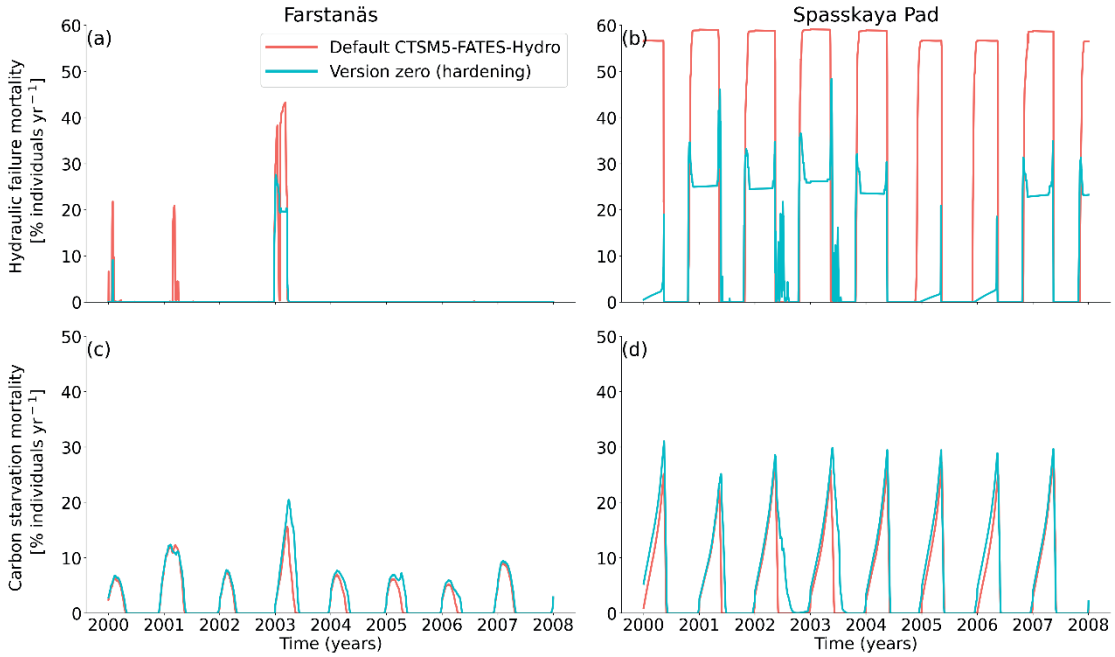

Figure 8: Mortality rates for evergreen needleleaf trees at the sites of: Left) Farstanäs, and Right) Spasskaya Pad, during the period 2000-2008. Top: hydraulic failure mortality, and bottom: carbon starvation mortality. The default simulation is shown in red, and the hardening simulation is shown in blue.

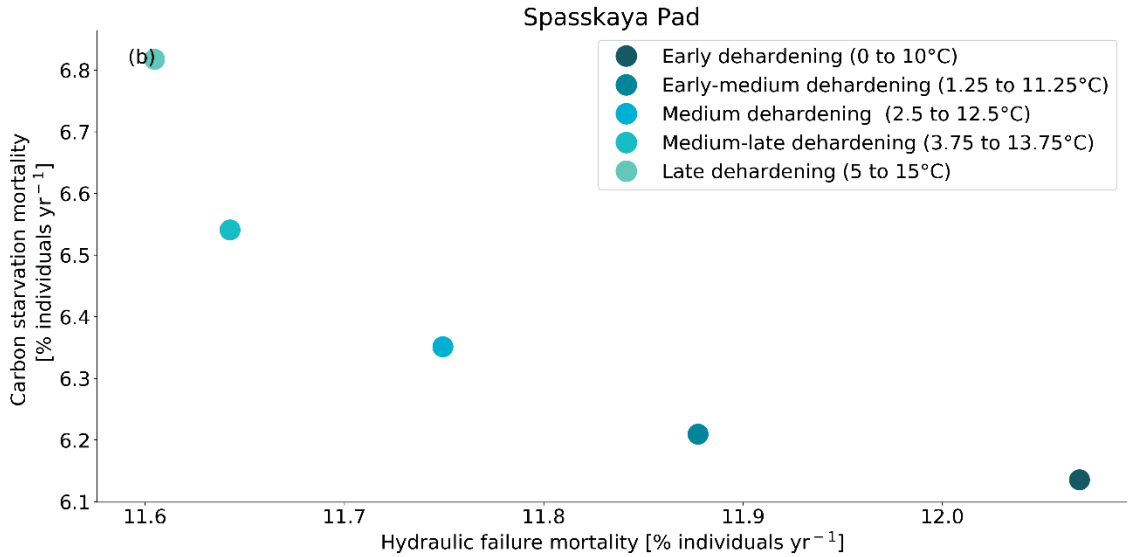

Figure 9: Trade-off between hydraulic failure mortality and carbon starvation mortality for evergreen needleleaf trees at Spasskaya Pad for 5 dehardening sensitivity experiments. The mortality rates are averaged over the 30 year period 1981 to 2011.

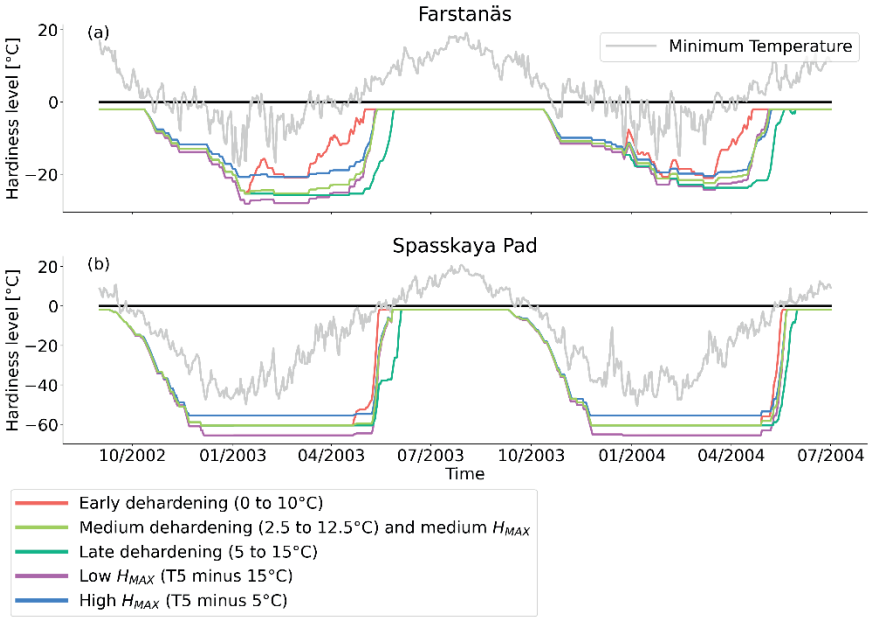

Figure 10: Hardiness level from dehardening and maximum hardiness level sensitivity analysis simulations for needleleaf evergreen trees at the sites of: a) Farstanäs, and b) Spasskaya Pad, during the period 2002/09-2004/07. The grey line corresponds to the minimum daily temperature, the black line is 0°C and the colored lines are the dehardening and maximum level hardiness sensitivity experiments.

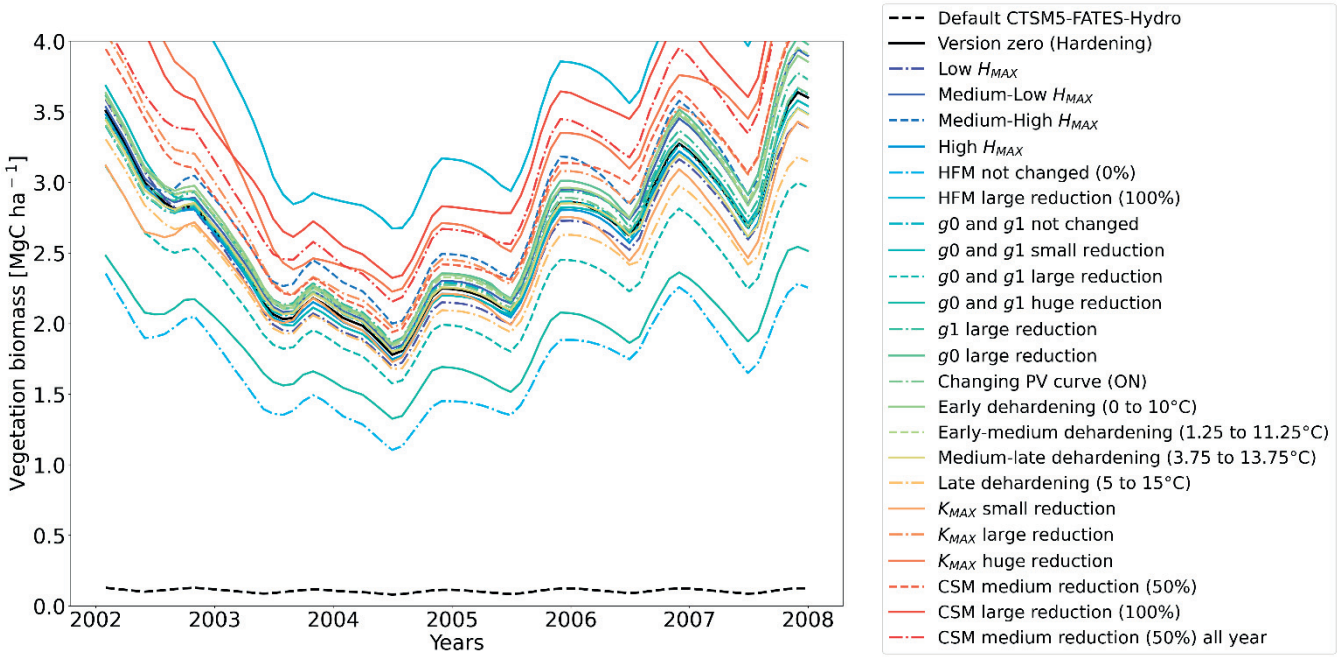

Figure 11: Ensemble of living biomass simulations for needleleaf evergreen trees at the site of Spasskaya Pad during the period 2002-2008.

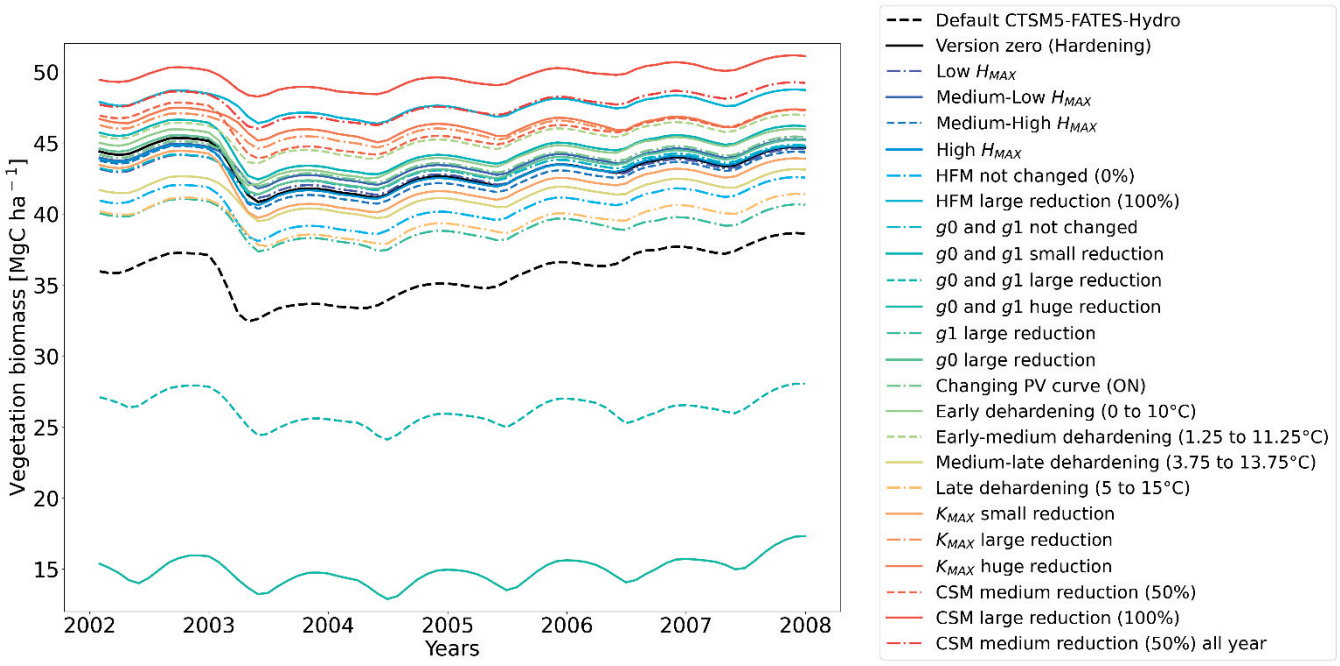

Figure 12: Ensemble of living biomass simulations for needleleaf evergreen trees at the site of Farstanäs during the period 2002-2008.

Simulation	***KMAX***	***g0, g1***	**HFM**	**CSM**	**PV**	***DR***	***HMAX***
Version zero (hardening)	$10^{\left(\frac{HD+3}{11}\right)}$	$10^{\left(\frac{HD+3}{40}\right)}$	50%	0%	OFF	2.5-12.5°C	T5-10°C

Table 1: Configuration of the version zero simulation. This simulation was run at the sites of Spasskaya Pad and Farstanäs for evergreen needleleaf and deciduous broadleaf trees. T5 is the 5-year running mean of the minimum 2m daily temperature of each year.

g0, g1	Not changed	Small $10^{\left(\frac{HD+3}{60}\right)}$	Medium $10^{\left(\frac{HD+3}{40}\right)}$	Large $10^{\left(\frac{HD+3}{20}\right)}$	Huge $10^{\left(\frac{HD+3}{10}\right)}$	Large only g0 $10^{\left(\frac{HD+3}{20}\right)}$	Large only g1 $10^{\left(\frac{HD+3}{20}\right)}$
DR	Early 0-10°C	Early-medium 1.25-11.25°C	Medium 2.5-12.5°C	Medium-late 3.75-13.75°C	Late 5-15°C		
HMAX	High T5 - 5°C	High-medium T5 – 7.5°C	Medium T5 -10°C	Medium-low T5 -12.5°C	Low T5 - 15°C		
KMAX	Small $10^{\left(\frac{HD+3}{13}\right)}$	Medium $10^{\left(\frac{HD+3}{11}\right)}$	Large $10^{\left(\frac{HD+3}{9}\right)}$	Huge $10^{\left(\frac{HD+3}{7}\right)}$			
CSM	Small 0%	Medium 50%	Large 100%	Medium all year 50%			

HFM	Small 0%	Medium 50%	Large 100%
PV	OFF	ON	

Table 2: Sensitivity experiments ran from the version zero hardening simulation (cells highlighted in orange). The simulations were run at the sites of Spasskaya Pad and Farstanäs for evergreen needleleaf trees. HD is the hardiness level and T5 is the 5-year running mean of the minimum 2m daily temperature of each year.

Supplemental

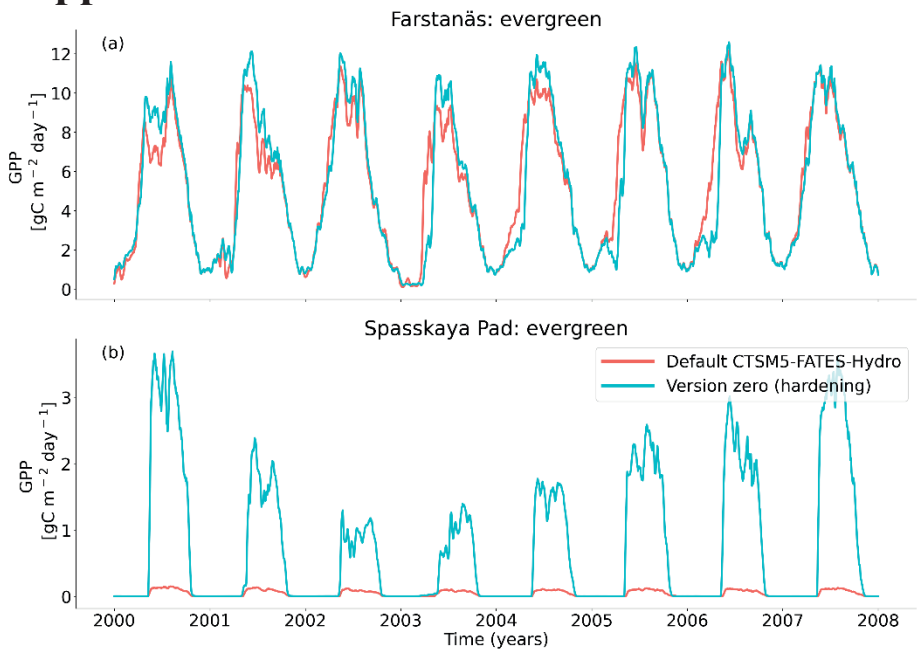

Figure S1: Gross primary productivity for needleleaf evergreen trees at the sites of a) Farstanäs, and b) Spasskaya Pad, during the period 2000-2008. The default simulation is shown in red, and the hardening simulation is shown in blue.

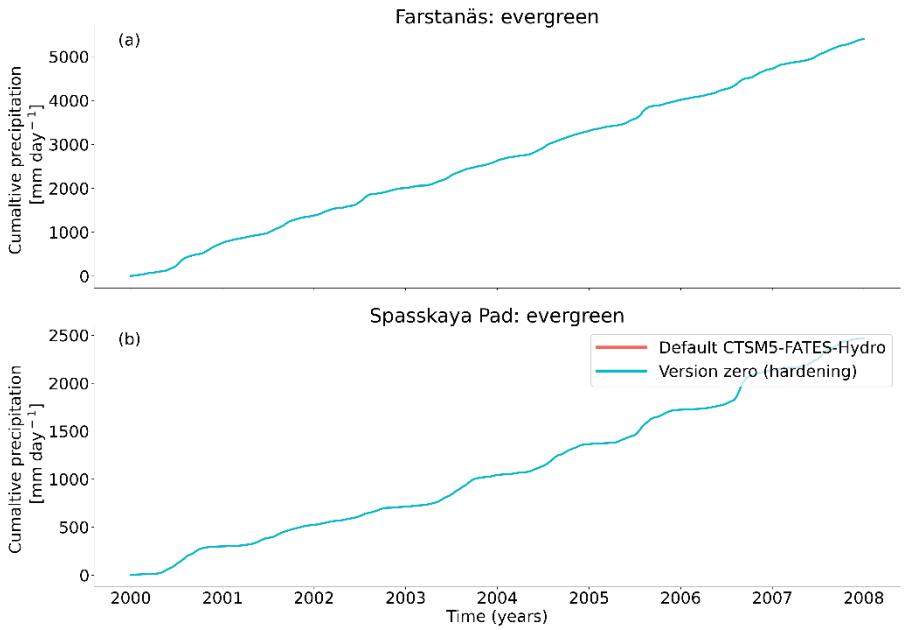

Figure S2: Cumulative total precipitation for needleleaf evergreen trees at the sites of a) Farstanäs, and b) Spasskaya Pad, during the period 2000-2008. The default simulation is shown in red, and the hardening simulation is shown in blue.

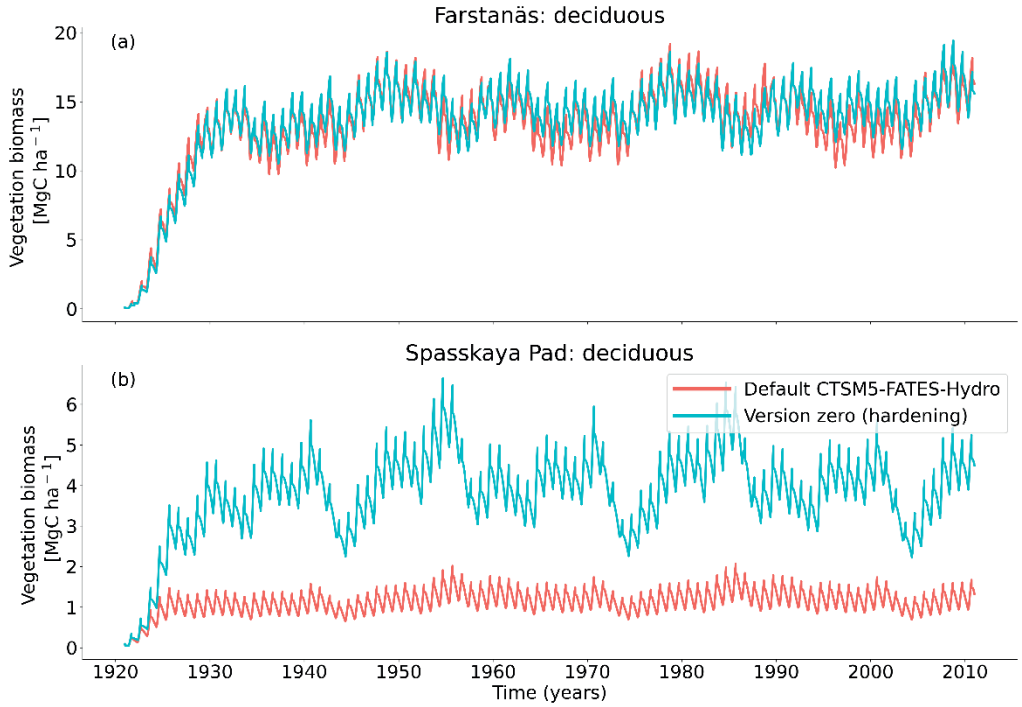

Figure S3: Living biomass for broadleaf deciduous trees at the sites of a) Farstanäs, and b) Spasskaya Pad, during the period 1921-2011 (atmospheric forcing: 3*[1981-2011]). The default simulation is shown in red, and the hardening simulation is shown in blue.

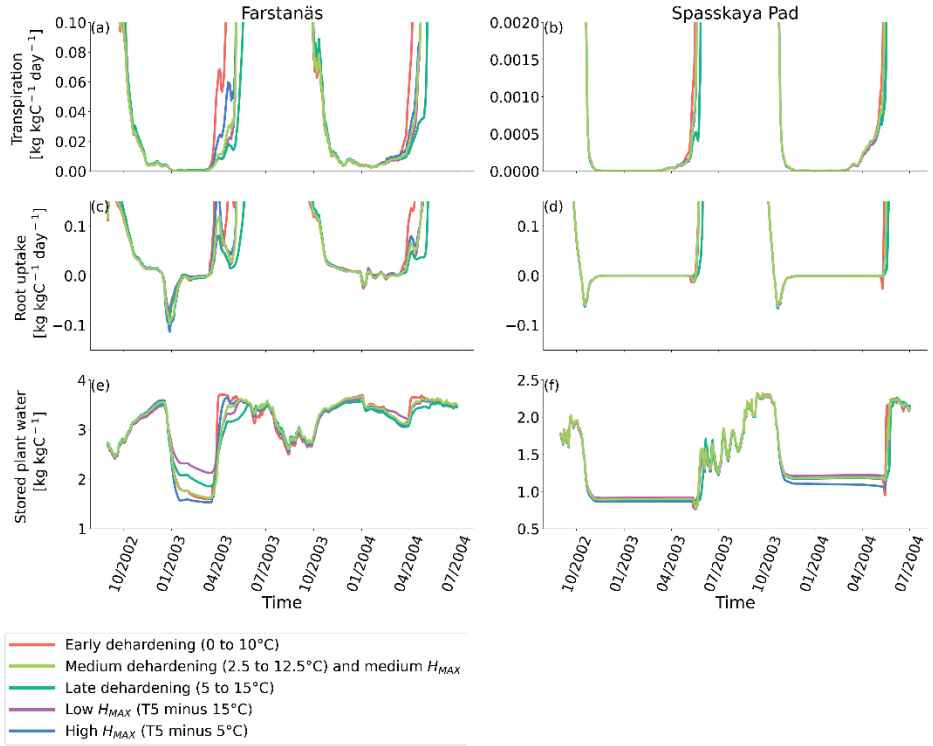

Figure S4: Plant water fluxes from dehardening and maximum hardiness level sensitivity analysis simulations for needleleaf evergreen trees at the sites of: Left) Farstanäs, and Right) Spasskaya Pad, during the period 2002/09-2004/07. Top: transpiration, middle: root water uptake, and bottom: stored plant water.

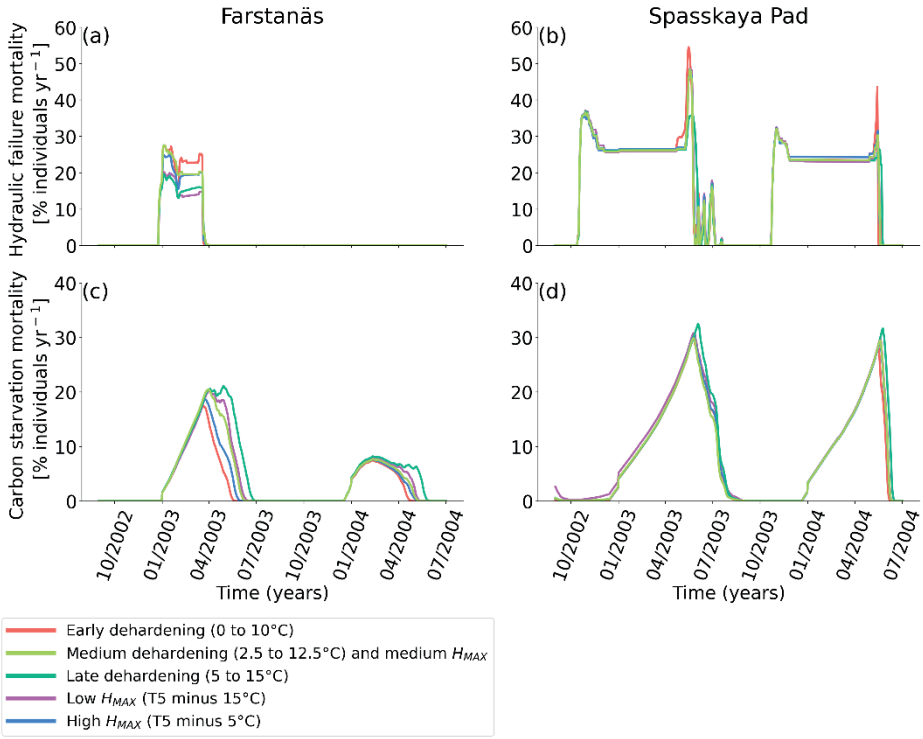

Figure S5: Mortality rates from dehardening and maximum hardiness level sensitivity analysis simulations for needleleaf evergreen trees at the sites of: Left) Farstanäs, and Right) Spasskaya Pad, during the period 2002/09-2004/07. Top: hydraulic failure mortality, and bottom: carbon starvation mortality.

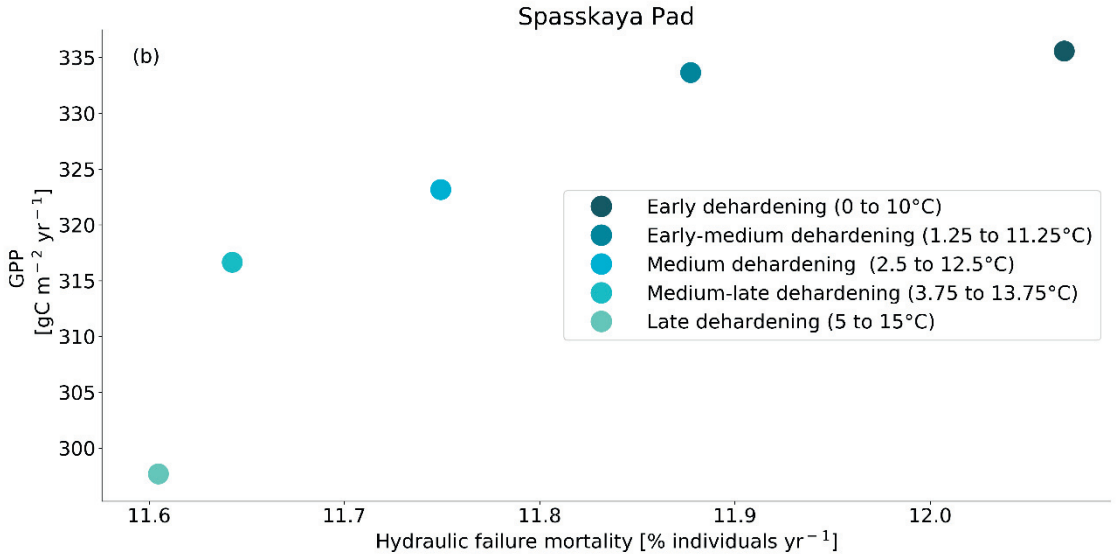

Figure S6: Trade-off between hydraulic failure mortality and gross primary productivity for evergreen needleleaf trees at Spasskaya Pad for 5 dehardening sensitivity experiments. The mortality rates are averaged over the 30 year period 1981 to 2011.

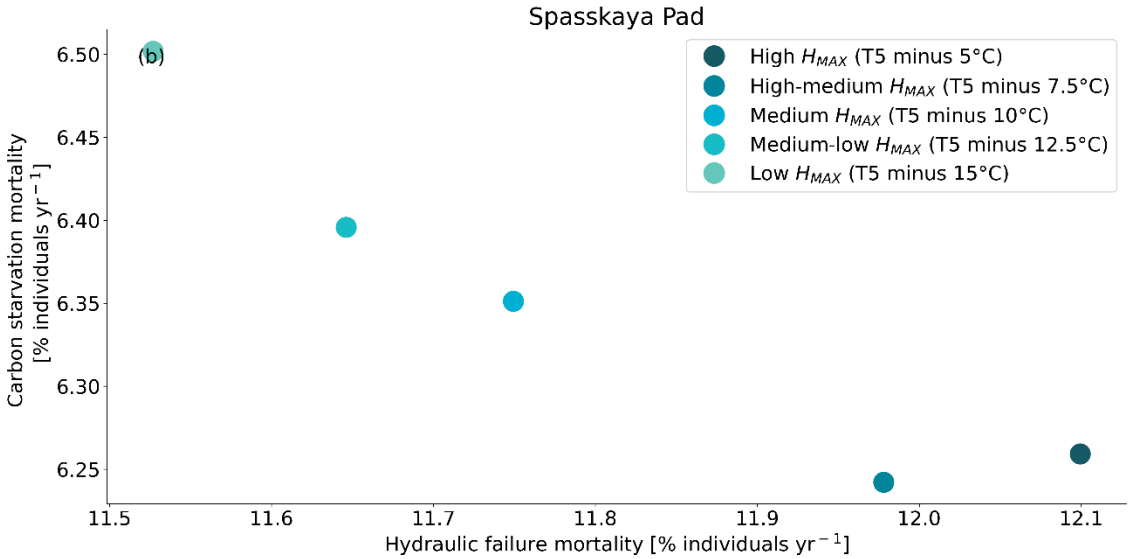

Figure S7: Trade-off between hydraulic failure mortality and carbon starvation mortality for evergreen needleleaf trees at Spasskaya Pad for 5 maximum hardiness level sensitivity experiments. The mortality rates are averaged over the 30 year period 1981 to 2011.

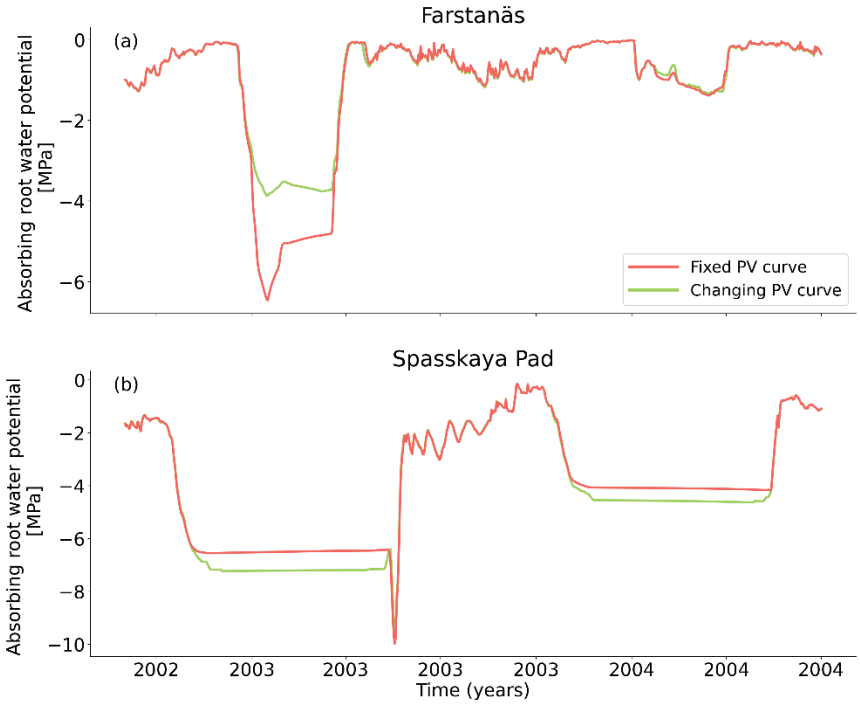

Figure S8: Absorbing root water potential from PV curve sensitivity analysis simulations for needleleaf evergreen trees at the sites of a) Farstanäs, and b) Spasskaya Pad, during the period 2002/09-2004/07.

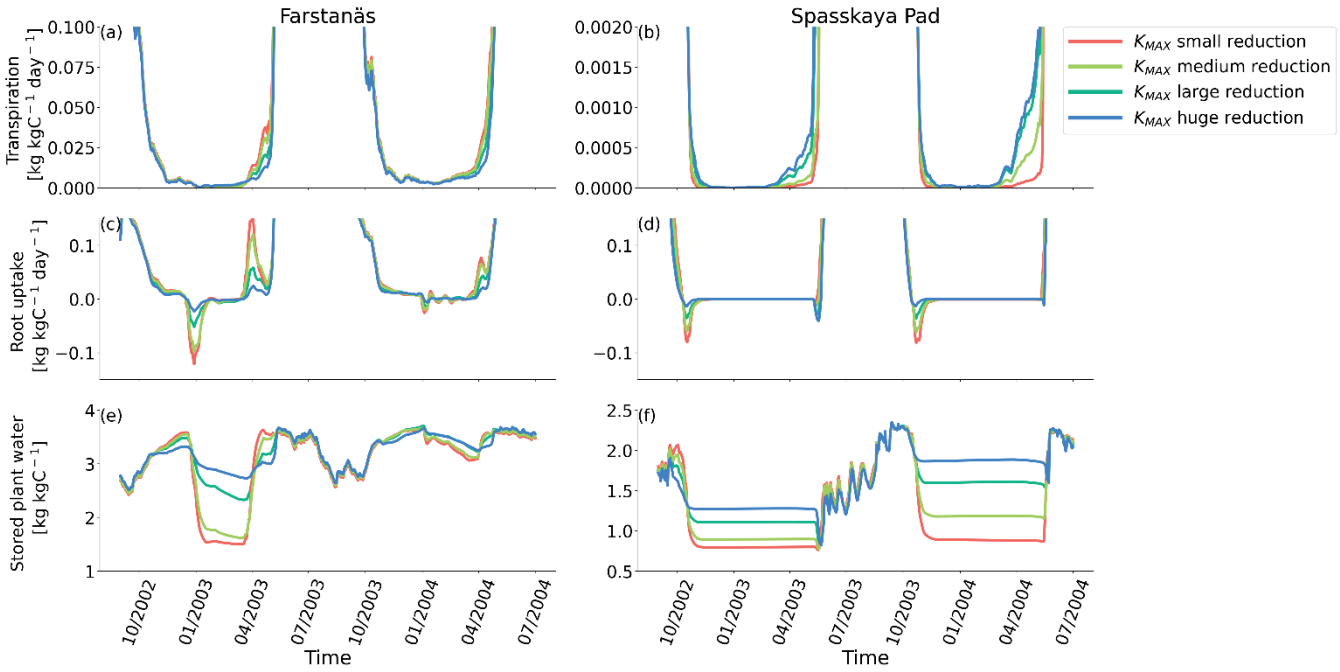

Figure S9: Plant water fluxes from Kmax sensitivity analysis simulations for needleleaf evergreen trees at the sites of: Left) Farstanäs, and Right) Spasskaya Pad, during the period 2002/09-2004/07. Top: transpiration, middle: root water uptake, and bottom: stored plant water.

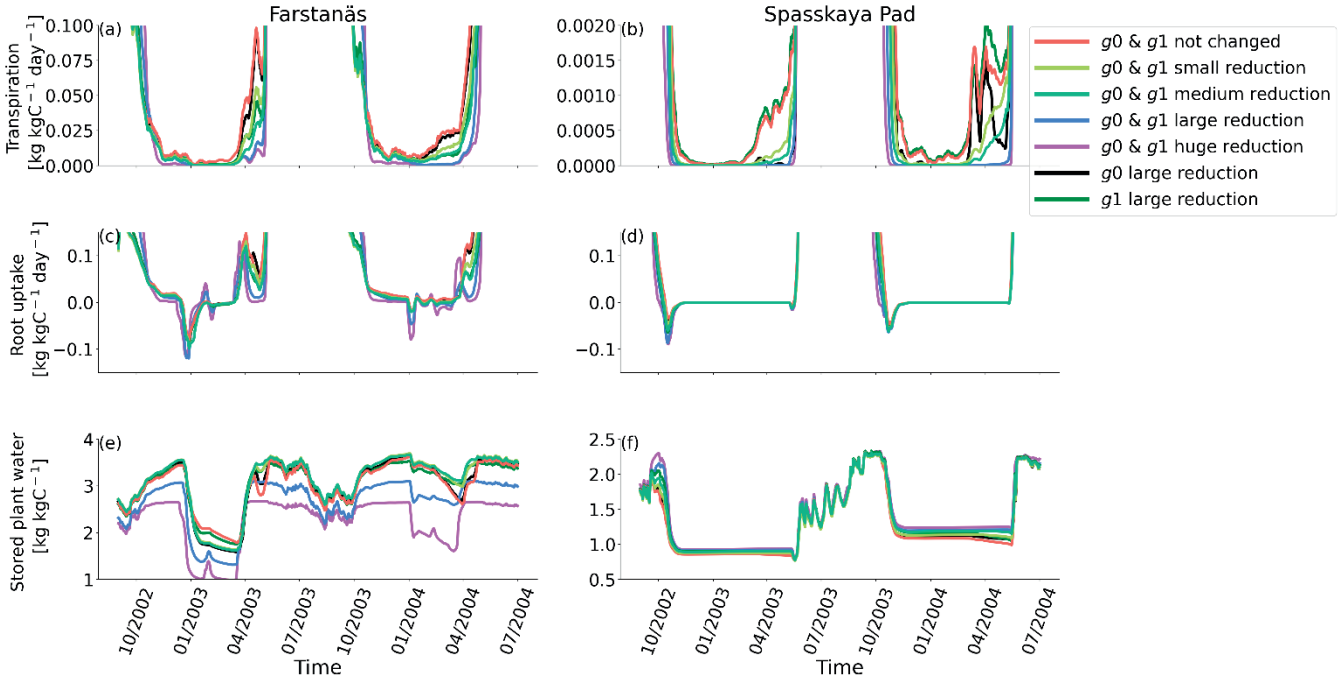

Figure S10: Plant water fluxes from g0 sensitivity analysis simulations for needleleaf evergreen trees at the sites of: Left) Farstanäs, and Right) Spasskaya Pad, during the period 2002/09-2004/07. Top: transpiration, middle: root water uptake, and bottom: stored plant water.

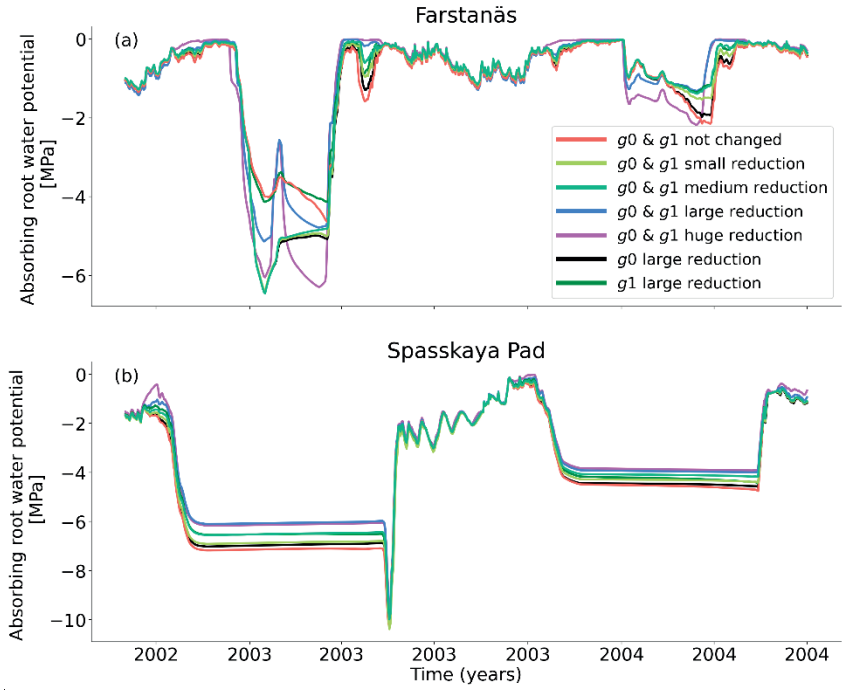

40 **Figure S11: Leaf water potential from g0 sensitivity analysis simulations for needleleaf evergreen trees at the sites of a) Farstanäs, and b) Spasskaya Pad, during the period 2002/09-2004/07.**

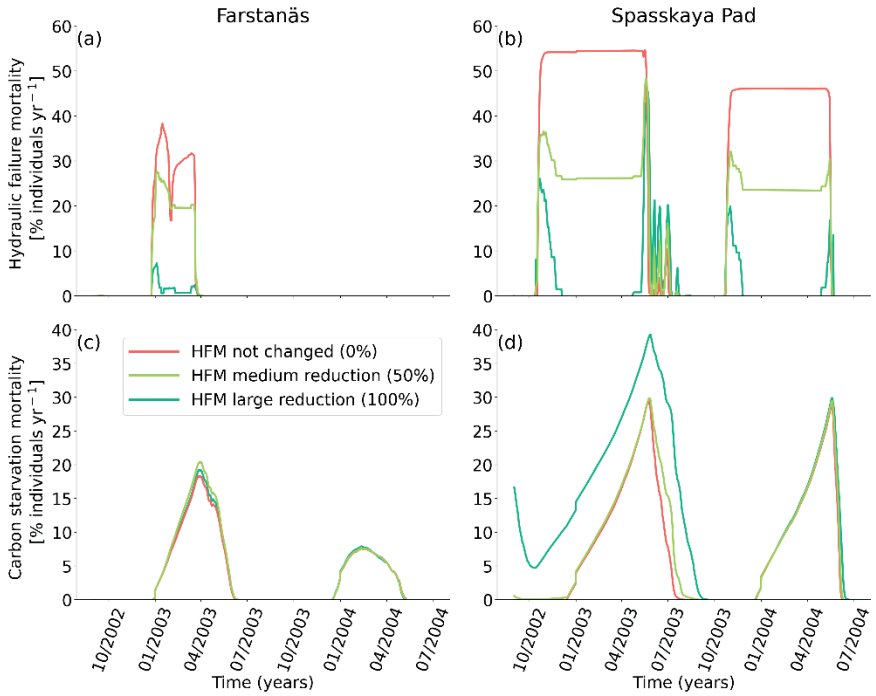

Figure S12: Mortality rates from hydraulic failure mortality sensitivity analysis simulations for needleleaf evergreen trees at the sites of: Left) Farstanäs, and Right) Spasskaya Pad, during the period 2002/09-2004/07. Top: hydraulic failure mortality, and bottom: carbon starvation mortality.

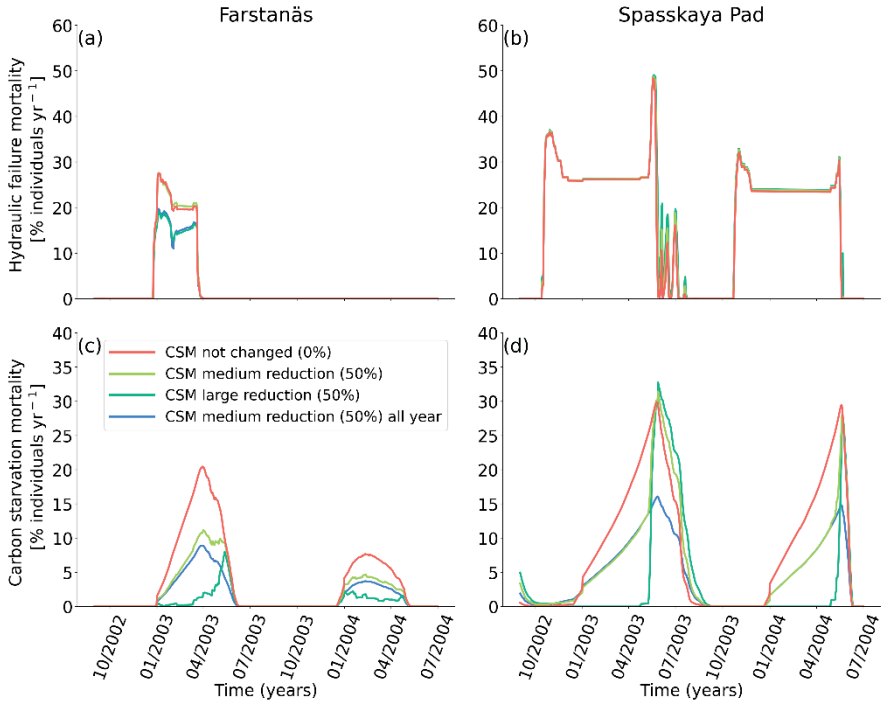

Figure S13: Carbon starvation mortality rate from carbon starvation mortality sensitivity analysis simulations for needleleaf evergreen trees at the sites of a) Farstanäs, and b) Spasskaya Pad, during the period 2002/09-2004/07.

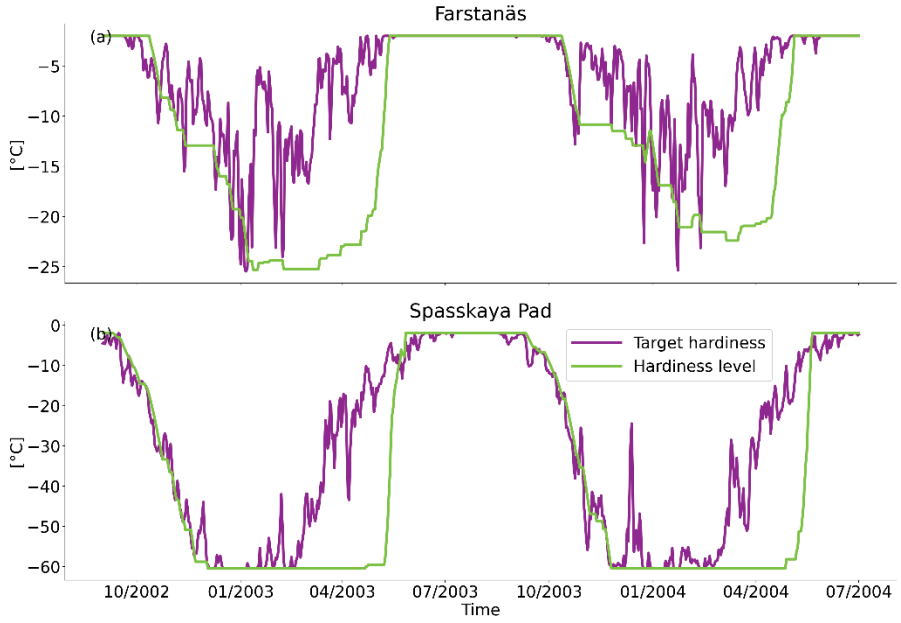

Figure S14: Target hardiness and hardiness level for needleleaf evergreen trees at the sites of a) Farstanäs, and b) Spasskaya Pad, during the period 2002/09-2004/07.

Parameters for standard runs	Description	Value and unit
Parameters for hardiness model		
H_{min}	Minimum hardiness level[a]	−2 °C
H_{max}	Maximum hardiness level[c]	−30 °C
S_{aut}	Start of autumn (start of hardening)[a]	Julian day 210
S_{spr}	Start of spring (start of dehardening) for Southern Sweden[a]	Julian day 1
H_t^*	Target hardiness level[a]	F (daily mean temperature)
r_h^*	Rate of hardening[a]	0–1 °C/day
r_{dh}^*	Rate of dehardening[a]	0–5 °C/day
W_d	Winter dormancy[a]	From days 260 to 365
Parameters for calculation of the growth reducing factor		
b	Slope parameter[b]	0.2 $°C^{-1}$
$LT50$	"Lethal temperature"[c]	20 °C

Table S1: Parameters for the frost hardiness and frost damage model (Rammig et al. 2010).

[a] Values from Jönsson et al. (2004).

[b] Values from Kellomäki et al. (1995).

[c] Values from Bigras and Colombo (2000).

Paper II: Integration of a frost mortality scheme into the demographic vegetation model FATES

Marius S. A. Lambert, Hui Tang, Kjetil S. Aas, Frode Stordal, Rosie A. Fisher, Jarle W. Bjerke, Jennifer A. Holm, and Frans-Jan W. Parmentier

Submitted to Journal of Advances in Modeling Earth Systems, 2022

II

Paper III: Modelled plant mortality due to an extreme winter event shows a divergent mortality for deciduous and evergreen species

Marius S. A. Lambert, Rosie A. Fisher, Kjetil S. Aas, Hui Tang, Frode Stordal, Jarle W. Bjerke and Frans-Jan W. Parmentier

Not submitted

III